MODELING, DYNAMICS AND OPTIMAL CONTROL OF WEST NILE VIRUS WITH SEASONALITY

AHMED ABDELRAZEC

A DISSERTATION SUBMITTED TO
THE FACULTY OF GRADUATE STUDIES
IN PARTIAL FULFILLMENT OF THE REQUIREMENTS
FOR THE DEGREE OF
DOCTOR OF PHILOSOPHY

GRADUATE PROGRAM IN MATHEMATICS AND STATISTICS
YORK UNIVERSITY
TORONTO, ONTARIO
June 2014

Abstract

West Nile virus (WNv) is a mosquito-borne disease which arrived in Canada in 2001. It has kept spreading across the country and still remains a threat to public health. In this dissertation, we formulate dynamical models and apply theory of dynamical systems to investigate the behavior of the transmission of WNv in the mosquito-bird cycle and humans. In the first part, we propose a system of ordinary differential equations to model the role of corvids and non-corvids birds in the transmission of WNv in the mosquito-bird cycle in a single season and proved the existence of backward bifurcation in the model. In the second part, we consider another deterministic model to study the impact of seasonal variations of the mosquito population on the transmission dynamics of WNv. We prove the existence of periodic solutions under specific conditions. As for the third part, the latter model is extended to assess the impact of some anti-WNv control measures; by re-formulating the model as an optimal control problem. For mosquito-borne diseases, it is essential to access and forcast the virus risk. Therefore in the final part, we generalize the risk index, minimum infection rate (MIR) by using a compartment model for WNv,

to define a dynamical minimum infection rate (DMIR) for assessing risk of WNv. By using the data from Peel region, we test and forecast the weekly risk of WNv which can help identify the optimal mitigation strategies.

Acknowledgements

Foremost, I would like to express my sincere gratitude to my advisor Professor Huaiping Zhu for the continuous support of my Ph.D study and research, for his patience, motivation, enthusiasm, and immense knowledge. His guidance helped me in all the time of research and writing of this thesis. I could not have imagined having a better advisor and mentor for my Ph.D study. I would also like to thank Dr. Michael Chen and Dr. Kaz Higuchi for their comments on my research and continuous support during my Ph.D. studies. In addition, I have been very privileged to get to know and to collaborate with Professor Suzanne Lenhart from University of Tennessee, my sincere thanks goes to her.

I express my gratitude to York University and Department of Mathematics Statistics for the financial support and help they provided throughout my graduate studies. I thank my fellows at LAMPS lab for the stimulating discussions and for all the fun we have had during my PhD. I am especially grateful to my wife Sherine and my kids Noura and Omar for their continuous care, constant encouragement, understanding and love on my way to this degree. My warm and sincere thanks also go to my friends and colleagues

for all the assistance in my research, fruitful discussions and encouragement during my stay at York.

Table of Contents

List of Tables

List of Figures

List of Variables

M_s	Number of susceptible mosquitoes
M_i	Number of infectious mosquitoes
L_s	Number of susceptible larval
L_i	Number of infectious larval
M	Total number of adult mosquitoes
L	Total number of larval
N_m	Total number of mosquitoes
B_{1s}	Number of susceptible corvid birds
B_{1i}	Number of infectious corvid birds
B_{1r}	Number of recovered corvid birds
N_{b1}	Total number of corvid birds
B_{2s}	Number of susceptible non-corvid birds
B_{2i}	Number of infectious non-corvid birds
B_{2r}	Number of recovered non-corvid birds

N_{b2}	Total number of non-corvid birds
B_s	Total number of susceptible birds
B_i	Total number of infectious birds
B_r	Total number of recovered birds
B, N_b	Total number of birds
S, H_s	Number of susceptible humans
E	Number of exposed humans
I, H_i	Number of infectious humans
H	Number of hospitalized humans
R, H_r	Number of recovered humans
H, N_h	Total number of humans
A	Number of mammals that mosquitoes bite
N	Total of all organisms that mosquitoes bite

1 Introduction

West Nile virus (WNv) is a mosquito-borne arbovirus belonging to the genus *Flavivirus* in the family Flaviviridae that can cause swelling and inflammation of the brain and spinal cord in birds, humans and many other species of animals (e.g. horses, cats, bats, and squirrels) [16]. The virus was first isolated from the serum of a febrile woman in 1937 in the West Nile district of Uganda [77]. Prior to the mid-1990s, WNv disease occurred only sporadically and was considered a minor risk for humans, until an outbreak in Algeria in 1994, with cases of WNv-caused encephalitis (50 human cases, including 8 fatalities), Romania in 1996 (393 human cases, 17 fatalities), Tunisia 1997 (111 human cases, 8 fatalities), Russia 1999 (361 human cases, 40 fatalities), and Israel 2000 (326 human cases, 33 fatalities) [6, 16, 61, 81, 82]. WNv has become an endemic pathogen in Africa, Asia, Australia, the Middle East, Europe and North America.

WNv first detected in the Western Hemisphere in 1999 in New York City [49]. Subsequently, the virus spread across the continental USA, leading to unparalleled morbidity and mortality rates in humans and equids, then continued its progression northward into

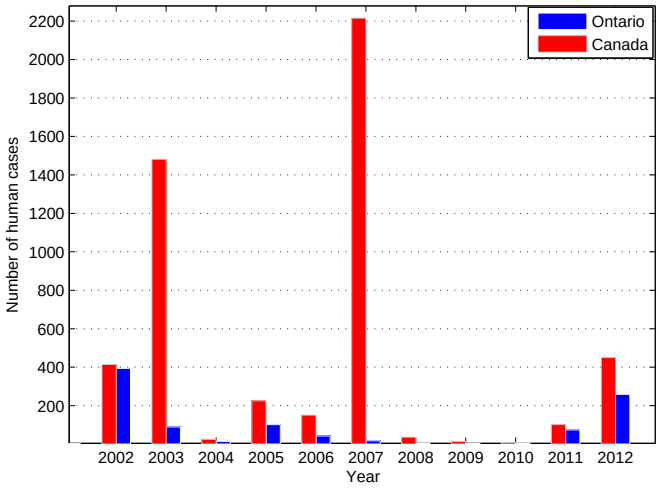

Figure 1.1: Reported human cases of WNv in Ontario and Canada [67]

Canada and southward into the Caribbean Islands and Latin America [46, 94]. In the USA, 1,263 fatal cases and 31,392 reported cases of WNv infection occurred between 1999 and 2011 [17]. In 2012, the USA had experienced one of its worst epidemics; there were 5387 cases of infections in humans. These were considered very high numbers of infection among humans knowing that the total number of infections in humans in the four years preceding 2012 was 3809 cases [17].

The WNv activity was first reported in Canada in 2001, when the virus was found in dead birds and mosquito pools in southern Ontario [16, 18]. In Fig.1.1, we present the reported WNv positive human cases in Ontario and Canada from 2002 to 2012 [67]. From the figure, one can see that the number of WNv infected humans in Canada was re-

markably decreasing during the years of 2007-2010. However, it started increasing once again in Ontario in 2010-2012 despite the immense efforts by the specialized agencies to control the virus. There are no indications that the spread of the virus has stopped. This fact reveals that the disease is evolving towards an endemic situation where the infected proportion is rather small. West Nile disease will most probably continue to be a public health concern because the virus has the most widespread geographical distribution and the largest vector and host range of all mosquito-borne flaviviruses. Thus, in this dissertation, we formulate dynamical models and theory of dynamical systems to discuss factors that could be involved in the changes of WNv dynamics in Canada. In addition to this, we develop a new risk assessment index.

1.1 Transmission cycle

WNv is an arthropod-borne virus (arbovirus) with a natural transmission cycle between mosquito vectors and wild birds that serve as amplification hosts [16]. When an infected mosquito bites a bird or some other mammal including a human, it transmits the virus; the bird may then develop sufficiently high viral titers during the next three to five days to infect another mosquito [83]. The WNv is different from other mosquito-born diseases since it involves a cross-infection between the host birds and mosquitoes and those birds could travel with no natural (spatial) boundaries. The virus can also be passed via vertical transmission from a mosquito to its offspring which increases the survival of WNv in

Figure 1.2: WNv transmission cycle.

nature [28, 78].

There are no documented cases from direct person-to-person or animal-to-person contact. However, it has been found that birds from certain species may become infected by WNv after ingesting it from an infected dead animal or infected mosquitoes, both of which are natural food items of some species [47]. Although mosquitoes can transmit the virus to humans and many other species of animals (e.g. horses, cats, bats, and squirrels), it cannot be transmitted back to mosquitoes (see Fig.1.2).

1.2 Mathematical modeling of WNv

Mathematical models for the WNv have been proposed in an attempt to study the transmission dynamics, in order to elucidate control strategies. The first WNv model was pre-

sented by Thomas and Urena in 2001 [79] to determine the amount of spraying (killing the mosquitoes) needed to eliminate the virus on New York City. In 2004 another model was presented and suggested that the most plausible method of eradication of WNv in a closed population would be to reduce the mosquito population or reduce the biting rate [69]. The authors in [53] made a comparative study of the discrete-time model in [79] and the continuous-time model in [93] confirmed that adulticiding is a more effective preventive strategy for controlling WNv in comparison to the use of personal protection. Paper [40] derived sufficient conditions in terms of the frequencies and rates of larvicides and insecticide spray. An age-structured WNv model was applied to the WNv dynamics in Southern Europe and Western Africa in [29]. The authors in [8] determined the cost-effective strategies for combating the spread of WNv in a given population. In [90] the authors compared four WNv compartmental models and proved that the dynamics of vector mosquitoes itself does not guarantee the existence of the backward bifurcation. All the above models share the feature of the interaction of WNv among mosquitoes, birds and humans.

Moreover, many other researches work on the transmission dynamics of WNv among mosquitoes and birds. Wonham et al. [92], presented a single season model with a system of differential equations for WNv transmission in the mosquito-bird population. Their work, using local stability results and simulations, showed that while mosquito control decreases WNv outbreak threshold, controlling birds increases it. They also focused on

how different assumptions of host-vector interaction affect the disease-transmission term in [93]. Paper [22] presented and analyzed a mathematical model for the transmission of WNv infection between mosquito and avian populations and by using experimental and field data as well as numerical simulations, they found the phenomena of damped oscillations of the infected bird population. A theoretical framework for the analysis of the WNv epidemic and for dealing with mosquito diffusion and bird's migration was provided in [45]. In [52] the authors studied the spatial spread of the virus, established the existence of traveling waves and computed the spatial spreading speed of the infection. The impact of directional dispersal of birds on the spatial spreading of WNv was studied in [54]. Paper [41] obtained a subthreshold condition for the backward bifurcation. The authors in [23] concluded numerically that the frequency of the new outbreaks depends on the relationship between the intrinsic and seasonal frequencies.

A common feature of all the previous WNv models is that they are formulated with constant parameters. There have been some models using a time-varying rate of some parameters like the one in [50] which estimated the proportion of actual WNv-induced dead birds by about $0.8\%, 7.3\%$ of equine and 10.7% of human cases- as reported by the Centers for Disease Control and Prevention. Another one presented by Abdelrazec et al. [2] considered the model that studied the impact of seasonal variations of the mosquito population on the dynamics of WNv; and by using the theory of optimal control, it confirmed that larviciding is the most effective strategy. Papers [1,11,30,60] categorized

the birds into two groups and studied the effects in transmission of the virus. Likewise, the article [24] studied the effect of the interaction between different species of birds and mosquitoes living in the same locality on the emergence and prevalence of the disease.

1.3 Risk assessment and control of WNv

Although studies are underway, there is no human vaccine currently available for WNv. The methods used to reduce the risk of WNv infection are based on mosquito reduction strategies (such as larvaciding, adulticiding, and elimination of breeding sites) and personal protection (based on the use of appropriate insect repellents). These measures are intensified during mosquito seasons.

Since 2002, the Public Health Agency of Canada has established a surveillance program to monitor the risk of WNv transmission to humans through surveillance and to reduce it through control efforts and public education. Both scientists and vector control practitioners have considered various means of assessing the spatiotemporal human risk of transmission to reduce potential health threats. Some studies have used entomological risk of vector exposure as a key determinant of WNv disease risk in humans, whereas others have focused on disease risk based on avian and equine surveillance or mandatory human case reports. In practice, the entomological risk measures based on vector mosquito abundance are considered effective means to assess and predict human WNv infection risk [85].

In general, risk assessment is a formalized basis for the objective evaluation of risk in which assumptions and uncertainties are clearly considered and presented. The Public Health Agency of Canada has utilized mosquitoes testing (through pooling mosquitoes of the same species) to estimate the risk assessment in order to monitor the spread of the virus. The risk assessment of WNv infection depends on seven surveillance factors: seasonal temperatures, adult mosquito vector abundance, virus isolation rate in vector mosquito species, human cases of WNv, local WNv activity (horse, mosquito), time of year and WNv activity in proximal urban or suburban region [85]. The risk assessment of WNv, based on mosquito, can help identify areas that are at greatest risk for humans so that control and prevention measures can be taken to reduce the human infection.

1.4 Overview of the dissertation

The overall goal of this thesis aims at understanding the behavior of the transmission of WNv in the mosquito-bird cycle and humans, as well as developing systems and procedures to reduce human risk by formulating dynamical models and using the optimal control to minimize the spread of WNv. This work consists of six chapters.

We begin with Chapter one as the introduction and in Chapter two, we propose a system of ordinary differential equations (by taking corvids and non-corvids birds as the primary reservoir hosts and mosquitoes as vectors) to model the role of corvids and non-corvids birds in the transmission of WNv in the mosquito-bird cycle in a single season.

The system of eight differential equations can have up to two positive equilibria. We find the basic reproduction number and analyze the existence and stability of the equilibria. Using normal theory and center-manifold theorem, we also prove the existence of a backward bifurcation which gives a further sub-threshold condition beyond the basic reproduction number for the spread of the virus. The existence of the backward bifurcation also suggests that the long term WNv activity in a given region depends on the initial population sizes of birds and density of mosquitoes. The result of this part also suggests that even though dead corvids (American crow) may not be seen in a given region, like in the early years of the endemic of the virus, there might be still a possibility of an outbreak due to the existence of the non-corvids as reservoirs. In this part we also suggest that it is essential to consider the diversity of the avian species, as well as the quantity of other mammals, when modeling WNv.

In Chapter three, we consider another deterministic model to study the impact of seasonal variations on mosquito population and the dynamics of WNv. Firstly, we establish and study the model without seasonality and prove the existence of the backward bifurcation of the model. Secondly, we expand the model to include the seasonal variations to study the impact of seasonal changes on the transmission of the virus. We prove the existence of periodic solutions under specific condition. We also introduce and calculate the basic reproduction number for this seasonal forced model. Furthermore, we examine the dynamics of the model when the seasonal variation becomes stronger.

In Chapter four, we use the optimal control theory to study the strategies of control and minimize the spread of WNv. The controls represent the level at which pesticide is applied to the mosquito population and the prevention efforts to minimize human-mosquito contacts. The model formulated in chapter three is extended to assess the impact of some anti-WNv control measures; by re-formulating the model as an optimal control problem. This entails the use of three control functions: adulticide, larvicide and human protection. The numerical simulations of this optimal control problem lead to the following outcomes: 1) Larvicide is the most effective strategy to control an ongoing epidemic in reducing disease cost. (2) The results emphasize the importance of using the information about quantity of other animals that could be infected and the percentage of the non-corvids bird at any region before applying the control strategies. (3) Identifying the ultimate time of applying the control to achieve the best control strategy.

In Chapter five, we establish a criterion to access the risk of WNv in any region. We utilise the dynamical models to measure the risk of WNv by considering the influence of birds. This is done by developing a new index, the dynamical minimum infection rate (DMIR) of WNv introduction into Ontario-Canada through different pathways. DMIR is considered the first WNv dynamical index to test and forecast the weekly risk of WNv by explicitly considering the temperature impact in the mosquito abundance, estimated by statistical tools. This chapter is followed by conclusions and future work.

2 Dynamics of West Nile virus in mosquitoes and corvids and non-corvids

2.1 Introduction

In North America, the WNv has been found in more than 300 species of birds [48]. From the study of [36], the dynamics of WNv transmission are influenced strongly by a few key super spreader bird species, and their results showed that the WNv mosquitoes fed predominantly (83%) on birds with a high diversity of species used as hosts (25 species), and WNv mosquitoes also fed on mammals (19%; 7 species with humans representing 16%). Their study indicated that approximately 66% of WNv-infectious mosquitoes became infected from feeding on just a few species of birds. Yet, as far as we know, the past modeling effects to understand the transmission dynamics of WNv have treated the avian species as one family. The study by [36] suggested that it is essential to consider the impact of avian species diversity in one system to understand the transmission dynamics of WNv.

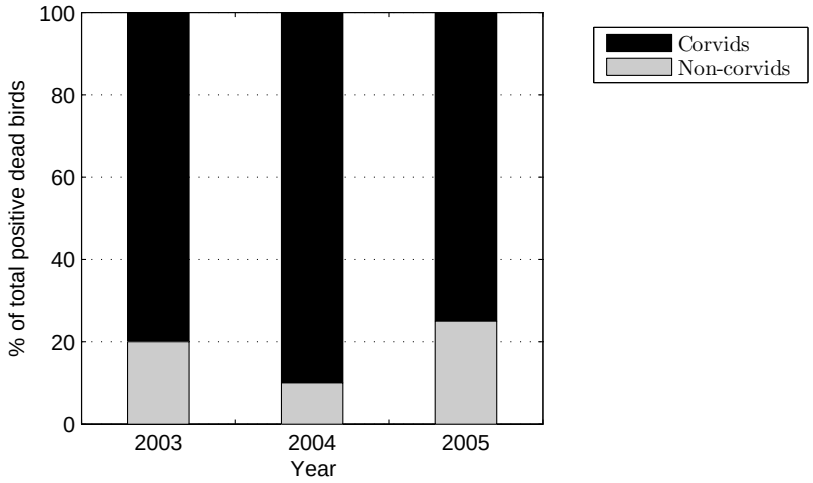

Figure 2.1: Percentages of WNv positive dead birds in Peel region [64].

However, it is not realistic to consider over 300 species of birds in one model. Note that of those many bird species, corvids are the most susceptible to infection and comprise an auspicious component of the mortality [66]. The surveillance data for WNv in southern Ontario, Canada, suggest that the corvids and non-corvids have different disease-induced mortality rates. In Fig.2.1, we present the percentages of dead birds from corvids and other bird species in Peel region, Ontario from 2003 to 2005 [64]. From Fig.2.1, one can see that corvids account up to 80% in 2003, 90% in 2004 and 75% in 2005 of total of deaths due to this disease.

In this chapter, we propose a system of ordinary differential equations to model the role of corvids and non-corvids in the transmission of WNv in the mosquito-bird cycle in a single season. The system of eight differential equations can have up to two positive

equilibria. The analysis of the model including a backward bifurcation gives a further sub-threshold condition beyond the reproduction number for the control of the virus. The existence of the backward bifurcation also suggests that the long term WNv activity in a given region depends on the initial population sizes of birds and density of mosquitoes. The results of this chapter also suggests that even though dead corvids (American crow) may not be seen in a given region, like in the early years of the endemic of the virus, there might be still a possibility of an outbreak due to the existence of the non-corvids as reservoirs. This chapter also suggests that it is essential to consider the diversity of the avian species when modeling WNv.

This chapter is organized as follows: We formulate the model, with birds being classified as corvids and non-corvids, in Section 2.2; and in the next section, we find and analyze the equilibrium points of the model. The backward bifurcation analysis is given in Section 2.4. Our numerical simulations and discussion are presented in Section 2.5 and 2.6 respectively.

2.2 Model formulation

According to the transmission cycle (between mosquitoes and birds) of the virus, we plot the flow chart in Fig.2.2. In the flow chart, $M_s(t)$ and $M_i(t)$ are the number of susceptible and infectious mosquitoes at time t, respectively. The total number of mosquitoes is $N_m(t) = M_s(t) + M_i(t)$. Due to its short life span, a mosquito never recovers from

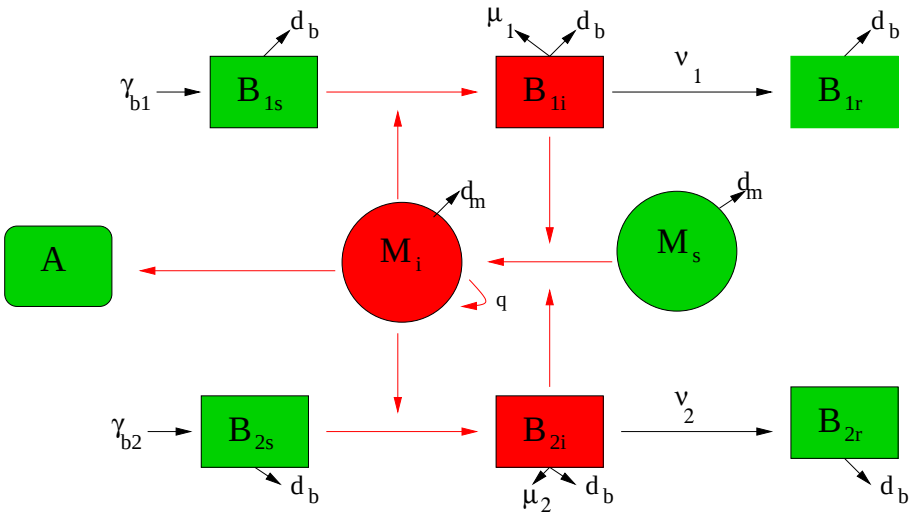

Figure 2.2: Flow chart of the WNv [1].

the infection and we do not consider the recovered class in the mosquitoes [28, 78]. The number of susceptible, infected and recovered corvid birds at time t are denoted by $B_{1s}(t)$, $B_{1i}(t)$ and $B_{1r}(t)$, respectively. Similarly, the number of susceptible, infected and recovered non-corvid birds at time t are denoted by $B_{2s}(t)$, $B_{2i}(t)$ and $B_{2r}(t)$. Thus, $N_{b1} = B_{1s} + B_{1i} + B_{1r}$ and $N_{b2} = B_{2s} + B_{2i} + B_{2r}$ are the total number of corvid and non-corvid birds, and the total number of birds will be $N_b = N_{b1} + N_{b2}$. Moreover, the total number of infected birds at time t is denoted by $B_i(t) = B_{1i}(t) + B_{2i}(t)$. According to [36], WNv mosquitoes also feed on mammals (humans, horses, cats, bats, and squirrels, etc.); hence, we let A be the total of mammals that mosquitoes will bite for blood meals. In this chapter we assume that A is constant.

Let us define the biting rate b_m of mosquitoes as the average number of bites per

mosquito per day. The transmission probability is the probability when an infectious bite produces a new case in a susceptible member of the other species. The probability that a mosquito chooses a particular bird or other animal to bite can be assumed as $\frac{1}{N_b+A}$. Thus, a bird receives in average $b_m\left(\frac{N_m}{N_b+A}\right)$ bites per unit of time. Then, the infection rate per susceptible bird (corvids or non-corvids) is given by $\beta_b b_m\left(\frac{N_m}{N_b+A}\right)\frac{M_i}{N_m} = \beta_b b_m \frac{M_i}{N_b+A}$, where β_b is the WNv transmission probability from mosquitoes to birds. Similarly, the infection rate per susceptible mosquito is $\beta_m b_m \frac{B_{1i}+B_{2i}}{N_b+A}$, where β_m is the WNv transmission probability from birds to mosquitoes. As was mentioned in the introduction, mosquitoes can transmit WNv vertically [78], and the fraction of progeny of infectious mosquitoes that is infectious is denoted by q, with $0 \leq q < 1$.

For the corvid and non-corvid bird populations, we assume constant recruitment rates γ_{b1} and γ_{b2} respectively due to birth and immigration. Usually the bird population remains unchanged over years if there are no avian diseases or environmental changes. For simplicity in this chapter, we assume that the natural death rate of non-corvid birds is the same as that of corvid birds d_b. Another assumption is that infected corvid and non-corvid birds recover at constant rates of ν_1 and ν_2, respectively. The specific death rates associated with WNv infection in the corvid and non-corvid birds population are μ_1 and μ_2, respectively. The corvids family is more competent than the non-corvids family of birds, i.e, the number of secondary infections produced by individuals of those species is greater than the corresponding number produced by the non-corvids [47]. Moreover,

from Fig.2.1, we noticed that the disease mortality rates of the corvids family are significantly greater than the corresponding ones for the non-corvids family [47]. So we can assume that $\mu_1 > \mu_2$.

Based on the above assumptions, and extending the ideas in [11, 22, 52, 92] our WNv model is given by

$$\begin{cases} \frac{dM_s}{dt} &= (r_m M_s + (1-q) r_m M_i)\left(1 - \frac{N_m}{K_m}\right) - d_m M_s - \beta_m b_m \frac{B_{1i}+B_{2i}}{N_b+A} M_s, \\ \frac{dM_i}{dt} &= q r_m M_i \left(1 - \frac{N_m}{K_m}\right) - d_m M_i + \beta_m b_m \frac{B_{1i}+B_{2i}}{N_b+A} M_s, \\ \frac{dB_{1s}}{dt} &= \gamma_{b1} - d_b B_{1s} - \beta_b b_m \frac{B_{1s}}{N_b+A} M_i, \\ \frac{dB_{1i}}{dt} &= -(d_b + \mu_1 + \nu_1) B_{1i} + \beta_b b_m \frac{B_{1s}}{N_b+A} M_i, \\ \frac{dB_{1r}}{dt} &= -d_b B_{1r} + \nu_1 B_{1i}, \\ \frac{dB_{2s}}{dt} &= \gamma_{b2} - d_b B_{2s} - \beta_b b_m \frac{B_{2s}}{N_b+A} M_i, \\ \frac{dB_{2i}}{dt} &= -(d_b + \mu_2 + \nu_2) B_{2i} + \beta_b b_m \frac{B_{2s}}{N_b+A} M_i, \\ \frac{dB_{2r}}{dt} &= -d_b B_{2r} + \nu_2 B_{2i}, \end{cases} \tag{2.2.1}$$

where the definitions and values of the parameters used in the model (2.2.1) are summarized in Table 2.1.

Adding the first two equations of the model (2.2.1), the total number of mosquitoes N_m satisfies

$$\frac{dN_m}{dt} = r_m N_m \left(1 - \frac{N_m}{K_m}\right) - d_m N_m. \tag{2.2.2}$$

For any given positive initial condition $N_m(0) > 0$, the total number of mosquitoes approaches a steady value $\tilde{M} = (1 - \frac{d_m}{r_m})K_m$.

The equation (2.2.2) indicates that the mosquito population will die out if $d_m \geq r_m$, while the mosquito population will eventually stabilize at a positive equilibrium $\tilde{M}$ if $d_m < r_m$. That is why in this chapter we are assuming the latter case.

For the two species of birds, their totals satisfy

$$\frac{dN_{bj}}{dt} = \gamma_{bj} - d_b N_{b_j} - \mu_i B_{ji}, \quad j = 1, 2, \tag{2.2.3}$$

respectively. From (2.2.3), one can see that if there is no virus involved ($B_{ji} = 0$), the total populations of corvids and non-corvids will approach $\tilde{B_j} = \frac{\gamma_{bj}}{d_b}$, $j = 1, 2$, respectively.

To better organize the analysis, we denote $\delta_j = d_b + \mu_j + \nu_j$, $j = 1, 2$. From the definition of μ_j and ν_j we can define $\frac{1}{\delta_1}$ and $\frac{1}{\delta_2}$ as the adjusted infectious period taking into account the mortality rates of corvid and non-corvid birds, respectively. Let $\tilde{B} = \tilde{B_1} + \tilde{B_2} + A$, which is the total number of birds and other mammals that mosquitoes will bite for blood meals.

2.3 Equilibria and reproduction number

The model (2.2.1) has two disease free equilibrium (DFE) points, $E_0 = (0, 0, \tilde{B_1}, 0, 0, \tilde{B_2}, 0, 0)$ and $E_1 = (\tilde{M}, 0, \tilde{B_1}, 0, 0, \tilde{B_2}, 0, 0)$. For the DFE E_0, one can verify that its Jacobian matrix has eigenvalues $\lambda_1 = \lambda_2 = \lambda_3 = \lambda_4 = -d_b$, $\lambda_5 = -\delta_1$, $\lambda_6 = -\delta_2$, $\lambda_7 = (qr_m - d_m)$ and $\lambda_8 = (r_m - d_m) > 0$, so E_0 is a hyperbolic saddle point.

The local stability of E_1 is governed by the basic reproduction number R_0 which can be calculated from the next generation matrix for the system (2.2.1). Note that the model has five

Par.	Definition	Range	Ref.
r_m	Mosquitoes per capita birth rate	$(0.036 - 42.5)/(day^{-1})$	[92]
K_m	Environmental carrying capacity of mosquitoes	$(10^5 - 10^6)$	[92]
d_m	Natural death rate of mosquitoes	$(0.016 - 0.07)/(day^{-1})$	[92]
d_b	Natural death rate of birds	$(10^{-4} - 10^{-3})/(day^{-1})$	[92]
β_m	WNv transmission probability from birds to mosquitoes	$(0.018 - 0.24)$	[92]
β_b	WNv transmission probability from mosquitoes to birds	$(0.088 - 0.9)$	[92]
b_m	Biting rate of mosquitoes	$(0.2 - 0.75)$	[92]
γ_{b1}	Recruitment rate of corvid birds	$(800 - 1100)/(day)$	[47]
γ_{b2}	Recruitment rate of non-corvid birds	$(800 - 1000)/(day)$	[47]
ν_1	Recovery rate of corvid birds	$(0 - 0.1)/(day^{-1})$	[47]
ν_2	Recovery rate of non-corvid birds	$(0 - 0.2)/(day^{-1})$	[47]
μ_1	Death rate of corvid birds due to the infection	$(0.2 - 0.3)/(day^{-1})$	[47]
μ_2	Death rate of non-corvid birds due to the infection	$(0.01 - 0.16)/(day^{-1})$	[47]

Table 2.1: Parameters used in the model (2.2.1).

infected groups, namely $M_i, B_{1i}, B_{1r}, B_{2i}$ and B_{2r}. Using the notation of [84], the new infection terms and the remaining transfer terms for those five groups are given below, in partitioned form.

In the following, let

$$\Im = \begin{pmatrix} qr_m M_i(1-\frac{N_m}{K_m}) + \beta_m b_m \frac{B_{1i}+B_{2i}}{N_b+A} M_s \\ \beta_b b_m \frac{B_{1s}}{N_b+A} M_i \\ 0 \\ \beta_b b_m \frac{B_{2s}}{N_b+A} M_i \\ 0 \end{pmatrix}, \quad \upsilon = \begin{pmatrix} d_m M_i \\ \delta_1 B_{1i} \\ d_b B_{1r} - \nu_1 B_{1i} \\ \delta_2 B_{2i} \\ d_b B_{2r} - \nu_2 B_{2i} \end{pmatrix}.$$

Thus, at point E_1, the Jacobian matrices of $\Im$ and υ with respect to the five groups leads to

$$F = \begin{pmatrix} qd_m & \frac{\beta_m b_m \tilde{M}}{\tilde{B}} & 0 & \frac{\beta_m b_m \tilde{M}}{\tilde{B}} & 0 \\ \frac{\beta_b b_m \tilde{B_1}}{\tilde{B}} & 0 & 0 & 0 & 0 \\ 0 & 0 & 0 & 0 & 0 \\ \frac{\beta_b b_m \tilde{B_2}}{\tilde{B}} & 0 & 0 & 0 & 0 \\ 0 & 0 & 0 & 0 & 0 \end{pmatrix}, \quad V^{-1} = \begin{pmatrix} \frac{1}{d_m} & 0 & 0 & 0 & 0 \\ 0 & \frac{1}{\delta_1} & 0 & 0 & 0 \\ 0 & \frac{\nu_1}{d_b \delta_1} & \frac{1}{d_b} & 0 & 0 \\ 0 & 0 & 0 & \frac{1}{\delta_2} & 0 \\ 0 & 0 & 0 & \frac{\nu_2}{d_b \delta_2} & \frac{1}{d_b} \end{pmatrix},$$

where F is a non-negative matrix and V is non-singular. It is not difficult to find the basic reproduction number defined by $R_0 = \rho(FV^{-1})$, the spectral radius of the matrix FV^{-1}. If we denote

$$\Re = \sqrt{\beta_m \beta_b b_m^2 \frac{\tilde{M}}{d_m \tilde{B}^2} \left(\frac{\tilde{B_1}}{\delta_1} + \frac{\tilde{B_2}}{\delta_2} \right)}, \tag{2.3.4}$$

then the basic reproduction number

$$R_0 = \frac{q}{2} + \frac{1}{2}\sqrt{q^2 + 4\Re^2}. \tag{2.3.5}$$

Note that for the WNv infection, the number of infections produced by a single corvid or non-corvid bird during its infectious period in a completely susceptible mosquito population is given

by $\beta_m b_m \frac{\tilde{M}}{\tilde{B}^2}\left(\frac{\tilde{B}_1}{\delta_1}+\frac{\tilde{B}_2}{\delta_2}\right)$. In the same way, the number of infections in a completely susceptible avian population produced by a single infectious mosquito is given by $\frac{\beta_b b_m}{d_m}$. Then $\Re$ is the basic reproductive number in the absence of vertical transmission.

From Theorem 2 of [84], the following proposition is obtained

Proposition 2.3.1. *For system (2.2.1), the disease-free equilibrium E_1 is locally asymptotically stable if $R_0 < 1$ and unstable if $R_0 > 1$.*

The epidemiological implication of Proposition 2.3.1 is that, in general, when $R_0 < 1$, a small influx of infected mosquitoes into the community would not generate a large outbreak, and the disease dies out in time. However, we show in the next subsection that the disease may still persist even when $R_0 < 1$.

2.3.1 Endemic equilibrium points (EEP)

To obtain all the endemic equilibrium points (EEP), or the positive equilibrium points, first we set the right hand sides in equations (2.2.1) equal to zero:

$$
\begin{aligned}
(r_m M_s + (1-q) r_m M_i)\left(1 - \frac{N_m}{K_m}\right) - d_m M_s - \beta_m b_m \frac{B_{1i} + B_{2i}}{N_b + A} M_s &= 0, && (2.3.6)\\
q r_m M_i \left(1 - \frac{N_m}{K_m}\right) - d_m M_i + \beta_m b_m \frac{B_{1i} + B_{2i}}{N_b + A} M_s &= 0, && (2.3.7)\\
\gamma_b - d_b B_{1s} - \beta_b b_m \frac{B_{1s}}{N_b + A} M_i &= 0, && (2.3.8)\\
-(d_b + \mu_1) B_{1i} - \nu_1 B_{1i} + \beta_b b_m \frac{B_{1s}}{N_b + A} M_i &= 0, && (2.3.9)\\
-d_b B_{1r} + \nu_1 B_{1i} &= 0, && (2.3.10)\\
\gamma_{b2} - d_b B_{2s} - \beta_b b_m \frac{B_{2s}}{N_b + A} M_i &= 0, && (2.3.11)\\
-(d_b + \mu_2) B_{2i} - \nu_2 B_{2i} + \beta_b b_m \frac{B_{2s}}{N_b + A} M_i &= 0, && (2.3.12)\\
-d_b B_{2r} + \nu_2 B_{2i} &= 0. && (2.3.13)
\end{aligned}
$$

Then we write the susceptible and recovered bird variables in terms of B_{1i} and B_{2i}

$$
\begin{aligned}
B_{1s} &= \tilde{B_1} - \tfrac{\delta_1}{d_b} B_{1i},\\
B_{2s} &= \tilde{B_2} - \tfrac{\delta_2}{d_b} B_{2i},\\
B_{1r} &= \tfrac{\nu_1}{d_b} B_{1i},\\
B_{2r} &= \tfrac{\nu_2}{d_b} B_{2i}.
\end{aligned} \qquad (2.3.14)
$$

By adding (2.3.6) and (2.3.7), we have $N_m \left(N_m - K_m \left(1 - \frac{d_m}{r_m}\right)\right) = 0$. At any positive equilibrium, we have $N_m = M_s + M_i = K_m \left(1 - \frac{d_m}{r_m}\right) = \tilde{M}$.

In case $M_s + M_i = \tilde{M}$, it follows from (2.3.9), (2.3.12) and (2.3.14) that one can verify

$$
B_{2i} = \frac{\delta_1 \tilde{B_2}}{\delta_2 \tilde{B_1}} B_{1i}. \qquad (2.3.15)
$$

From equation (2.3.7), we have $(1-q)d_m M_i = \beta_m b_m M_s \frac{B_{1i}+B_{2i}}{N_b+A}$, and then

$$M_i = \frac{\beta_m b_m \tilde{M}(B_{1i}+B_{2i})}{(1-q)d_m(N_b+A)+\beta_m b_m(B_{1i}+B_{2i})}. \tag{2.3.16}$$

Equations (2.3.9) and (2.3.12) imply that

$$B_{1i}+B_{2i} = \left(\frac{\beta_b b_m M_i}{N_b+A}\right)\left(\frac{\tilde{B_1}}{\delta_1}+\frac{\tilde{B_2}}{\delta_2}-\frac{B_{1i}}{d_b}-\frac{B_{2i}}{d_b}\right). \tag{2.3.17}$$

Eliminating M_i from equations (2.3.16) and (2.3.17), a straight forward calculation gives that if an endemic equilibrium exists, its B_i-coordinates should satisfy the following quadratic equation:

$$c_{20}B_{1i}^2 + c_{11}B_{1i}B_{2i} + c_{02}B_{2i}^2 + c_{10}B_{1i} + c_{01}B_{2i} + c_{00} = 0, \tag{2.3.18}$$

where

$$\begin{aligned}
c_{20} &= (1-q)d_m\left(\tfrac{\mu_1}{d_b}\right)^2 - \beta_m b_m \tfrac{\mu_1}{d_b},\\
c_{11} &= 2(1-q)d_m \tfrac{\mu_1}{d_b}\tfrac{\mu_2}{d_b} - \beta_m b_m(\tfrac{\mu_1}{d_b}+\tfrac{\mu_2}{d_b}),\\
c_{02} &= (1-q)d_m\left(\tfrac{\mu_2}{d_b}\right)^2 - \beta_m b_m \tfrac{\mu_2}{d_b},\\
c_{10} &= \beta_m b_m \tilde{B} - 2(1-q)d_m\tilde{B}\tfrac{\mu_1}{d_b} + \beta_m\beta_b b_m^2 \tfrac{\tilde{M}}{d_b},\\
c_{01} &= \beta_m b_m \tilde{B} - 2(1-q)d_m\tilde{B}\tfrac{\mu_2}{d_b} + \beta_m\beta_b b_m^2 \tfrac{\tilde{M}}{d_b},\\
c_{00} &= (1-q)d_m\tilde{B}^2 - \tilde{M}\beta_m\beta_b b_m^2\left(\tfrac{\tilde{B_1}}{\delta_1}+\tfrac{\tilde{B_2}}{\delta_2}\right).
\end{aligned} \tag{2.3.19}$$

Using the expression for R_0 in (2.3.5) we can write

$$\beta_b\beta_m\frac{\tilde{M}}{\tilde{B}^2}\left(\frac{\tilde{B_1}}{\delta_1}+\frac{\tilde{B_2}}{\delta_2}\right) = d_m(R_0^2 - qR_0),$$

so we can rewrite c_{00} in (2.3.19) as

$$c_{00} = \tilde{B}^2 d_m\,(1-q+R_0)\,(1-R_0). \tag{2.3.20}$$

To obtain the positive equilibrium points, we find the intersection of the line (2.3.15) with the quadratic curve (2.3.18).

For the curve defined by (2.3.18), let $D = c_{02}c_{20} - \frac{1}{4}c_{11}^2$. One can verify that

$$D = -\frac{\beta_m^2}{4d_b^2}\left(\mu_1 - \mu_2\right)^2 < 0.$$

Therefore, the quadratic curve (2.3.18) is a hyperbola. In order to better understand the intersection of this hyperbola with line (2.3.15), we make the following rotation of B_{1i} and B_{2i} axes by letting

$$\begin{aligned} x &= \left[(1-q)d_m\tfrac{\mu_1}{d_b} - \beta_m b_m\right]B_{1i} + \left[(1-q)d_m\tfrac{\mu_2}{d_b} - \beta_m b_m\right]B_{2i}, \\ y &= \tfrac{\mu_1}{d_b}B_{1i} + \tfrac{\mu_2}{d_b}B_{2i}. \end{aligned} \tag{2.3.21}$$

The inverse of the rotation operator is given by

$$\begin{aligned} B_{1i} &= \tfrac{1}{\beta_m b_m(\mu_1-\mu_2)}\left(\mu_2 x - \left[(1-q)d_m\mu_2 - \beta_m b_m d_b\right]y\right), \\ B_{2i} &= \tfrac{1}{\beta_m b_m(\mu_1-\mu_2)}\left(-\mu_1 x + \left[(1-q)d_m\mu_1 - \beta_m b_m d_b\right]y\right), \end{aligned} \tag{2.3.22}$$

provided $\mu_1 \neq \mu_2$. By using this transformation we can conclude that,

$$N_b + A = \tilde{B} - \frac{\mu_1}{d_b}B_{1i} - \frac{\mu_2}{d_b}B_{2i} = \tilde{B} - y. \tag{2.3.23}$$

Using the new coordinates, it follows from (2.3.21) that the line (2.3.15) and the hyperbola (2.3.18) become

$$L: \quad y = \frac{x}{k}, \tag{2.3.24}$$

$$C: \quad y = \left(\tilde{B} + \beta_b b_m \frac{\tilde{M}}{d_b}\right)\frac{x - x_0}{x - x_1}, \tag{2.3.25}$$

where

$$\begin{aligned} k &= (1-q)d_m - \frac{\beta_m b_m d_b\left(\frac{\tilde{B_1}}{\delta_1}+\frac{\tilde{B_2}}{\delta_2}\right)}{\mu_1\frac{\tilde{B_1}}{\delta_1}+\mu_2\frac{\tilde{B_2}}{\delta_2}}, \\ x_0 &= \frac{c_{00}}{\tilde{B}+\beta_b b_m\frac{\tilde{M}}{d_b}}, \\ x_1 &= (1-q)d_m\left(\tilde{B}-\beta_b b_m\frac{\tilde{M}}{d_b}\right). \end{aligned} \tag{2.3.26}$$

Since $1 > \mu_1 > \mu_2 > 0$, $q \in (0,1)$, and from the Table 2.1, we have $(1-q)d_m\mu_2 - \beta_m b_m d_b > 0$, then $(1-q)d_m\mu_1 - \beta_m d_b > 0$, and then $0 < k < 1$. For the equation of a hyperbola (2.3.25) whose (mutually orthogonal) asymptotes are $x = x_1$ and $y = \tilde{B} + \beta_b b_m\frac{\tilde{M}}{d_b}$, respectively, the horizontal asymptote intersects the $y-$axis at a positive point while the intersection of the vertical asymptote with the $x-$axis depends on the sign of x_1.

To obtain the intersection between the hyperbola (2.3.25) and the line (2.3.24), we have to find the roots of the following equation:

$$x^2 - \left[x_1 + \left(\tilde{B} + \beta_b b_m\frac{\tilde{M}}{d_b}\right)k\right]x + c_{00}k = 0. \tag{2.3.27}$$

The discriminant Δ for the quadratic equation (2.3.27) satisfies,

$$\Delta = \left[((1-q)d_m + k)\tilde{B} - ((1-q)d_m - k)\beta_b b_m\frac{\tilde{M}}{d_b}\right]^2 - 4kc_{00}.$$

Depending on the sign of Δ, we can have up to two positive equilibria.

Let $E = (M_s^*,\ M_i^*,\ B_{1s}^*,\ B_{1i}^*,\ B_{1r}^*,\ B_{2s}^*, B_{2i}^*, B_{2r}^*)$ be any one of the arbitrary endemic equilibrium of the model (2.2.1), represented as

$$B_{1i}^* = \frac{\frac{d_b}{\delta_1}\tilde{B_1}x}{k\left(\mu_1\frac{\tilde{B_1}}{\delta_1}+\mu_2\frac{\tilde{B_2}}{\delta_2}\right)},\quad B_{2i}^* = \frac{\delta_1\tilde{B_2}}{\delta_2\tilde{B_1}}B_{1i}^*,\quad B_{1s}^* = \tilde{B_1} - \frac{\delta_1}{d_b}B_{1i}^*,\quad B_{2s}^* = \tilde{B_2} - \frac{\delta_2}{d_b}B_{2i}^*,$$

$$B_{1r}^* = \frac{\nu_1}{d_b}B_{1i}^*,\quad B_{2r}^* = \frac{\nu_2}{d_b}B_{2i}^*,\quad M_i^* = \frac{\beta_m b_m\tilde{M}(B_{1i}^* + B_{2i}^*)}{(1-q)d_m(\tilde{B} - \frac{\mu_1}{d_b}B_{1i}^* - \frac{\mu_2}{d_b}B_{2i}^*) + \beta_m b_m(B_{1i}^* + B_{2i}^*)}.$$

If $R_0 > 1$, then $c_{00} < 0$ and we always have only one positive root,

$$x_{E_2} = \frac{\left[x_1 + \left(\tilde{B} + \beta_b b_m \frac{\tilde{M}}{d_b}\right) k\right] + \sqrt{\Delta}}{2},$$

and we denote the corresponding equilibrium by E_2.

If $R_0 = 1$, then $c_{00} = 0$; subsequently, we have one positive root if

$$x_1 + \left(\tilde{B} + \beta_b b_m \frac{\tilde{M}}{d_b}\right) k > 0.$$

This condition can be written in another form as:

$$\frac{\beta_b b_m}{d_b} \frac{\tilde{M}}{\tilde{B}} < \left(\frac{(1-q)d_m + k}{(1-q)d_m - k}\right). \tag{2.3.28}$$

Now we consider the case $R_0 < 1$. Since $c_{00} > 0$, we always have one or two positive roots if $\Delta \geq 0$.

First if $x_1 > x_0$, then

$$\frac{(1-q)d_m}{d_b}\tilde{B} > \beta_m b_m \left(\frac{\tilde{B_1}}{\delta_1} + \frac{\tilde{B_2}}{\delta_2}\right) > (1-q)d_m \beta_b b_m \frac{\tilde{M}}{d_b^2},$$

which implies $\tilde{B} > \beta_b b_m \frac{\tilde{M}}{d_b}$. Since $c_{00} > 0$, then $x_0 > 0$ and $R_0 < 1$. Moreover, the hyperbolic curve C will intersect the x, y axes at positive points as shown in Fig.2.3(a).

So the line L has two positive intersection points with the hyperbola C as shown in Fig. 2.3(a), with one being above the line $y = \tilde{B} + \beta_b b_m \frac{\tilde{M}}{d_b}$. Let x-coordinates of L and C with $y = \tilde{B}$ be denoted by x_{10} and x_{11}, then (2.3.24) and (2.3.25) give,

$$x_{10} = k\tilde{B} = \left((1-q)d_m - \frac{\beta_m b_m d_b \left(\frac{\tilde{B_1}}{\delta_1} + \frac{\tilde{B_2}}{\delta_2}\right)}{\mu_1 \frac{\tilde{B_1}}{\delta_1} + \mu_2 \frac{\tilde{B_2}}{\delta_2}}\right)\tilde{B},$$

and

$$x_{11} = \left((1-q)d_m - \beta_m b_m \frac{\frac{d_b}{\delta_1}\tilde{B}_1 + \frac{d_b}{\delta_2}\tilde{B}_2}{\tilde{B}}) \right) \tilde{B}.$$

As shown in Fig.2.3(a), one can verify that $x_{10} < x_{11}$ which means the other intersection of L with C is also above the line $y = \tilde{B}$. Thus, from (2.3.23) that total number of birds would be negative, so this case does not occur biologically.

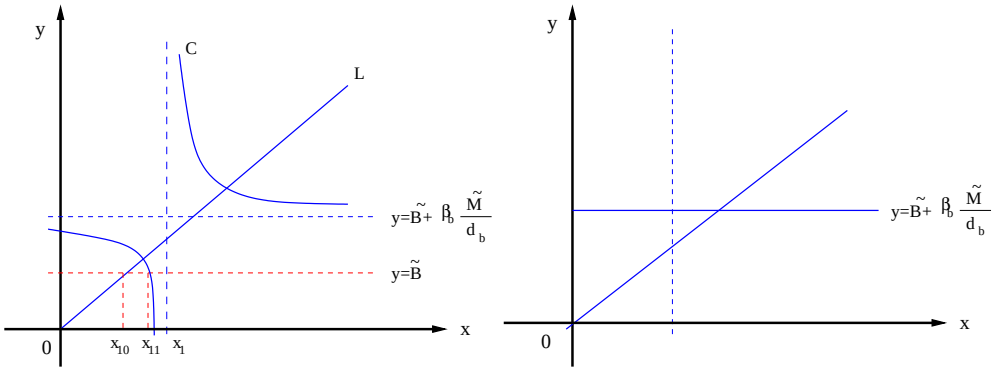

(a) $x_1 > x_0 \quad (R_0 < 1)$, no EEP. (b) $x_1 = x_0 \quad (R_0 < 1)$, no EEP.

Figure 2.3: If $x_1 \geq x_0$, the system does not have any (EEP).

If $x_1 = x_0$, then $c_{00} = (1-q)d_m \left(\tilde{B^2} - \beta_b^2 b_m^2 \frac{\tilde{M}^2}{d_b^2} \right) > 0$, which implies $R_0 < 1$. Note in this case the hyperbola C will be reduced to a line $y = \tilde{B} + \beta_b b_m \frac{\tilde{M}}{d_b}$, as shown in Fig. 2.3(b). Thus, we have one positive equilibrium point that satisfies $y = \tilde{B} + \beta_b b_m \frac{M_i}{d_b}$. Again, from (2.3.23) the total number of birds would be negative, and this case has no positive equilibrium. Hence there is no positive equilibria if $x_1 \geq x_0$. Now we consider the case $x_1 < x_0$. Here we need to consider the following five cases.

CASE 1. If $x_1 < 0$ with $x_0 < 0$, then $R_0 > 1$, and therefore $c_{00} < 0$ which leads to $\Delta > 0$. Consequently, the hyperbolic curve C intersects the x-axis with one negative component. So there is one intersecting point as shown in Fig. 2.4. From the case $x_1 > x_0$ we proved that $x_{10} < x_{11}$ which leads to the intersection between L and C at point below the line $y = \tilde{B}$. Thus, it follows from (2.3.23) that the total number of birds would be positive, so if $R_0 > 1$ there exists a unique endemic equilibrium.

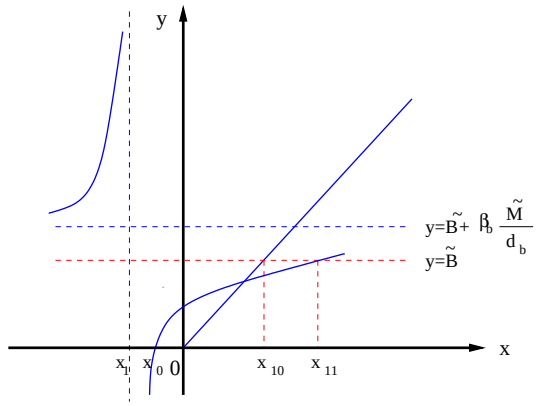

Figure 2.4: CASE 1. The system always has a unique EEP.

CASE 2. If $x_1 < 0$ with $x_0 = 0$, then $R_0 = 1$. Therefore, the hyperbolic curve C passes through the origin, and we have $\Delta = \left(x_1 + \left(\tilde{B} + \beta_b \frac{\tilde{M}}{d_b}\right) k\right)^2$. In this case and under condition (2.3.28) we have one positive intersection point, otherwise we will not have any positive intersection point. These subcases are shown in Fig. 2.5(a) and (b). Also by the same way as in CASE 1, this intersection point is below the line $y = \tilde{B}$.

CASE 3. If $x_1 < 0$ with $x_0 > 0$, then $\tilde{B} < \beta_b b_m \frac{\tilde{M}}{d_b}$ and $R_0 < 1$. Therefore, under condition (2.3.28), we can see that we do not have any positive intersection points if $\Delta < 0$ and we have

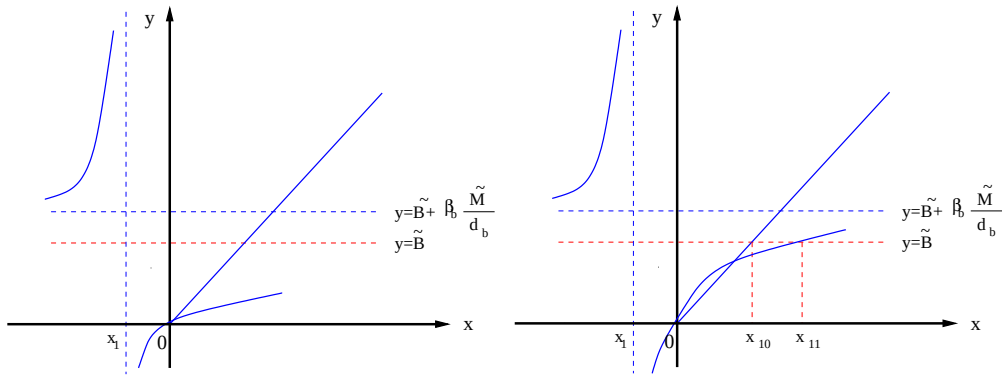

(a) No EEP. (b) One EEP.

Figure 2.5: CASE 2. The system has at most one EEP

one or two intersection points if and only if $\Delta \geq 0$. Moreover, from the definition of c_{00}, we can conclude that $c_{00} < k\tilde{B}\left(\tilde{B} + \beta_b b_m \frac{\tilde{M}}{d_b}\right)$ which means $\frac{1}{k}x_0 < \tilde{B}$ and then $x_0 < x_{10} < x_{11}$. Then any intersection between L and C occurs at a point below the line $y = \tilde{B}$. It is important to note here that if $\Delta = 0$, then we denote the basic reproduction number by $R_0 = R_0^1$. Case 3 is shown in Fig.2.6.

CASE 4. If $x_1 = 0$ then $\tilde{B} = \beta_b b_m \frac{\tilde{M}}{d_b}$ and

$$\Delta = -4k\tilde{B}\beta_m b_m \left(\tilde{B} - \left(\frac{\mu_1}{\delta_1}\tilde{B}_1 + \frac{\mu_2}{\delta_2}\tilde{B}_2\right)\right) < 0.$$

So we do not have any real intersection points.

CASE 5. If $x_1 > 0$ with $x_0 > 0$, then $R_0 < 1$ and

$$\frac{\beta_m b_m d_b}{(1-q)d_m}\left(\frac{\tilde{B}_1}{\delta_1} + \frac{\tilde{B}_2}{\delta_2}\right) < \beta_b b_m \frac{\tilde{M}}{d_b} < \tilde{B}.$$

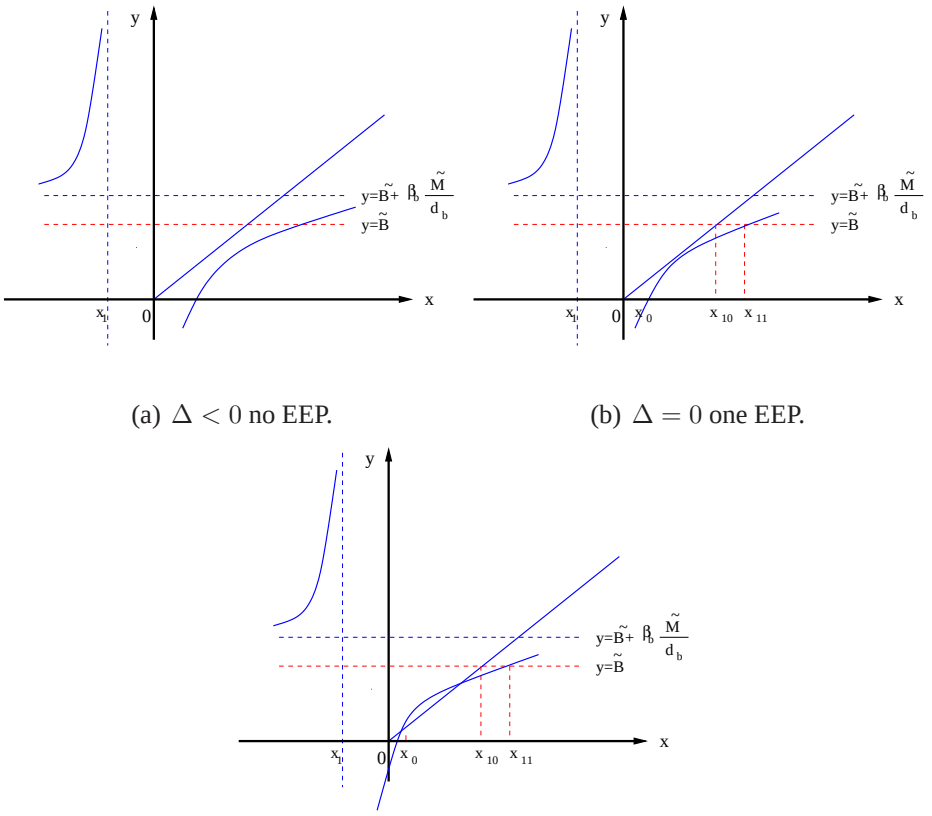

(a) $\Delta < 0$ no EEP.

(b) $\Delta = 0$ one EEP.

(c) $\Delta > 0$ two EEP.

Figure 2.6: CASE 3. The system has at most two EEPs.

By the same way in CASE 3, we can have a maximum of two positive intersection points. However, in the case that we have positive intersection points, we can conclude that $c_{00} > k\tilde{B}\left(\tilde{B} + \beta_b b_m \frac{\tilde{M}}{d_b}\right)$ which means $\frac{1}{k}x_0 > \tilde{B}$ and then $x_{11} > x_0$. This leads to the intersection between L and C at a point above the line $y = \tilde{B}$. Hence, from (2.3.23) the total number of birds is negative, and this case does not occur biologically. CASE 5 is shown in Fig.2.7.

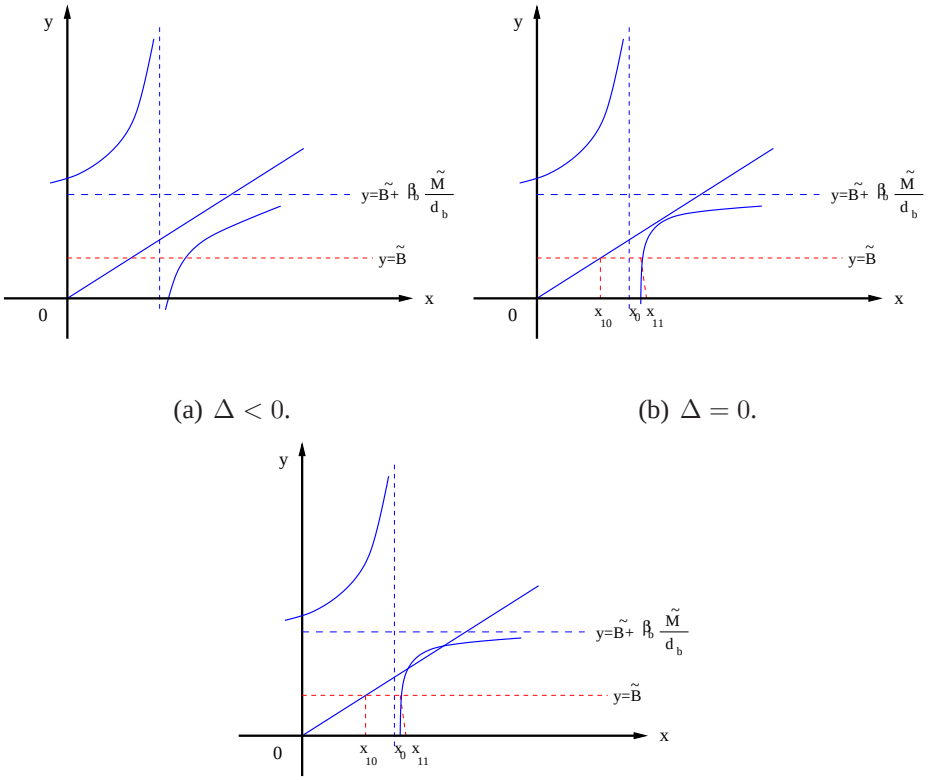

(a) $\Delta < 0$.

(b) $\Delta = 0$.

(c) $\Delta > 0$.

Figure 2.7: CASE 5. The system has no EEP.

Now, if we use x_{E_2} and x_{E_3} to define equilibrium points E_2 and E_3 we are able to state the principal results about the existence and number of the equilibrium points.

Proposition 2.3.2. *If we suppose that* $(1-q)d_m\mu_2 - \beta_m b_m d_b > 0$, *the system (2.2.1) can have up to two positive equilibrium. More precisely,*

1. *If* $R_0 > 1$, *there exists a unique endemic equilibrium* E_2.

2. *If* $R_0 < 1$, *then*

(a) *If* $\frac{d_b}{\beta_b b_m} < \frac{\tilde{M}}{\tilde{B}} < \frac{d_b}{\beta_b b_m}\left(\frac{(1-q)d_m+k}{(1-q)d_m-k}\right)$ *and* $\Delta > 0$, *there exists two endemic equilibria* E_2 *and* E_3.

(b) *If* $\frac{d_b}{\beta_b b_m} < \frac{\tilde{M}}{\tilde{B}} < \frac{d_b}{\beta_b b_m}\left(\frac{(1-q)d_m+k}{(1-q)d_m-k}\right)$ *and* $\Delta = 0$, *these two equilibria coalesce.*

(c) *Otherwise, there is no endemic equilibrium.*

3. *If* $R_0 = 1$, *then*

(a) *If* $\frac{\tilde{M}}{\tilde{B}} < \frac{d_b}{\beta_b b_m}\left(\frac{(1-q)d_m+k}{(1-q)d_m-k}\right)$, *there exists a unique endemic equilibrium* E_2.

(b) *Otherwise, there is no endemic equilibrium.*

The epidemiological implication of Proposition 2.3.2 is that when $R_0 < 1$ the virus may or may not become endemic (at any region) depending on the ratio between the quantity of mosquitoes on one hand and that of birds and other mammals on the other hand.

2.3.2 Local stability

In this section, we study the local stability of the EEP in the system (2.2.1). By using the Jacobian matrix, at any equilibrium point, the eigenvalues satisfy: the first $-(r_m - d_m)$, the second $-d_b$ that is repeated four times, as well as the eigenvalues from the matrix W with

$$W = \begin{pmatrix} -(1-q)d_m\frac{\tilde{M}}{M_s} & \frac{\left((1-q)d_m\frac{\mu_1}{d_b}-\beta_m b_m\right)M_i+\beta_m b_m\tilde{M}}{N_b+A} & \frac{\left((1-q)d_m\frac{\mu_2}{d_b}-\beta_m b_m\right)M_i+\beta_m b_m\tilde{M}}{N_b+A} \\ \beta_b b_m\frac{B_{1s}}{N_b+A} & -\left(\delta_1+\delta_1\frac{\left(\beta_b b_m\frac{M_i}{d_b}-\frac{\mu_1}{d_b}B_{1i}\right)}{N_b+A}\right) & \delta_1\frac{\frac{\mu_2}{d_b}B_{1i}}{N_b+A} \\ \beta_b b_m\frac{B_{2s}}{N_b+A} & \delta_2\frac{\frac{\mu_1}{d_b}B_{2i}}{N_b+A} & -\left(\delta_2+\delta_2\frac{\left(\beta_b b_m\frac{M_i}{d_b}-\frac{\mu_2}{d_b}B_{2i}\right)}{N_b+A}\right) \end{pmatrix}.$$

We can find the eigenvalues of W by finding the roots of the cubic equation

$$\lambda^3 + A_2\lambda^2 + A_1\lambda + A_0 = 0, \tag{2.3.29}$$

where

$$
\begin{aligned}
A_2 &= (1-q)d_m\frac{\tilde{M}}{M_s} + (\delta_1+\delta_2) + \delta_1\left(\frac{\frac{\beta_b b_m M_i}{d_b} - \frac{\mu_1}{d_b}B_{1i}}{N_b+A}\right) + \delta_2\left(\frac{\frac{\beta_b b_m M_i}{d_b} - \frac{\mu_2}{d_b}B_{2i}}{N_b+A}\right),\\
A_1 &= (1-q)d_m\frac{\tilde{M}}{M_s}(\delta_1+\delta_2) + \delta_1\delta_2\left(1+\frac{\frac{\beta_b b_m M_i}{d_b}}{N_b+A}\right)\left(1+\frac{\frac{\beta_b b_m M_i}{d_b} - \frac{\mu_1}{d_b}B_{1i} - \frac{\mu_2}{d_b}B_{2i}}{N_b+A}\right)\\
&+ (1-q)d_m\frac{\tilde{M}}{M_s}\left(\frac{\delta_1\left(\frac{\beta_b b_m M_i}{d_b} - \frac{\mu_1}{d_b}B_{1i}\right) + \delta_2\left(\frac{\beta_b b_m M_i}{d_b} - \frac{\mu_2}{d_b}B_{1i}\right)}{N_b+A}\right) - \beta_m b_m\frac{\tilde{M}}{M_i}\frac{\delta_1 B_{1i} + \delta_2 B_{2i}}{N_b+A}\\
&- \frac{\delta_1\left((1-q)d_m\frac{\mu_1}{d_b} - \beta_m b_m\right)B_{1i} + \delta_2\left((1-q)d_m\frac{\mu_2}{d_b} - \beta_m b_m\right)B_{2i}}{N_b+A},\\
A_0 &= \delta_1\delta_2(1-q)d_m\left(1+\frac{\beta_b b_m\frac{M_i}{d_b}}{N_b+A}\right)\frac{\tilde{M}}{M_s}\left(\frac{\frac{\beta_b b_m M_i}{d_b} - \frac{\mu_1}{d_b}B_{1i} - \frac{\mu_2}{d_b}B_{2i}}{N_b+A}\right)\\
&- \delta_1\delta_2\left(1+\frac{\beta_b b_m\frac{M_i}{d_b}}{N_b+A}\right)\frac{\left((1-q)d_m\frac{\mu_1}{d_b} - \beta_m b_m\right)B_{1i} + \left((1-q)d_m\frac{\mu_2}{d_b} - \beta_m b_m\right)B_{2i}}{N_b+A}.
\end{aligned}
$$

For any endemic equilibrium point $E = (M_s^*, M_i^*, B_{1s}^*, B_{1i}^*, B_{1r}^*, B_{2s}^*, B_{2i}^*, B_{2r}^*)$ of the system (2.2.1), we have the following proposition to determine the sign of the eigenvalues and the roots for the characteristic equation (2.3.29).

Proposition 2.3.3. *For the system (2.2.1), E_2 is stable while E_3 is unstable when they exist.*

Proof. For both E_2 and E_3, from equation (2.3.9) we have $\beta_b b_m\frac{M_i^*}{d_b} > \frac{\delta_1}{d_b}B_{1i}^* > \frac{\mu_1}{d_b}B_{1i}^*$. Similarly by (2.3.12) we have $\beta_b b_m\frac{M_i^*}{d_b} > \frac{\mu_2}{d_b}B_{2i}^*$. Hence, $A_2 > 0$ (in (2.3.29)) for both E_2 and E_3.

By using equations (2.3.6) and (2.3.13) we can conclude that, for any positive equilibrium with $M_s^* = \frac{\tilde{M}(1-q)d_m(\tilde{B}-y_E)}{(1-q)d_m\tilde{B}-x_E}$ and $M_i^* = \frac{\tilde{M}((1-q)d_m y_E - x_E)}{(1-q)d_m\tilde{B}-x_E}$, we can rewrite A_0 as

$$
A_0 = \frac{\delta_1\delta_2}{k(\tilde{B}-y_E)^2}\left(1+\frac{\beta_b b_m\frac{M_i^*}{d_b}}{\tilde{B}-y_E}\right)\left(2x_E^2 - x_E\left[((1-q)d_m+k)\tilde{B} - ((1-q)d_m-k)\beta_b\frac{\tilde{M}}{d_b}\right]\right).
$$

If $R_0 < 1$ and case (3)(a) of Proposition 2.3.2 holds, then we have two positive equilibrium

points denoted by (x_{E_2}, y_{E_2}) and (x_{E_3}, y_{E_3}). For E_3 from (2.3.27) we can see that

$$x_{E_3} < \frac{1}{2}\left[((1-q)d_m + k)\tilde{B} - ((1-q)d_m - k)\beta_b b_m \frac{\tilde{M}}{d_b}\right],$$

therefore $A_0 < 0$, the roots of (2.3.29) will have different signs, and E_3 is unstable. While for E_2, from (2.3.27) we have $x_{E_2} > \frac{1}{2}\left[((1-q)d_m + k)\tilde{B} - ((1-q)d_m - k)\beta_b b_m \frac{\tilde{M}}{d_b}\right]$. Hence, we conclude that $A_0 > 0$.

In the same way, if $R_0 > 1$, from Proposition 2.3.2, we have one positive equilibrium point denoted by (x_{E_2}, y_{E_2}) and from (2.3.27),

$$x_{E_2} > \frac{1}{2}\left[((1-q)d_m + k)\tilde{B} - ((1-q)d_m - k)\beta_b b_m \frac{\tilde{M}}{d_b}\right]$$

and $A_0 > 0$.

Finally, to prove that all roots of equation (2.3.29) are negative at E_2, in the two cases $R_0 < 1$ and $R_0 > 1$, we need to prove that if $A_0 > 0$ then $A_1 A_2 - A_0 > 0$.

By (2.3.7) we conclude that at E_2, $(1-q)d_m M_i^* > \beta_m b_m M_s^* \frac{B_{1i}^*}{N_b^* + A}$, so this leads to $(1-q)d_m \frac{\tilde{M}}{M_s^*} > \beta_m b_m \frac{\tilde{M}}{M_i^*} \frac{B_{1i}^*}{N_b^* + A}$, and in the same way, $(1-q)d_m \frac{\tilde{M}}{M_s^*} > \beta_m b_m \frac{\tilde{M}}{M_i^*} \frac{B_{2i}^*}{N_b^* + A}$. Therefore,

$$\delta_1\left[(1-q)d_m - \beta_m b_m \frac{B_{1i}^*}{N_b^* + A}\right] + \delta_2\left[(1-q)d_m - \beta_m b_m \frac{B_{2i}^*}{N_b^* + A}\right] > 0. \tag{2.3.30}$$

From (2.3.9) at E_2 we can conclude that $\frac{\beta_b b_m M_i^*}{d_b} > \frac{\mu_1}{d_b} B_{1i}^* + \frac{\mu_2}{d_b} B_{2i}^*$. Then we have

$$\delta_1 \delta_2 \left(1 + \frac{\frac{\beta_b b_m M_i^*}{d_b}}{N_b^* + A}\right)\left(1 + \frac{\frac{\beta_b b_m M_i^*}{d_b} - \frac{\mu_1}{d_b} B_{1i}^* - \frac{\mu_2}{d_b} B_{2i}^*}{N_b^* + A}\right) > 0. \tag{2.3.31}$$

It follows from (2.3.30) and (2.3.31) that $A_0 > 0$ implies that $A_1 > 0$ and

$$\begin{aligned} A_1A_2 &- A_0 \\ &= \left((1-q)^2 d_m^2 \frac{\tilde{M}}{M_s^*} + A_1\right)\left[(\delta_1+\delta_2) + \frac{\delta_1\left(\frac{\beta_b b_m M_i^*}{d_b} - \frac{\mu_1}{d_b}B_{1i}^*\right) + \delta_2\left(\frac{\beta_b b_m M_i^*}{d_b} - \frac{\mu_2}{d_b}B_{1i}^*\right)}{N_b^*+A}\right] \\ &+ \delta_1\delta_2\left[1 + \frac{\frac{\beta_b b_m M_i^*}{d_b}}{N_b^*+A}\right]\frac{\left((1-q)d_m\frac{\mu_1}{d_b} - \beta_m b_m\right)B_{1i}^* + \left((1-q)d_m\frac{\mu_2}{d_b} - \beta_m b_m\right)B_{2i}^*}{N_b^*+A} \\ &- (1-q)d_m\frac{\tilde{M}}{M_s^*}\left(\frac{\delta_1\left((1-q)d_m\frac{\mu_1}{d_b} - \beta_m b_m\right)B_{1i}^* + \delta_2\left((1-q)d_m\frac{\mu_2}{d_b} - \beta_m b_m\right)B_{2i}^*}{N_b^*+A}\right) \end{aligned}.$$

Thus $A_1A_2 - A_0 > 0$, and the proof is complete.

□

2.4 Backward bifurcation

To discuss the backward bifurcation, we choose $\delta_1 = \mu_1 + \nu_1 + d_b$ and $\delta_2 = \mu_2 + \nu_2 + d_b$ as the bifurcation parameters. We will express the two conditions $R_0 = 1$ and $\Delta = 0$ in terms of the parameters δ_1 and δ_2 $(\delta_1 > \delta_2)$, and then present the bifurcation diagram in (δ_1, δ_2) plane.

First, with $R_0 = 1$, equation (2.3.5) can be presented as follows,

$$\delta_1 = \alpha\tilde{B}_1 + \frac{\alpha^2\tilde{B}_1\tilde{B}_2}{\delta_2 - \alpha\tilde{B}_2} \tag{2.4.32}$$

where $\alpha = \frac{\beta_b\beta_m b_m^2\tilde{M}}{(1-q)d_m\tilde{B}^2}$.

The second curve can be obtained by letting $\Delta = 0$ in equation (2.3.27). Solving $\Delta = 0$ in terms of δ_1 one can get

$$\delta_1 = \rho\tilde{B}_1 + \frac{\rho^2\tilde{B}_1\tilde{B}_2}{\delta_2 - \rho\tilde{B}_2}, \tag{2.4.33}$$

where

$$\rho = \frac{\beta_b \beta_m b_m^2 \tilde{M}}{(1-q)d_m \tilde{B}^2 - \frac{1}{4k}\left(((1-q)d_m + k)\tilde{B} - ((1-q)d_m - k)\beta_b b_m \frac{\tilde{M}}{d_b}\right)^2}.$$

In the positive quadrant of the parameters plane (δ_1, δ_2), equation (2.4.32) is a hyperbola, whose (mutually orthogonal) asymptotes are $\delta_1 = \alpha\tilde{B}_1$ and $\delta_2 = \alpha\tilde{B}_2$. Similarly, equation (2.4.33) represents a hyperbola with (mutually orthogonal) asymptotes, $\delta_1 = \rho\tilde{B}_1$ and $\delta_2 = \rho\tilde{B}_2$. From the above we can conclude that if $((1-q)d_m + k)\tilde{B} = ((1-q)d_m - k)\beta_b b_m \frac{\tilde{M}}{d_b}$, then the two hyperbolas (2.4.32) and (2.4.33) are the same, and $x_1 + \left(\tilde{B} + \beta_b b_m \frac{\tilde{M}}{d_b}\right) k = 0$ in equation (2.3.27). Then when $\frac{\tilde{M}}{\tilde{B}} = \frac{d_b}{\beta_b b_m}\left(\frac{(1-q)d_m + k}{(1-q)d_m - k}\right)$, we do not have any positive equilibrium points if $R_0 \leq 1$, while if $R_0 > 1$, we have one positive equilibrium point, where $\rho > \alpha > 0$.

One can verify that the two hyperbolas (2.4.32) and (2.4.33) do not intersect in the positive quadrant, and a region for the existence of two endemic equilibria to occur is well defined in the shadow area as shown in Fig.2.8.

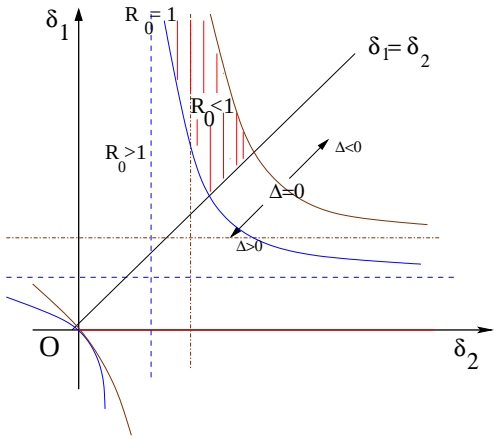

Figure 2.8: In the plane (δ_1, δ_2), we have two EEPs in the dashed area.

Then from the above and from Proposition 2.3.2, if the discriminant Δ is set to zero and solved for the critical value of R_0, which we denote by R_0^1, then we have

$$R_0^1 = \frac{q + \sqrt{q^2 + \frac{((1-q)d_m+k)^2}{kd_m}\left(\frac{4k(1-q)d_m}{((1-q)d_m+k)^2} - \left(1 - \frac{(1-q)d_m-k}{(1-q)d_m+k}\frac{\beta_b b_m}{d_b}\frac{\tilde{M}}{\tilde{B}}\right)^2\right)}}{2}. \quad (2.4.34)$$

Thus, the backward bifurcation scenario involves the existence of a subcritical transcritical bifurcation at $R_0 = 1$ and of a saddle-node bifurcation at $R_0 = R_0^1 < 1$. The qualitative bifurcation diagrams describing two types of bifurcation at $R_0 = 1$ are depicted in Fig.2.9(a) and (b).

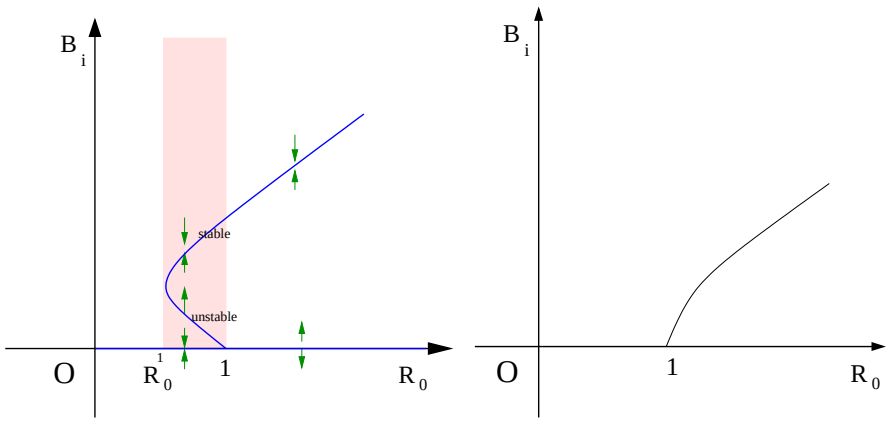

(a) Backward bifurcation. (b) Forward bifurcation.

Figure 2.9: Basic reproduction number and bifurcation diagram.

Theorem 2.4.1. *Consider model (2.2.1) with positive parameters. If*

$$A < \left(\mu_1 - (\nu_1 + d_b(1 + \frac{\beta_m b_m}{(1-q)d_m}))\right)\frac{\tilde{B}_1}{\delta_1} + \left(\mu_2 - (\nu_2 + d_b(1 + \frac{\beta_m b_m}{(1-q)d_m}))\right)\frac{\tilde{B}_2}{\delta_2}, \quad (2.4.35)$$

then system (2.2.1) undergoes a backward bifurcation when $R_0 = 1$.

Proof. The proof employs Theorem 2.4.2, which is adopted from [14] that is, in turn, based on the use of the center manifold theory [13, 33].

Theorem 2.4.2. *[14]. Consider the following general system of ordinary differential equations with a parameter*

$$\frac{dx}{dt} = f(x, \phi), \quad f : R^n \longrightarrow R, \quad and \quad f \in C^2(R \times R). \tag{2.4.36}$$

Without loss of generality, it is assumed that 0 *is an equilibrium for system (2.4.36) for all values of the parameter* ϕ*, (that is* $f(0, \phi) = 0 \quad \forall \phi$*). Assume*

1. $B = D_x f(0,0) = \left(\frac{\partial f_j}{\partial x_i}(0,0)\right)$ *is the linearized matrix of system (2.4.36) around the equilibrium* 0 *with* ϕ *evaluated at* 0*. Zero is a simple eigenvalue of* B *and all other eigenvalues of* B *have negative real parts;*

2. *Matrix* B *has a right eigenvector* w *and a left eigenvector* v *corresponding to the zero eigenvalue. Let* f_k *be the* k^{th} *component of* f *and*

$$a = \sum_{k,i,j=1}^{8} v_k w_i w_j \frac{\partial^2 f_k}{\partial x_i \partial x_j}(0,0)$$

$$b = \sum_{k,i=1}^{8} v_k w_i \frac{\partial^2 f_k}{\partial x_i \partial \phi}(0,0).$$

The local dynamics of system (2.4.36) around 0 *are totally determined by* a *and* b*.*

   (a) *In the case where* $a > 0; b > 0$*, we have that when* $\phi < 0$ *with* $|\phi|$ *close to zero,* 0 *is locally asymptotically stable and there exists a positive unstable equilibrium; when* $0 < \phi << 1$*,* 0 *is unstable and there exists a negative and locally asymptotically stable equilibrium.*

(b) *In the case where* $a < 0; b < 0$, *we have that when* $\phi < 0$ *with* $|\phi|$ *close to zero,* 0 *is unstable; when* $0 < \phi << 1$, *0 is locally asymptotically stable, and there exists a positive unstable equilibrium;*

(c) *In the case where* $a > 0; b < 0$, *we have that when* $\phi < 0$ *with* $|\phi|$ *close to zero, 0 is unstable and there exists a locally asymptotically stable negative equilibrium; when* $0 < \phi << 1$, 0 *is stable and a positive unstable equilibrium appears*

(d) *In the case where* $a < 0; b > 0$, *we have that when* ϕ *changes from negative to positive,* 0 *changes its stability from stable to unstable. Correspondingly, a negative unstable equilibrium becomes positive and locally asymptotically stable.*

To apply Theorem 2.4.2, the following simplification and change of variables are made on the system (2.2.1). First of all, let $x_1 = M_s, x_2 = M_i, x_3 = B_{1s}, x_4 = B_{1i}, x_5 = B_{1r}, x_6 = B_{2s}, x_7 = B_{2i}, x_8 = B_{2r}$. Further, by using the vector notation $X = (x_1, x_2, x_3, x_4, x_5, x_6, x_7, x_8)^T$, the system (2.2.1) can be written in the form of $\frac{dX}{dt} =$

$F(x)$, with $F = (f_1, f_2, f_3, f_4, f_5, f_6, f_7, f_8)^T$, such that

$$\begin{cases} \frac{dx_1}{dt} &= (r_m x_1 + (1-q) r_m x_2)\left(1 - \frac{x_1+x_2}{K_m}\right) - d_m x_1 - \beta_m b_m \frac{x_4+x_7}{\sum_{j=3}^{8} x_j + A} x_1, \\ \frac{dx_2}{dt} &= q r_m x_2 \left(1 - \frac{x_1+x_2}{K_m}\right) - d_m x_2 + \beta_m b_m \frac{x_4+x_7}{\sum_{j=3}^{8} x_j + A} x_1, \\ \frac{dx_3}{dt} &= \gamma_{b1} - d_b x_3 - \beta_b b_m \frac{x_3}{\sum_{j=3}^{8} x_j + A} x_2, \\ \frac{dx_4}{dt} &= -\delta_1 x_4 + \beta_b b_m \frac{x_3}{\sum_{j=3}^{8} x_j + A} x_2, \\ \frac{dx_5}{dt} &= -d_b x_5 + \nu_1 x_4, \\ \frac{dx_6}{dt} &= \gamma_{b2} - d_b x_6 - \beta_b b_m \frac{x_6}{\sum_{j=3}^{8} x_j + A} x_2, \\ \frac{dx_7}{dt} &= -\delta_2 x_7 + \beta_b b_m \frac{x_6}{\sum_{j=3}^{8} x_j + A} x_2, \\ \frac{dx_8}{dt} &= -d_b x_8 + \nu_2 x_7. \end{cases} \tag{2.4.37}$$

Assume that $(1-q) d_m \mu_2 - \beta_m b_m d_b > 0$. Choose (δ_1, δ_2) as a bifurcation parameters. As a result of solving $R_0 = 1$, backward bifurcation occurs at any point on the curve defined at equation (2.4.32).

The Jacobian matrix of the system (2.2.1) at E_1 (with (δ_1, δ_2) satisfying equation (2.4.32)) is given by

$$\begin{pmatrix}
-(r_m-d_m) & d_m(1-q)+(d_m-r_m) & 0 & -\beta_m b_m\frac{\tilde{M}}{\tilde{B}} & 0 & 0 & -\beta_m b_m\frac{\tilde{M}}{\tilde{B}} & 0\\
0 & -(1-q)d_m & 0 & \beta_m b_m\frac{\tilde{M}}{\tilde{B}} & 0 & 0 & \beta_m b_m\frac{\tilde{M}}{\tilde{B}} & 0\\
0 & -\beta_b b_m\frac{\tilde{B_1}}{\tilde{B}} & -d_b & 0 & 0 & 0 & 0 & 0\\
0 & \beta_b b_m\frac{\tilde{B_1}}{\tilde{B}} & 0 & -\delta_1 & 0 & 0 & 0 & 0\\
0 & 0 & 0 & \nu_1 & -d_b & 0 & 0 & 0\\
0 & -\beta_b b_m\frac{\tilde{B_2}}{\tilde{B}} & 0 & 0 & 0 & -d_b & 0 & 0\\
0 & \beta_b b_m\frac{\tilde{B_2}}{\tilde{B}} & 0 & 0 & 0 & 0 & -\delta_2 & 0\\
0 & 0 & 0 & 0 & 0 & 0 & \nu_2 & -d_b.
\end{pmatrix},$$

The eigenvalues of the Jacobian matrix can be obtained by the following equation:

$$\chi(\lambda) = \lambda(\lambda+d_b)^4(\lambda+(r_m-d_m))(\lambda^2+a_2\lambda+a_1),$$

where $a_2 = \delta_1+\delta_2+(1-q)d_m$ and $a_1 = \delta_2(\delta_1+(1-q)d_m)$.

Thus, the Jacobian matrix has a simple zero eigenvalue and all the other eigenvalues have negative real parts for all $r_m > d_m$. Hence, Theorem 2.4.2 can be used to analyze the dynamics of the system (2.2.1).

When $R_0 = 1$, it can be shown that the Jacobian matrix has a right eigenvector (associated to the zero eigenvalue), given by $w = (w_1, w_2, w_3, w_4, w_5, w_6, w_7, w_8)^T$, where $w_1 = -w_2, w_2 = w_2, w_3 = -\beta_b b_m\frac{\tilde{B_1}}{d_b\tilde{B}}w_2, w_4 = \beta_b b_m\frac{\tilde{B_1}}{\delta_1\tilde{B}}w_2, w_5 = \beta_b b_m\frac{\nu_1\tilde{B_1}}{\delta_1 d_b\tilde{B}}w_2, w_6 = -\beta_b b_m\frac{\tilde{B_2}}{d_b\tilde{B}}w_2, w_7 = \beta_b b_m\frac{\tilde{B_2}}{\delta_2\tilde{B}}w_2, w_8 = \beta_b b_m\frac{\nu_2\tilde{B_2}}{\delta_2 d_b\tilde{B}}w_2$.

Similarly, the components of the left eigenvector of Jacobian matrix (corresponding to the zero eigenvalue), denoted by $v = (v_1, v_2, v_3, v_4, v_5, v_6, v_7, v_8)^T$, are given by $v_1 = 0, v_2 =$

$v_2, v_3 = 0, v_4 = \beta_m b_m \frac{\tilde{M}}{\tilde{B}} v_2, v_5 = 0, v_6 = 0, v_7 = \beta_m b_m \frac{\tilde{M}}{\tilde{B}} v_2, v_8 = 0.$

Let a and b be the coefficients defined in Theorem 2.4.2. We can calculate a as follows: for the transformed system (2.4.37), the associated non-zero partial derivatives of f (evaluated at the DFE E_1) are given by

$$\begin{aligned}
&\frac{\partial^2 f_2}{\partial x_1 \partial x_2} = -\frac{q r_m}{K_m}, \quad \frac{\partial^2 f_2}{\partial x_1 \partial x_j} = \frac{\beta_m b_m}{\tilde{B}}, \ (j = 4, 7),\\
&\frac{\partial^2 f_2}{\partial x_2 \partial x_2} = -2\frac{q r_m}{K_m}, \quad \frac{\partial^2 f_2}{\partial x_i \partial x_j} = -\beta_m b_m \frac{\tilde{M}}{\tilde{B}^2}, \ (i = 3, 4, 5, 6, 7, 8; j = 4, 7),\\
&\frac{\partial^2 f_4}{\partial x_2 \partial x_j} = -\beta_b b_m \frac{\tilde{B}_1}{\tilde{B}^2}, \ (j = 4, 5, 6, 7, 8),\\
&\frac{\partial^2 f_4}{\partial x_2 \partial x_3} = \beta_b b_m \frac{\tilde{B} - \tilde{B}_1}{\tilde{B}^2}, \quad \frac{\partial^2 f_7}{\partial x_2 \partial x_j} = -\beta_b b_m \frac{\tilde{B}_2}{\tilde{B}^2}, \ (j = 3, 4, 5, 7, 8),\\
&\frac{\partial^2 f_7}{\partial x_2 \partial x_6} = \beta_b b_m \frac{\tilde{B} - \tilde{B}_2}{\tilde{B}^2}.
\end{aligned}$$

Then,

$$\begin{aligned}
a &= \sum_{k,i,j}^{8} v_k w_i w_j \frac{\partial^2 f_k}{\partial x_i \partial x_j}(0,0)\\
&= \frac{2\beta_m \beta_b^2 b_m^3}{d_b} \frac{\tilde{M}}{\tilde{B}^4} v_2 w_2^2 (\tilde{B}_1 + \tilde{B}_1) \left(\tilde{B}_1 (\frac{\nu_1 + d_b}{\delta_1} - 1) + \tilde{B}_2 (\frac{\nu_2 + d_b}{\delta_2} - 1) \right)\\
&+ \frac{2\beta_m \beta_b^2 b_m^3}{d_b} \frac{\tilde{M}}{\tilde{B}^4} v_2 w_2^2 (\tilde{B}_1 + \tilde{B}_1) \left(A + \tilde{B}_1 (1 - \frac{\mu_1}{\delta_1}) + \tilde{B}_2 (1 - \frac{\mu_2}{\delta_2}) + \frac{\beta_m b_m d_b}{(1-q) d_m} \Big(\frac{\tilde{B}_1}{\delta_1} + \frac{\tilde{B}_2}{\delta_2} \Big) \right)\\
&= \frac{2\beta_m \beta_b^2 b_m^3}{d_b} \frac{\tilde{M}(\tilde{B}_1 + \tilde{B}_2)}{\tilde{B}^4} v_2 w_2^2 (A - (\mu_1 - \nu_1 - d_b - \frac{d_b \beta_m b_m}{(1-q) d_m}) \frac{\tilde{B}_1}{\delta_1}\\
&- (\mu_2 - \nu_2 - d_b - \frac{d_b \beta_m b_m}{(1-q) d_m}) \frac{\tilde{B}_2}{\delta_2}).
\end{aligned}$$

Then, from the above equation we can conclude that a is negative if and only if A satisfies the equation (2.4.35).

From equation (2.4.32) we can see that $\delta_1 \geq \frac{\alpha \tilde{B}_1 \delta_2}{\delta_2 - \alpha \tilde{B}_2}$, if and only if $R_0 \leq 1$. Using the same notation as in [14], $\phi = \frac{\alpha \tilde{B}_1 \delta_2}{\delta_2 - \alpha \tilde{B}_2} - \delta_1$, then $\phi \geq 0$ if and only if $R_0 \geq 1$, and $\phi < 0$ if and only if $R_0 < 1$.

We can calculate b by substituting the vectors v and w and the respective partial derivatives (evaluated at the DFE E_1) into the expression

$$b = \sum_{k,i}^{8} v_k w_i \frac{\partial^2 f_k}{\partial x_i \partial \phi}(0,0),$$

which implies

$$b = \frac{2\beta_m \beta_b b_m^2}{d_b} \frac{\tilde{M}\tilde{B}_1}{\tilde{B}^2} v_2 w_2 > 0.$$

Since coefficient b is always positive, it follows that the system (2.2.1) will undergo backward bifurcation if the coefficient a is negative.

□

The parameter A measuring the effects of other animals bitten by mosquitoes to take blood meals is usually ignored in many compartment models for mosquito-borne diseases. So if we assume that all the birds as one family (corvids) and $A = 0$, then the condition for occurrence of the backward bifurcation in the Theorem 2.4.1 can be simplified as

$$\mu_1 > \nu_1 + d_b \left(1 + \frac{\beta_m b_m}{(1-q)d_m}\right) \tag{2.4.38}$$

which is consistent with the results on backward bifurcation in [41] and [90].

The epidemiological significance of the phenomenon of backward bifurcation is that if R_0 is nearly below unity, then the disease control strongly depends on the initial sizes of the various sub-populations of the models. On the other hand, reducing R_0 below the saddle-node bifurcation value R_0^1 may result in disease eradication.

2.5 Simulations and discussion

In this section, we carry out numerical simulations to illustrate the effects and role of two avian species, corvids and non-corvids, on the transmission of WNv and its dynamics. Numerical results are obtained using values for parameters given in Table 2.1 .

2.5.1 R_0 in case of corvid and non-corvid populations

Let $h \in [0,1]$ be the percentage of corvids in new recruitment of birds. If γ_b is the recruitment rate, then in the model (2.2.1) we have $\gamma_{b1} = h\gamma_b$ and $\gamma_{b2} = (1-h)\gamma_b$. If $h = 0$, then all birds are non-corvid, and if $h = 1$, all birds are corvids.

It follows from (2.3.5) that we can rewrite the basic reproduction number as $R_0 = \frac{q}{2} + \frac{1}{2}\sqrt{q^2 + 4\Re^2}$ with $\Re = \sqrt{\beta_m b_m^2 \frac{\gamma_b}{d_b} \frac{\tilde{M}}{d_m(\frac{\gamma_b}{d_b}+A)^2}\left(\frac{\beta_{b1}h}{\delta_1} + \frac{\beta_{b2}(1-h)}{\delta_2}\right)}$.

For the case of $h = 1$ and $h = 0$, if we denote

$$R_{0j} = \frac{q}{2} + \frac{1}{2}\sqrt{q^2 + 4\beta_m b_m^2 \frac{\gamma_b}{d_b} \frac{\tilde{M}}{d_m(\frac{\gamma_{bj}}{d_b}+A)^2}\left(\frac{\beta_{bj}}{\delta_j}\right)}, \quad j = 1,2, \tag{2.5.39}$$

then R_{01} and R_{02} are the basic reproduction numbers in the case that all birds are corvids ($j = 1$) and non-corvids ($j = 2$), respectively. One can verify that we have

$$(R_0 - \frac{q}{2})^2 = h(R_{01} - \frac{q}{2})^2 + (1-h)(R_{02} - \frac{q}{2})^2, \quad h \in [0,1]. \tag{2.5.40}$$

Since corvids are more competent in transmitting the virus as the primary host for the virus [47], therefore we have $\frac{\beta_{b1}}{\delta_1} > \frac{\beta_{b2}}{\delta_2}$. So from (2.5.39), we have $R_{01} > R_{02}$. One can further verify that $R_{02} < R_0 < R_{01}$.

For the reproduction number as a function of the percentage $h \in [0,1]$, it follows from (2.5.40) that we have

$$R_0 = \frac{q}{2} + \sqrt{(R_{02} - \frac{q}{2})^2 + h(R_{01} + R_{02} - q)(R_{01} - R_{02})}, \quad h \in [0,1]. \tag{2.5.41}$$

Since $R_{01} > R_{02}$, so for the case with a small vertical transmission rate q, as shown in Fig. 2.10, the basic reproduction number R_0 is an increasing function of h which defines a segment of a parabola (2.5.41) for $h \in [0,1]$.

Another important observation is that if we do not distinguish the birds as corvids and non-corvids, and take the bird population as only one species (using corvid parameters), just like what have been done in available modeling for WNv, we have $R_0 < R_{01}$, resulting in over estimation of the epidemic of the virus in the birds population. This observation suggests that it will be essential to further classify the birds into more species according to their responses, or death rates due to the infection of the virus.

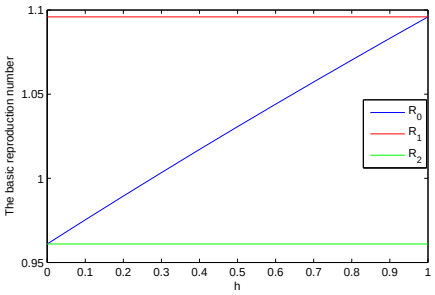

Figure 2.10: R_0 as a function of h.

As shown in Fig. 2.10, one can see that R_0 is an increasing function of $h \in [0,1]$. This means that in regions with high percentage of corvids, the virus becomes epidemic with higher basic

reproduction number. This is consistent with the observation in Peel region, Ontario, Canada in early years when the virus first arrived and caused the outbreak. It is well known that a large number of corvid birds died due to the infection and thus, leading to the decrease of their numbers. Yet in regions with a lower percentage, the epidemic either did not occur or was not as severe as regions with higher percentages of corvid birds. In later years after the virus had established in the region, when $R_0 < 1$ the outbreak of the virus may still occur (inspite of the lower number of corvid birds) due to existence of the backward bifurcation.

2.5.2 A discussion on the backward bifurcation

By Theorem 2.4.1, the backward bifurcation will occur when $R_0 = 1$ and the condition (2.4.35) is satisfied. The existence of the backward bifurcation is illustrated by simulating the model (2.2.1) with the values of the parameters from Table 2.1 and $A = \frac{\tilde{B_1}}{20}$. We keep μ_1, μ_2 as bifurcation parameters and we plot the two curves (2.4.32) and (2.4.33) in the (μ_1, μ_2) planes. As shown in Fig. 2.11, we note that the two positive equilibria exist only in a small area S between the two hyperbola curves.

By taking $(\mu_1, \mu_2) = (0.24, 0.07) \in S$, a time series of B_i is plotted in Fig.2.12 showing the DFE and two endemic equilibria. Also using (2.4.34), we can find $R_0^1 = 0.9922 < R_0 = 0.9962 < 1$. Moreover, the value of the right hand side of condition (2.4.35) can be calculated as $0.2386 \times \tilde{B_1}$; subsequently, the value of $A = \frac{\tilde{B_1}}{20}$ satisfies the condition (2.4.35). Therefore, the backward bifurcation will occur (when R_0 is nearly below unity). We can then find B_{1i} in the two endemic equilibria E_2, E_3 for all $B_{1i}^{E2} = 1779$, $B_{1i}^{E3} = 409$.

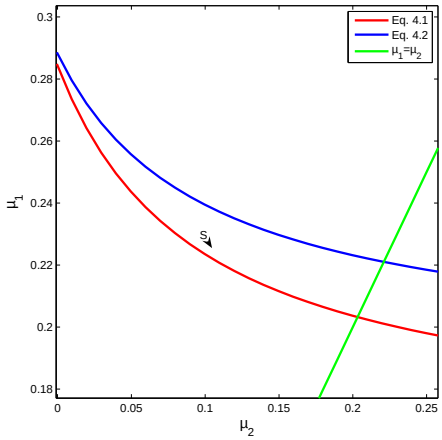

Figure 2.11: Bifurcation curves in the plane (μ_1, μ_2).

Further, Fig.2.12 shows that one of the endemic equilibria E_2 is stable, the other E_3 is unstable (saddle), and the DFE is stable. This clearly shows the co-existence of two locally-asymptotically stable equilibria when $R_0 < 1$.

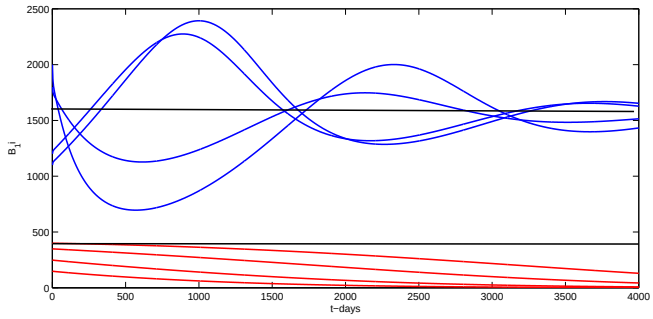

Figure 2.12: The trajectories of infected corvid birds with different initial values.

2.5.3 The impact of other mammals A

From the expression in (2.3.5) and (2.5.40), we can conclude that the basic reproduction number increases as A decreases.

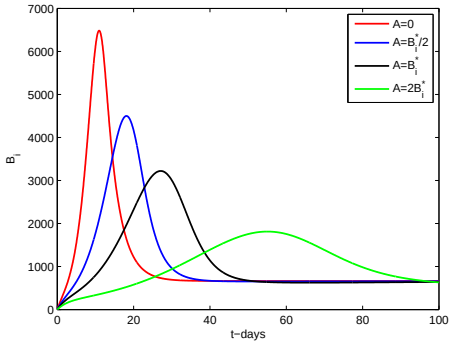

Figure 2.13: Infected bird population with different values of A.

In Fig.2.13, we simulate and present the total number of infected birds with different sizes of A. We compare the cases when $A = 0$, $\frac{B_s^*}{2}$, B_s^* and $2B_s^*$, where B_s^* is the initial number of birds and we also assume that all birds are of one family. One can see that the peak value of infected bird population increases and the peak time occurs earlier when A decreases. This is due to the fact that some of the mosquito bites are shared by other mammals which causes the decrease of the incidence of the birds.

2.5.4 The impact of bird species diversity

In Section 2.5.1, we see that the basic reproduction number is an increasing function of h (the percentage of corvids of the total birds population). By using the same parameters as in Table

2.1, in Fig.2.14 we present the total number of infected birds (B_i) for $h \in [0, 1]$.

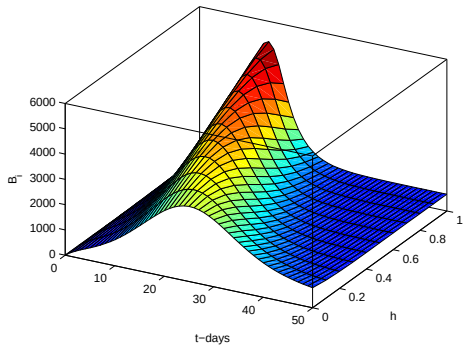

Figure 2.14: Total of all infected birds with different values of h.

Usually, registers of WNv cases in the avian population are based on the number of dead birds found. Thus, epidemiological reports indicate high WNv prevalence in avian species with high disease mortality rate. In Fig.2.15, using the parameters given in Table 2.1, we present the corvids and non-corvid birds population with initial total bird population 15000. We can observe in Fig.2.15(a) that the peak time of the infected mosquitoes appears earlier with higher percentage of corvid birds. It suggests that if we ignore the weather and environmental factors for a region with higher percentage of corvids, the peak time of the total infected mosquitoes (correspondingly the risk of WNv risk) in the region arrives earlier.

From Fig.2.15(b), we can observe that the peak time of the infected non-corvid subpopulation occurs later with the increase of its percentage that ranges between 40% and 80%. On the other hand, the peak time of the infected corvid subpopulation occurs earlier with the increase of its percentage. This observation together with the simulations in Fig. 2.15(a) suggests that for a re-

gion with more corvids, usually one would observe a large amount of dead corvids, the virus first causes the outbreak in the bird populations, and is followed with the peak of infected mosquitoes which can potentially induce the outbreak in the human population. But for a region with less corvids, it takes longer time for the epidemic of the virus to reach a peak in the birds population which would postpone the peak of infection in mosquito population. In this case if the cold wind arrives earlier in the region, it can blow away the epidemic of the virus in human population. The above observation is consistent with the endemic of the virus in regions in Southern Ontario [67]. The first year Ontario had more cases of WNv was in 2002, a total of 394 human cases reported.

Yet, if warmer weather promotes the abundance of total mosquitoes to reach a peak earlier, it can still cause outbreak in humans even if there are fewer number of corvids in the region. Recent outbreak of WNv in regions like Durham, Ontario verifies our observation. In 2012 the hot summer in Southern Ontario allows mosquitoes to breed more quickly, which allows the WNv in infected mosquitoes, and therefore in birds, to replicate faster. As in 2012, a total of 450 cases of human infection were reported [67].

2.6 Conclusions and discussion

This Chapter presents a deterministic model for the transmission dynamics of WNv, by classifying avian populations as corvids and non-corvids. A detailed analysis of the model shows the presence of the locally stable disease free equilibrium whenever the associated reproduction number is less than unity. The model undergoes backward bifurcation where the stable disease free equilibrium co-exists with a stable endemic equilibrium. The existence of the backward bifurca-

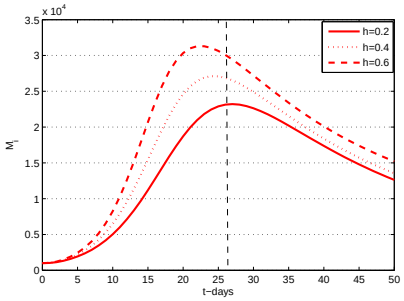

(a) Infected mosquitoes

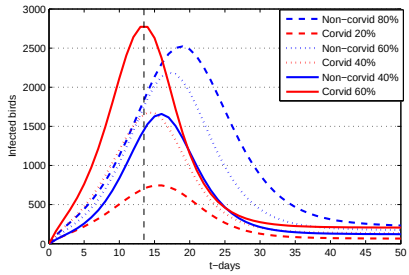

(b) Infected corvids and non-corvids.

Figure 2.15: The peak time of infected mosquitoes, and infected birds.

tion indicates that the spread of the virus when R_0 is nearly below unity could be dependent on the initial sizes of the sub-population of the model. Moreover, in this chapter we generalizes the results of backward bifurcation in previous work [41] and [90]. Furthermore, We analyzed the effects of two avian populations, corvid and non-corvid family of birds with different responses to the virus, and we found that the level of incidence (measured by the peak) and the basic reproduction number are completely different when assuming one family of bird population. We also discussed the impact of other mammals on the transition of WNv. Thus, from the above, we can conclude that if we do not classify the bird population into different species and if we do not include other mammals, any epidemic calculations will be overestimated

3 Dynamics of a West Nile virus model with seasonality

3.1 Introduction

Seasonal variations in temperature, rainfall and resource availability are ubiquitous and can exert strong pressures on density of vector mosquitoes. Three different mechanisms are responsible for seasonality: host behavior changes, climate and environmental changes, and pathogen appearance and disappearance [25]. Because WNv mosquitoes *culex* are sensitive to temperature change, WNv shows very clear seasonal variation in any given year in Southern Ontario and other regions in Canada. This variation would not necessarily be labeled as an outbreak. The incidence during any part of the year should be compared to the situation in the previous years to demonstrate a clear increase to be declared as an epidemic.

There have been some epidemiological models using a time-varying rate of some parameters. Some models use a time varying rate of contact, between susceptible and infected individuals, called the seasonally forced function [9, 27, 32]. Other examples of seasonally forced functions may be found in [43, 91]. The authors in [89] proposed statistical relationships between environmental parameters and WNv by using the mosquito surveillance data, and temperature and precipitation records. Paper [23] is the only work that tackles the seasonal effects on new out-

breaks in WNv starting from an endemic situation. It numerically concluded that the frequency of the new outbreaks depends on the relationship between the intrinsic and seasonal frequencies.

By assuming that the birth rate of mosquitoes follows a periodic pattern, in this chapter we study the impact of seasonal variations of the mosquito population on the dynamics of WNv. We also prove the existence of periodic solutions under specific conditions. Moreover, we introduce and calculate the basic reproduction number for this seasonal forced model. Furthermore, we numerically study the effect of seasonality and the dynamics of the model when the seasonal variation becomes stronger.

The current chapter is organized as follows. We formulate our model in Section 3.2. In Section 3.3, we find and study the stability of the equilibrium points of the model and then existence of the backward bifurcation. The impact of seasonal variation, including proof of existence of periodic solutions, is demonstrated in Section 3.4. The discussion are presented in Section 3.5.

3.2 Model formulation

Based on the Chapter 2, on modeling the population of mosquitoes and hosts, and to extend the modeling for the WNv in [1, 7, 52, 92] we propose to study a new model:

$$
\begin{cases}
\dfrac{dL_s}{dt} = r_m(M_s + (1-q)M_i) - (d_L + m_L)L_s, \\
\dfrac{dL_i}{dt} = qr_m M_i - (d_L + m_L)L_i, \\
\dfrac{dM_s}{dt} = m_L L_s - \beta_m b_m \dfrac{B_{1i} + B_{2i}}{N} M_s - d_m M_s, \\
\dfrac{dM_i}{dt} = m_L L_i + \beta_m b_m \dfrac{B_{1i} + B_{2i}}{N} M_s - d_m M_i,
\end{cases}
$$

$$
\begin{cases}
\dfrac{dB_{js}}{dt} = \gamma_{bj} - d_b B_{js} - \beta_b b_m \dfrac{B_{js}}{N} M_i, \\
\dfrac{dB_{ji}}{dt} = -(d_b + \nu_j + \mu_j)B_{ji} + \beta_b b_m \dfrac{B_{js}}{N} M_i, \qquad j = 1, 2 \\
\dfrac{dB_{jr}}{dt} = -d_b B_{jr} + \nu_j B_{ji},
\end{cases}
\tag{3.2.1}
$$

$$
\begin{cases}
\dfrac{dS}{dt} = \gamma_h - \beta_h b_m \dfrac{S}{N} M_i - d_h S, \\
\dfrac{dE}{dt} = \beta_h b_m \dfrac{S}{N} M_i - \alpha E - d_h E, \\
\dfrac{dI}{dt} = \alpha E - (\gamma + \mu_l + r + d_h)I, \\
\dfrac{dH}{dt} = \gamma I - (\mu_h + \tau + d_h)H, \\
\dfrac{dR}{dt} = \tau H + rI - d_h R,
\end{cases}
$$

where $j = 1, 2$, correspond to different avian populations, 1 for corvid and 2 for non-corvid. The definitions and values of the parameters used in the model (3.2.1) are summarized in Table 2.1

and Table 3.1.

Par.	Value	Meaning	Ref.
r_m	Variable	Mosquitoes per capita birth rate	[92]
d_m	$(0.02 - 0.07)$	Natural death rate of adult mosquitoes	[92]
d_L	$(0.1 - 1.5)$	Natural death rate of larva mosquitoes	[92]
β_m	$(0.018 - 0.24)$	WNv transmission probability from birds to mosquitoes	[92]
m_L	$(0.07 - 0.1)$	Mosquito maturation rate	[92]
γ_h	0.05	The recruitment rate of humans	[8]
β_h	0.01	WNv transmission probability from mosquitoes to humans	[8]
α	0.1	The rate of development of clinical symptoms of WNv	[8]
γ	0.0009	The hospitalization rate of infected humans	[8]
μ_l	0.015	The WNv-induced death rate of humans	[8]
μ_h	0.0005	The death rate of hospitalized humans	[8]
τ	0.05	The treatment-induced recovery rate	[8]
r	0.0002	The natural recovery rate	[8]
d_h	0.00008	The natural death rate for humans	[8]

Table 3.1: Parameters used in the model (3.2.1).

In the model (3.2.1) the total human population denoted by N_h, is split into the populations of susceptible S, exposed E, infectious I, hospitalized H and recovered R humans. For the bird populations we considered the same as in Chapter 2. The parameter A denotes the number of other living organisms that mosquitoes will bite (not include human population), and $N = N_b + N_h + A$ represents the total of all organisms that mosquitoes will bite. Let $h \in [0, 1]$ be the percentage of corvids in new recruitment of birds. If γ_b is the recruitment rate, then in the model (3.2.1) we have $\gamma_{b1} = h\gamma_b$ and $\gamma_{b2} = (1 - h)\gamma_b$. If $h = 0$, then all birds are non-corvid, and if $h = 1$, all birds are corvids.

As we mentioned in the Chapter 2, the female mosquitoes can transmit WNv vertically [78], and the fraction of progeny of infectious mosquitoes that is infectious is denoted by q, with $0 \leq q < 1$. Then the larval population L is split into the populations of susceptible larval L_s and infectious larval L_i. Similarly the adult population M splits into susceptible adults M_s and infectious adults M_i. Thus, $N_m = L + M = L_s + L_i + M_s + M_i$ is the total number of mosquitoes. Due to its short life, a mosquito never recovers from the infection, so we do not consider the recovered class in the mosquitoes [34].

Strong pressure on population dynamics can be exerted by seasonal variations in temperature. Field observations show that the strength and mechanisms of seasonality can alter the spread and persistence of WNv. Hatching of the Culex mosquito eggs varies during the year; being low in the winter and high in the summer [37]. Fig.3.1 shows the relation between temperature and percentage of eggs hatching from *Culex* quinquefasciatus. The figure also demonstrates the percentage of hatching eggs from *Culex* quinquefasciatus in Toronto, ON, Canada in 2011. From

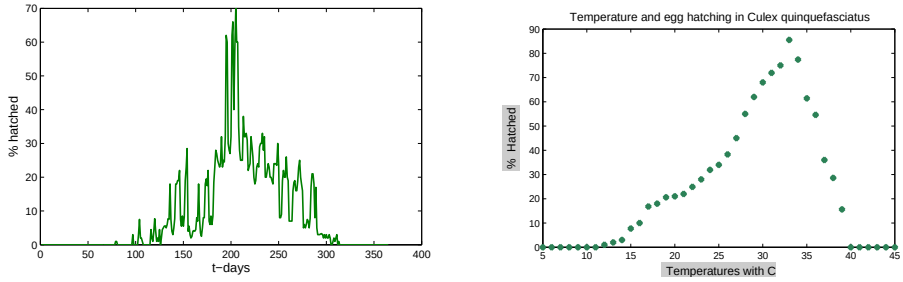

(a) Percentage egg hatching in *Culex* quinquefasciatus during the year 2011.

(b) Temperature and percentage egg hatching in *Culex* quinquefasciatus

Figure 3.1: Impact of the temperature in *Culex* quinquefasciatus in Toronto

the data in Fig.3.1, we can assume that the birth rate of mosquitoes follows a periodic pattern.

Therefore, we propose that:

$$r_m = r_1(1 - \epsilon\cos(\omega t)), \tag{3.2.2}$$

where r_1 is the mean of birth rate of mosquitoes, $0 \leq \epsilon \leq 1$ is a measure of the influence of the seasonality on the birth process and $\omega = \frac{2\Pi}{365} day^{-1}$ is the frequency.

3.3 Model without seasonality

We start by studying the model (3.2.1) without seasonality (i.e. $\epsilon = 0$). In this case each of the total subpopulations N_m, N_b and N_h is assumed to be positive for $t = 0$. Let us denote

$$\tilde{B_1} = \frac{\gamma_{b1}}{d_b}, \quad \tilde{B_2} = \frac{\gamma_{b2}}{d_b}, \quad \tilde{S} = \frac{\gamma_h}{d_h}, \quad \tilde{N} = \tilde{B_1} + \tilde{B_2} + \tilde{S} + A. \tag{3.3.3}$$

We begin analysis by making two assumptions; the first is the parameter constraint $r_m = \frac{d_m}{m_L}(m_L + d_L)$ so as to guarantee the existence of a disease-free equilibrium. The second is that the adult and larval mosquito populations satisfy: $M(0) = \tilde{M}$ and $L(0) = \tilde{L} = \frac{d_m}{m_L}\tilde{M}$. Then in a given period of time the mosquito population has constant size equal to $N_m(t) = (1 + \frac{d_m}{m_L})\tilde{M}$.

Next, we will determine the equilibrium points and assess their stability, and we will also prove the existence of backward bifurcation.

The model (3.2.1), with $\epsilon = 0$, has a disease-free equilibrium E_0, obtained by setting the right hand sides of (3.2.1) to zero, resulting in $E_0 = (\tilde{L}, 0, \tilde{M}, 0, \tilde{B}_1, 0, 0, \tilde{B}_2, 0, 0, \tilde{S}, 0, 0, 0, 0)$. The local stability of E_0 is governed by the basic reproduction number R_0. The basic reproduction number is obtained by [84]:

$$R_0 = \sqrt{q + \beta_m \beta_b b_m^2 \frac{\tilde{M}}{d_m \tilde{N}^2}\left(\frac{\tilde{B}_1}{\delta_1} + \frac{\tilde{B}_2}{\delta_2}\right)}, \tag{3.3.4}$$

where $\tilde{B}_1$, $\tilde{B}_2$, $\tilde{N}$ are defined in (3.3.3).

Theorem 2 of [84] gives the following stability result with R_0 given by (3.3.4).

Proposition 3.3.1. *For system (3.2.1), (with $\epsilon = 0$) under the assumption $r_m = \frac{d_m}{m_L}(m_L + d_L)$, the disease-free equilibrium E_0 is locally asymptotically stable if $R_0 < 1$ and unstable if $R_0 > 1$.*

An endemic equilibrium is given by the solution of the algebraic system obtained by setting the derivatives of model (3.2.1) equal to zero with $M_s = \tilde{M} - M_i$ and $L_s = \tilde{L} - L_i$.

$$
\begin{aligned}
qr_m M_i - (d_L + m_L)L_i &= 0, && (3.3.5)\\
m_L L_i + \beta_m b_m \frac{B_{1i} + B_{2i}}{N}(\tilde{M} - M_i) - d_m M_i &= 0, && (3.3.6)\\
\gamma_{bj} - d_b B_{js} - \beta_b b_m \frac{B_{js}}{N} M_i &= 0, && (3.3.7)\\
-\delta_j B_{ji} + \beta_b b_m \frac{B_{js}}{N_b + A} M_i &= 0, && (3.3.8)\\
-d_b B_{jr} + \nu_2 B_{ji} &= 0, && (3.3.9)\\
\gamma_h - \beta_h b_m \frac{S}{N} M_i - d_h S &= 0, && (3.3.10)\\
\beta_h b_m \frac{S}{N} M_i - \alpha E - d_h E &= 0, && (3.3.11)\\
\alpha E - (\gamma + \mu_l + r + d_h) I &= 0, && (3.3.12)\\
\gamma I - (\mu_h + \tau + d_h) H &= 0, && (3.3.13)\\
\tau H + rI - d_h R &= 0. && (3.3.14)
\end{aligned}
$$

First we write the susceptible and recovered birds variables in terms of B_{1i} and B_{2i}

$$B_{js} = \tilde{B_j} - \frac{\delta_j}{d_b} B_{ji}, \quad B_{jr} = \frac{\nu_j}{d_b} B_{ji}, \qquad j = 1, 2. \tag{3.3.15}$$

By combining (3.3.8) and (3.3.15) one can verify that

$$B_{2i} = \frac{\delta_1 \tilde{B_2}}{\delta_2 \tilde{B_1}} B_{1i}. \tag{3.3.16}$$

From (3.3.5) we have $qd_m M_i = m_L L_i$. As assumed above we know that at any positive equilibrium, we have $M = \tilde{M}$ and $L = \tilde{L}$. Then from equation (3.3.6), we have $(1-q)d_m M_i = \beta_m b_m (\tilde{M} - M_i)\frac{B_{1i}+B_{2i}}{N}$. As a result we get the following:

$$M_i = \frac{\beta_m b_m \tilde{M}(B_{1i} + B_{2i})}{(1-q)d_m N + \beta_m b_m (B_{1i} + B_{2i})}. \tag{3.3.17}$$

It follows from (3.3.8) that

$$B_{1i} + B_{2i} = \left(\frac{\beta_b b_m M_i}{N}\right)\left(\frac{\tilde{B_1}}{\delta_1} + \frac{\tilde{B_2}}{\delta_2} - \frac{B_{1i}}{d_b} - \frac{B_{2i}}{d_b}\right). \tag{3.3.18}$$

Eliminating M_i from equation (3.3.17) and (3.3.18), a straight forward calculation yields that if an endemic equilibrium exists, its B_{1i} and B_{2i} coordinates should satisfy the following quadratic equation:

$$c_{20}B_{1i}^2 + c_{11}B_{1i}B_{2i} + c_{02}B_{2i}^2 + c_{10}B_{1i} + c_{01}B_{2i} + c_{00} = 0, \tag{3.3.19}$$

where

$$\begin{aligned}
c_{20} &= (1-q)d_m\left(\tfrac{\mu_1}{d_b}\right)^2 - \beta_m b_m \tfrac{\mu_1}{d_b},\\
c_{11} &= 2(1-q)d_m\tfrac{\mu_1}{d_b}\tfrac{\mu_2}{d_b} - \beta_m b_m(\tfrac{\mu_1}{d_b} + \tfrac{\mu_2}{d_b}),\\
c_{02} &= (1-q)d_m\left(\tfrac{\mu_2}{d_b}\right)^2 - \beta_m b_m \tfrac{\mu_2}{d_b},\\
c_{10} &= \beta_m b_m\tilde{N} - 2(1-q)d_m\tilde{N}\tfrac{\mu_1}{d_b} + \beta_m\beta_b b_m^2\tfrac{\tilde{M}}{d_b},\\
c_{01} &= \beta_m b_m\tilde{N} - 2(1-q)d_m\tilde{N}\tfrac{\mu_2}{d_b} + \beta_m\beta_b b_m^2\tfrac{\tilde{M}}{d_b},\\
c_{00} &= (1-q)d_m\tilde{N}^2 - \tilde{M}\beta_m\beta_b b_m^2\left(\tfrac{\tilde{B_1}}{\delta_1} + \tfrac{\tilde{B_2}}{\delta_2}\right).
\end{aligned} \tag{3.3.20}$$

Using the expression for R_0 in (3.3.4) we can write $\beta_b\beta_m b_m^2\frac{\tilde{M}}{\tilde{N}^2}\left(\frac{\tilde{B_1}}{\delta_1} + \frac{\tilde{B_2}}{\delta_2}\right) = d_m(R_0^2 - q)$, so we can rewrite c_{00} in (3.3.20) as

$$c_{00} = \tilde{N}^2 d_m\left(1 - R_0^2\right). \tag{3.3.21}$$

To obtain the positive equilibrium points, we have to find the intersection of the line (3.3.16) with the quadratic curve (3.3.19). This is similar to the results illustrated in chapter 2.

Theorem 3.3.2. *If we set*

$$\Delta = (\beta_m b_m \frac{k_1}{k_2})^2 \left(\tilde{N} - \beta_b b_m \frac{\tilde{M}}{d_b}\right)^2 - 4\beta_m b_m \frac{k_1}{k_2}((1-q)d_m - \beta_m b_m \frac{k_1}{k_2})\beta_b b_m \frac{\tilde{M}}{d_b}(\tilde{N} - k_2),$$

with $k_1 = \frac{d_b \tilde{B_1}}{\delta_1} + \frac{d_b \tilde{B_2}}{\delta_2}$ *and* $k_2 = \frac{\mu_1 \tilde{B_1}}{\delta_1} + \frac{\mu_2 \tilde{B_2}}{\delta_2}$, *then under assumption* $(1-q)d_m > \beta_m b_m \frac{k_1}{k_2}$ *the system (3.2.1) (with* $\epsilon = 0$*) can have up to two positive equilibrium. More precisely,*

1. *If* $R_0 > 1$, *there exists a unique positive stable equilibrium* $E_2 = (L_s^*, L_i^*, M_s^*, M_i^*, B_{1s}^*, B_{1i}^*, B_{1r}^*, B_{2s}^*, B_{2i}^*, B_{2r}^*, S^*, E^*, I^*, H^*, R^*)$. *Moreover,*

$$B_{1i}^* = \frac{\frac{d_b \tilde{B_1}}{\delta_1}\left(2(1-q)d_m - \left(\frac{\beta_m b_m k_1}{k_2}\right)\left(\beta_b b_m \frac{\tilde{M}}{d_b} + \tilde{N}\right) + \sqrt{\Delta}\right)}{2\left((1-q)d_m k_2 - \beta_m b_m k_1\right)},$$

$$B_{2i}^* = \frac{\delta_1 \tilde{B_2}}{\delta_2 \tilde{B_1}} B_{1i}^*, \quad B_{1s}^* = \tilde{B_1} - \frac{\delta_1}{d_b} B_{1i}^*, \quad B_{2s}^* = \tilde{B_2} - \frac{\delta_2}{d_b} B_{2i}^*, \quad B_{1r}^* = \frac{\nu_1}{d_b} B_{1i}^*, \quad B_{2r}^* = \frac{\nu_2}{d_b} B_{2i}^*,$$

$$M_i^* = \frac{\beta_m b_m \tilde{M}(B_{1i}^* + B_{2i}^*)}{(1-q)d_m(\tilde{N} - \frac{\mu_1}{d_b} B_{1i}^* - \frac{\mu_2}{d_b} B_{2i}^*) + \beta_m b_m (B_{1i}^* + B_{2i}^*)}, \quad M_s^* = \tilde{M} - M_i^*$$

$$L_i^* = \frac{q d_m}{m_L} M_i^*, \quad L_s^* = \tilde{L} - L_i^*, \quad S^* = \tilde{S} \frac{B_{1s}^*}{B_{1s}^* + B_{1i}^* \frac{\delta_1 \beta_h}{d_h \beta_b}}, \quad E^* = \frac{d_h}{d_h + \alpha}(\tilde{S} - S^*),$$

$$I^* = \frac{\alpha}{\gamma + r + d_h} E^*, \quad H^* = \frac{\gamma}{\tau + d_h} I^*, \quad R^* = \frac{1}{d_h}(\tau H^* + r I^*).$$

2. *If* $R_0 < 1$, *then*

   (a) *If* $\frac{d_b}{\beta_b b_m} < \frac{\tilde{M}}{\tilde{N}} < \left(\frac{((1-q)d_m k_2 - \beta_m b_m k_1)}{\beta_m b_m k_1}\right)\frac{d_b}{\beta_b b_m}$, *and* $\Delta > 0$, *we have two positive equilibrium points,* $E_1 = (L_s^{**}, L_i^{**}, M_s^{**}, M_i^{**}, B_{1s}^{**}, B_{1i}^{**}, B_{1r}^{**}, B_{2s}^{**}, B_{2i}^{**}, B_{2r}^{**}, S^{**}, E^{**}, I^{**}, H^{**}, R^{**})$ *unstable point and* $E_2 = (L_s^*, L_i^*, M_s^*, M_i^*, B_{1s}^*, B_{1i}^*, B_{1r}^*, B_{2s}^*, B_{2i}^*, B_{2r}^*, S^*, E^*, I^*, H^*, R^*)$ *stable point. Moreover,*

$$B_{1i}^{**} = \frac{\frac{d_b \tilde{B_1}}{\delta_1}\left(2(1-q)d_m - \left(\frac{\beta_m b_m k_1}{k_2}\right)\left(\beta_b b_m \frac{\tilde{M}}{d_b} + \tilde{N}\right) - \sqrt{\Delta}\right)}{2\left((1-q)d_m k_2 - \beta_m b_m k_1\right)}.$$

By just replacing "" with "**", we can obtain the other values of the coordinates of E_1 by the same relations between the coordinates in E_2.*

These two equilibria coalesce if and only if $\Delta = 0$.

(b) Otherwise there is no positive equilibrium.

3. *If $R_0 = 1$, then*

(a) If $\frac{\tilde{M}}{\tilde{N}} < \left(\frac{((1-q)d_m k_2 - \beta_m b_m k_1)}{\beta_m b_m k_1}\right) \frac{d_b}{\beta_b b_m}$, there exists a unique endemic equilibrium E_2.

(b) Otherwise, there is no endemic equilibrium.

In general from the parameter assumptions, the system (3.2.1) (with $\epsilon = 0$) has infinitely many degenerate stationary points satisfying $L(t) = \frac{d_m}{m_L} M(t)$. From 2(a) in the Theorem 3.3.2 suggests the possibility of backward bifurcation at any given initial larval and adult mosquito population $(\frac{d_m}{m_L}\tilde{M}, \tilde{M})$ (where the locally-asymptotically stable DFE co-exists with a locally-asymptotically stable endemic equilibrium) when near to $R_0 = 1$. To check this, let $\Delta = 0$ and solve for the critical value of R_0, denoted by R_1:

$$R_1 = \sqrt{1 - \frac{((2(1-q)dm - \beta_m b_m \frac{k_1}{k_2}) - \beta_m b_m \frac{k_1}{k_2} \beta_b b_m \frac{\tilde{M}}{d_b \tilde{N}})^2}{4 d_m ((1-q)d_m - \beta_m b_m \frac{k_1}{k_2})}}. \tag{3.3.22}$$

Thus, the backward bifurcation scenario involves the existence of a subcritical transcritical bifurcation at $R_0 = 1$ and of a saddle-node bifurcation at $R_0 = R_1$. It should be mentioned that the proofs of stability and existence of the backward bifurcation are similar to the proofs in Chapter 2.

Similar to Theorem 2.4.1 in chapter 2 we can summarize and prove the next theorem. Note that the proof of the next theorem is based on the center manifold theory similar to the proof in

Theorem 3.3.3. *Consider model (3.2.1) with positive parameters. If*

$$A+\tilde{S}<\left(\mu_1-(\nu_1+d_b(1+\frac{\beta_m}{(1-q)d_m}))\right)\frac{\tilde{B}_1}{\delta_1}+\left(\mu_2-(\nu_2+d_b(1+\frac{\beta_m}{(1-q)d_m}))\right)\frac{\tilde{B}_2}{\delta_2},$$

then system (3.2.1) undergoes a backward bifurcation when $R_0=1$.

From Theorem 3.3.3 we can conclude that the backward bifurcation occurs at $R_0=1$. If we assume that all the birds as one family (Corvids) then the condition of the for occurrence of the backward bifurcation in Theorem 3.3.3 can be simplified as

$$\mu_1>\frac{\tilde{N}}{\tilde{B}-(\tilde{S}+A)}\left(\nu_1+d_b\left(1+\frac{\beta_m\tilde{B}}{(1-q)d_m\tilde{N}}\right)\right), \tag{3.3.23}$$

and is similar to one of the conditions in [8]; it is also considered a generalization of the same form in chapter 2 and in [90]. With reference to equation (3.3.23) we notice that the existence of another important condition that is required for occurrence the backward bifurcation and that is the ratio between total number of birds and the other mammals that can be infected by mosquitoes is greater than unity. When forward bifurcation occurs, the condition $R_0<1$ is a necessary and sufficient condition for disease eradication, whereas it is no longer sufficient when a backward bifurcation occurs.

The backward bifurcation is illustrated by simulating system (3.2.1) (with $\epsilon=0$) with the parameters of Table 2.1 and Table 3.1.

Fig.3.2 shows convergence to both the disease free equilibrium and the endemic equilibrium for system (3.2.1) when $\beta_b=0.3$, $\beta_m=0.05$ and $(\mu_1,\mu_2)=(0.27,0.07)$, (in this case $R_0=$

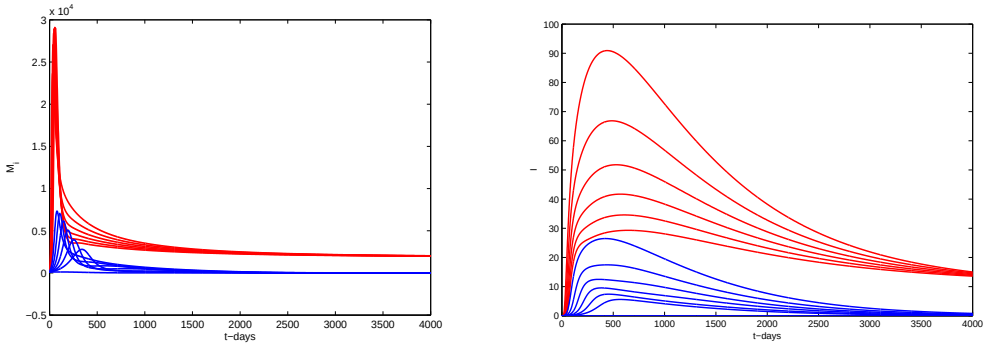

(a) Infected mosquitoes.

(b) Infected humans.

Figure 3.2: Time series of model (3.2.1) when $R_0 = 0.9908 > R_1 = 0.9846$.

$0.9908 > R_1 = 0.9846$). The profiles can converge to either the disease free equilibrium or an endemic equilibrium point for the trajectories of system (3.2.1), depending on the initial sizes of the population of the model.

The epidemiological significance of these is that the usual requirement of $R_0 < 1$ is, although necessary, no longer sufficient for disease elimination. In other words, for $R_0 < 1,$ a stable disease-free equilibrium coexists with two endemic equilibria: a smaller equilibrium (i.e., with a smaller number of infective individuals) which is unstable and a larger one (i.e., with a larger number of infective individuals) which is stable. In such a scenario, disease elimination would depend on the initial sizes of the sub-populations (state variables) of the model.

That is, the presence of backward bifurcation in model (3.2.1) (with $\epsilon = 0$) suggests that the feasibility of controlling WNv when R_0 is nearly below unity, may depend on the initial sizes of the sub-populations. On the other hand, reducing R_0 below the saddle-node bifurcation value $R_1,$

may result in disease eradication. It follows from (3.3.23) that one can see, in order for backward bifurcation to occur the virus induced death rate must be high enough and the total number of initial bird population should be greater than the sum of total number of initial other mammals.

3.4 The impact of seasonal variations

In this section, we consider the model with seasonal variations ($\epsilon \neq 0$) to study the impact of seasonal changes on the transmission of the virus. We prove the existence of periodic solutions, in the seasonal model, under specific conditions. We also introduce and calculate the basic reproduction number for this seasonal forced model. Furthermore, we examine the dynamics of the model when the seasonal variation becomes stronger.

3.4.1 Existence of periodic solutions

By replacing r_m given in (3.2.2) into system (3.2.1), we can conclude that the total number of larval and adult mosquitoes satisfy the following equations:

$$\begin{cases} \dfrac{dL}{dt} = (r_1(1 - \epsilon\cos(\omega t))M - (d_L + m_L)L, \\ \dfrac{dM}{dt} = -d_m M + m_L L. \end{cases} \tag{3.4.24}$$

Using the trajectories of (3.4.24) the equation for total number of adult mosquitoes M can be written as

$$\frac{d^2M}{dt^2} + d\frac{dM}{dt} - (\delta - \kappa\cos(\omega t))\, M = 0, \tag{3.4.25}$$

for all $d = d_m + d_L + m_L$, $\delta = (m_L r_1 - d_m(d_L + m_L))$ and $\kappa = m_L r_1 \epsilon$, where $d^2 + 4\delta > 4\kappa$ with $0 \leq \epsilon \leq 1$. From equation (3.4.25) we can conclude that the parametric resonance appears. Parametric resonance comes from changes in the parameters of the system as opposed to the classical resonance which originates from external forcing. The fundamental property of parametric resonance is that resonance peaks are expected at integer fractions of the natural period, once a control parameter has exceeded a certain threshold, with each parametric resonance peak having its own threshold value.

In general, the solutions of equation (3.4.25) are not periodic. However, for a given δ, periodic solutions exist for special values of κ. The most general method to analyze equation (3.4.25) is the classical Floquet method, which is based on the calculation of the monodromy matrix and an analysis of its eigenvalues. However, this method requires a large number of numerical integrations, which restricts its possibilities, especially if the coefficients of the equations depend on some parameters. Noted that the stability analysis of differential equations with periodic coefficients is rather cumbersome, but it can be successfully made with computer software such as the Maple program.

According to the general theory of linear differential equations with periodic coefficients, the behavior of solutions of (3.4.25) is determined by its characteristic multipliers ρ, which are the eigenvalues of the monodromy matrix $X(T)$ for (3.4.25), where $X(t)$ is the principal fundamental matrix which is defined

$$X(t) = \begin{pmatrix} M_1(t) & M_2(t) \\ \frac{dM_1}{dt} & \frac{dM_2}{dt} \end{pmatrix},$$

with $M_1(t)$ and $M_2(t)$ are two linearly independent solutions of (3.4.25) satisfying the initial conditions $M_1(0) = 1, M_2(0) = 0$, $\frac{dM_1}{dt}(0) = 0$ and $\frac{dM_2}{dt}(0) = 1$.

The characteristic equation $det(X(T) - \rho I_2) = 0$ can be rewritten as

$$\rho^2 - 2D\rho + B = 0,$$

where $D = \frac{1}{2}(M_1(T) + \frac{dM_2}{dt}(T))$ and $B = M_1(T) \times \frac{dM_2}{dt}(T) - M_2(T) \times \frac{dM_1}{dt}(T)$. Thus, the characteristic roots $\rho_{1,2}$ are functions of two parameters D and B which are given by the formula

$$\rho_{1,2} = D \pm \sqrt{D^2 - B}. \tag{3.4.26}$$

The parameter B can be found without solving equation (3.4.25). Indeed, since the functions $M_1(t)$ and $M_2(t)$ satisfy (3.4.25), we can write

$$\frac{d^2M_j}{dt^2} + d\frac{dM_j}{dt} - (\delta - \kappa\cos(\omega t))\, M_j = 0, \qquad (j = 1, 2).$$

By solving these two equations together, we can conclude that the function $y(t) = M_1(t) \times \frac{dM_2}{dt}(t) - M_2(t) \times \frac{dM_1}{dt}(t)$ satisfies the following differential equation:

$$\frac{dy}{dt} = -dy(t).$$

Thus, the parameter B is given by the formula

$$B = e^{-dT}, \tag{3.4.27}$$

and then $0 < B < 1$. Hence, the system (3.4.25) is asymptotically stable for $|D| < \frac{1}{2}(B + 1)$, stable for $|D| = \frac{1}{2}(B+1)$, and unstable for $|D| > \frac{1}{2}(B+1)$. Next we use the Poincare-Lyapunov theorem to calculate D.

The general solution of (3.4.25) can be represented as a power series

$$M(t) = \sum_{j=0}^{n} N_j(t)\kappa^j, \tag{3.4.28}$$

where $N_j(t)$ are continuous functions, and sufficiently small κ.

In order to obtain differential equations determining the functions $N_j(t)$, we substitute expansion (3.4.28) into (3.4.25). Next, by equating the coefficients of $\kappa^j, j = 0, 1, ..$ on both sides of the equation, we obtain the following system of differential equations.

$$\frac{d^2N_0}{dt^2} + d\frac{dN_0}{dt} - \delta N_0 = 0,$$

and

$$\frac{d^2N_j}{dt^2} + d\frac{dN_j}{dt} - \delta N_j = -\cos(\omega t)N_{j-1}(t), \quad j = 1, 2, ...$$

Accordingly, we have two linearly independent solutions of $N_0(t)$, satisfying the initial condition of the fundamental matrix,

$$N_0(t) = e^{\frac{-d}{2}t}(\cosh(w_0 t) + \frac{d}{2w_0}\sinh(w_0 t)),$$

$$N_0(t) = \frac{1}{w_0}e^{\frac{-d}{2}t}\sinh(w_0 t),$$

where $w_0 = \sqrt{\frac{d^2}{4} + \delta}$. Then the initial conditions for the functions $N_j, j = 1, 2, ...$ can be written as $N_j(0) = \frac{dN_j}{dt}(0) = 0$. Using these initial conditions we can obtain the following expression for the functions $N_j(t), j = 1, 2, ...$ as

$$N_j(t) = \frac{1}{2w_0}\left(\int_0^t \cos(\omega s)N_{j-1}(s)e^{(\frac{d}{2}+w_0)(s-t)}ds - \int_0^t \cos(\omega s)N_{j-1}(s)e^{(\frac{d}{2}-w_0)(s-t)}ds\right). \tag{3.4.29}$$

It should be noted that the solution $N_0(t)$ is increases unboundedly as $t \to \infty$ (unstable) when $\delta > 0$ (i.e $r_1 > \frac{d_m(d_L+m_L)}{m_L}$), decreases to 0 as $t \to \infty$ (asymptotically stable) when $\delta < 0$

(i.e $r_1 < \frac{d_m(d_L+m_L)}{m_L}$), and stable when $\delta = 0$ (i.e $r_1 = \frac{d_m(d_L+m_L)}{m_L}$). This is achieved with previous results when $\epsilon = 0$ ($\kappa = 0$).

Using the recurrence relation (3.4.29), we can successively calculate the coefficients N_j in expansion (3.4.28). However, as j grows, the calculations become more and more cumbersome. Therefore, this method can be reasonably realized with computer software. With accuracy of κ^2, we have found the parameter D as a power series in ϵ :

$$\begin{aligned} D &= \frac{2d}{w_0} e^{\frac{-d}{2}T}(\sinh(w_0T) + \epsilon m_L\omega^2 + \epsilon^2((4w_0^2 - \omega^2)((w_0^2 - d^2)\sinh(w_0T) \\ &+ 2d\omega\cosh(w_0T)) + (w_0^2 - d^2(3w_0^2 - d^4))\sinh(w_0T) + 2w_0 d\cosh(w_0T))). \end{aligned} \tag{3.4.30}$$

From the above, we are able to state the principal results about the existence of the periodic solutions.

Theorem 3.4.1. *Let* $\Re = \frac{r_1}{\frac{d_m(d_L+m_L)}{m_L} - m_L\omega^2\epsilon + ((m_L+\omega-d_m)^2 + d_m\frac{\omega}{2})\epsilon^2}$, *and* (L, M) *be the solution of system (3.4.24) through* $(L(0), M(0)) \in R_+^2$. *Then the following statements are valid:*

1. *If* $\Re < 1$, *then* $lim_{t\to\infty}(L(t), M(t)) = (0, 0)$,

2. *If* $\Re > 1$, *then* $lim_{t\to\infty}(L(t), M(t)) = (\infty, \infty)$,

3. *The periodic solutions exists only if* $\Re = 1$.

Proof. By studying the dynamics of equation (3.4.25), we can conclude that the domain of stability of equation (3.4.25) is inside the triangle bounded by the lines $B = 1$ and $B = -1 \pm 2D$ in the $D - B$ plane. The points that lie on the boundary of the triangle determine the stable behavior of its solutions, while the domain outside the triangle is the domain of instability. Thus,

from (3.4.30) and (3.4.27) we can conclude that $D > 0$ and $0 < B < 1$. Furthermore, the line $B = -1 + 2D$ is periodical condition in the (D, B) plane. The periodic condition can be written in the form of the relation between (r_1, ϵ) as shown below

$$r_1 = \frac{d_m(d_L + m_L)}{m_L} - m_L\omega^2\epsilon + ((m_L + \omega - d_m)^2 + d_m\frac{\omega}{2})\epsilon^2. \tag{3.4.31}$$

□

Biologically, we can indicate from the previous result that the mosquito population will die out if $\Re < 1$, while it grows exponentially if $\Re > 1$. Whereas, it oscillate to the positive equilibrium if $\Re = 1$.

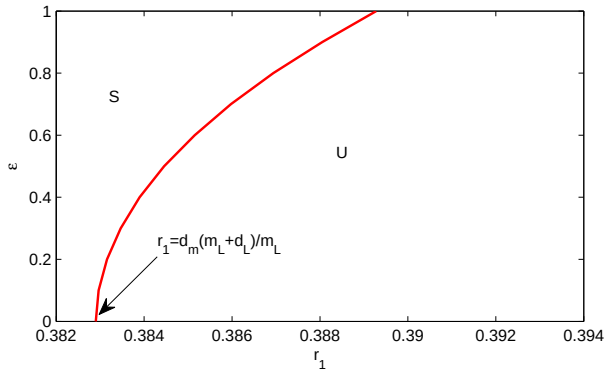

Figure 3.3: The stability domain of (3.4.25).

Fig.3.3, shows that the (r_1, ϵ) parameter plane (with the parameters values $d_m = 0.03, m_L = 0.068,$ and $d_L = 0.8$,) is divided into two regions. The first one is asymptotically stable (the amplitude M goes to zero at long times) where $\Re < 1$. The second region is unstable (the amplitude M grows exponentially without bound) where $\Re > 1$. Between these two zones there

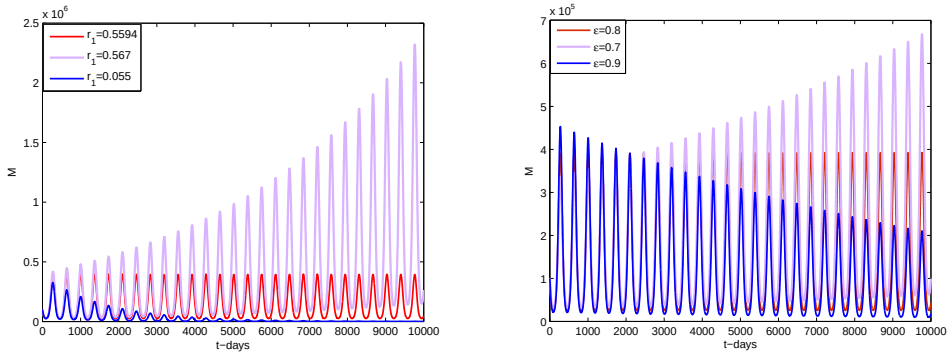

(a) $d_L = 1.2, m_L = 0.068, d_m = 0.03$ and $\epsilon = 0.8$. (b) $d_L = 0.8, m_L = 0.068, d_m = 0.03$ and $r_1 = 0.387$.

Figure 3.4: Long-term behavior of the total number of adult mosquitoes.

are bounded periodic solutions when $\Re = 1$.

Fig.3.4 explains these scenarios with different values of ϵ and r_1. Fig.3.4(a) introduces the total number of adult mosquitoes when $\epsilon = 0.8$ and r_1 has three different values. One of the latter satisfies the equation (3.4.31); where we have a periodic solution. The second value of r_1 is less than the first value; where we obtain asymptotically stable solution. Finally, we have unbounded unstable solution if r_1 is greater than the first value. Similarly, the same thing occurs in Fig.3.4(b) but with fixed $r_1 = 0.387$ and three different values of ϵ.

3.4.2 Reproduction number

In what follows, we introduce the basic reproduction number for the model with seasonality according to the theory developed in [88], which is a generalization of the work in [84] to the

periodic case. It is easy to see that the system (3.2.1) (when r_m satisfy (3.2.2) and $\Re = 1$) has one disease-free equilibrium $E_0^p = (\tilde{L}(t), 0, \tilde{M}(t), 0, \tilde{B_1}, 0, 0, \tilde{B_2}, 0, 0, \tilde{S}, 0, 0, 0, 0)$, where $\tilde{M}(t)$ is the positive periodic solution of (3.4.25). Linearizing the system at the disease-free periodic state E_0^p to obtain

$$F(t) = \begin{pmatrix} 0 & qr_m(t) & 0 & 0 & 0 & 0 & 0 & 0 & 0 & 0 \\ m_L & 0 & \frac{\beta_m b_m \tilde{M}(t)}{\tilde{N}} & 0 & \frac{\beta_m b_m \tilde{M}(t)}{\tilde{N}} & 0 & 0 & 0 & 0 & 0 \\ 0 & \frac{\beta_b b_m \tilde{B_1}}{\tilde{N}} & 0 & 0 & 0 & 0 & 0 & 0 & 0 & 0 \\ 0 & 0 & \nu_1 & 0 & 0 & 0 & 0 & 0 & 0 & 0 \\ 0 & \frac{\beta_b b_m \tilde{B_2}}{\tilde{N}} & 0 & 0 & 0 & 0 & 0 & 0 & 0 & 0 \\ 0 & 0 & 0 & 0 & \nu_2 & 0 & 0 & 0 & 0 & 0 \\ 0 & \frac{\beta_h b_m \tilde{S}}{\tilde{N}} & 0 & 0 & 0 & 0 & 0 & 0 & 0 & 0 \\ 0 & 0 & 0 & 0 & 0 & 0 & \alpha & 0 & 0 & 0 \\ 0 & 0 & 0 & 0 & 0 & 0 & 0 & \gamma & 0 & 0 \\ 0 & 0 & 0 & 0 & 0 & 0 & 0 & r & \tau & 0 \end{pmatrix},$$

and

$$V = \begin{pmatrix} d_L + m_L & 0 & 0 & 0 & 0 & 0 & 0 & 0 & 0 & 0 \\ 0 & d_m & 0 & 0 & 0 & 0 & 0 & 0 & 0 & 0 \\ 0 & 0 & \delta_1 & 0 & 0 & 0 & 0 & 0 & 0 & 0 \\ 0 & 0 & 0 & d_b & 0 & 0 & 0 & 0 & 0 & 0 \\ 0 & 0 & 0 & 0 & \delta_2 & 0 & 0 & 0 & 0 & 0 \\ 0 & 0 & 0 & 0 & 0 & d_b & 0 & 0 & 0 & 0 \\ 0 & 0 & 0 & 0 & 0 & 0 & (\alpha + d_h) & 0 & 0 & 0 \\ 0 & 0 & 0 & 0 & 0 & 0 & 0 & (\gamma + \mu_l + r + d_h) & 0 & 0 \\ 0 & 0 & 0 & 0 & 0 & 0 & 0 & 0 & (\mu_h + \tau + d_h) & 0 \\ 0 & 0 & 0 & 0 & 0 & 0 & 0 & 0 & 0 & d_h \end{pmatrix}.$$

Then we can write

$$\frac{dz}{dt} = (F(t) - V)z(t),$$

where $z(t) = (L_i(t), M_i(t), B_{1i}(t), B_{1r}(t), B_{2i}(t), B_{2r}(t), E(t), I(t), H(t), R(t))^T$. Assume $Y(t, s), t \geq s$, is the evolution operator of the linear periodic system $\frac{dy}{dt} = -Vy(t)$. That is, for each $s \in R$, the 10×10 matrix $Y(t, s)$ satisfies

$$\frac{dY(t, s)}{dt} = -VY(t, s) \quad \forall t \geq s, \quad Y(s, s) = I,$$

where I is the 10×10 identity matrix.

Let C_T be the Banach space of all T-periodic functions from R to R^{10} equipped with the maximum norm. Suppose $\Phi(s) \in C_T$ is the initial distribution of infectious individuals in this

periodic environment; then $F(s)\Phi(s)$ is the rate of new infections produced by the infected individuals who were introduced at time s, and represents the distribution of those infected individuals who were newly infected at time s and remain in the infected compartments at time t for $t \geq s$. Thus,

$$\Psi(t) = \int_{-\infty}^{t} Y(t,s)F(s)\Phi(s)ds = \int_{0}^{\infty} Y(t,t-a)F(t-a)\Phi(t-a)da,$$

is the distribution of accumulative new infections at time t produced by all those infected individuals $\Phi(s)$ introduced at the previous time. We define the linear operator $L : C_T \longrightarrow C_T$ by

$$(L\Phi)(t) = \int_{0}^{\infty} Y(t,t-a)F(t-a)\Phi(t-a)da \quad \forall t \in R, \quad \Phi \in C_T.$$

Following [88], we call L the next infection operator, and define the basic reproduction number as $R_0^p = \rho(L)$, the spectral radius of L. It should be pointed out that in the special case of $r_m(t) = r_1 = \frac{d_m}{m_L}(m_L + d_L)$ ($\epsilon = 0$) we obtain $F(t) = F$ for all t. By Lemma 2.2(ii) in [88] (see also [84]), we further obtain the basic reproduction number defined as in (3.3.4). In the periodic case, we let $W(t,\lambda)$ be the monodromy matrix of the linear T-periodic system:

$$\frac{du}{dt} = (-V + \frac{1}{\lambda}F(t))u,$$

with parameter $\lambda \in (0,\infty)$. It is easy to verify that our model with seasonality satisfies assumptions (A1)-(A7) in [88]. Thus, from Theorem 2.1 and 2.2 in [88], we have the following results, which will be used in our numerical computation of R_0^p

- If $\rho(W(T,\lambda))$ has a positive solution λ_0 (is an eigenvalue of the operator L), then $R_0^p > 1$.

- If $R_0^p > 1$, then $\lambda = R_0^p$ is the unique solution of $\rho(W(T, \lambda)) = 1$.
- $R_0^p = 1$ if and only if $\rho(\Phi_{F-V}(T)) = 1$.
- $R_0^p < 1$ if and only if $\rho(\Phi_{F-V}(T)) < 1$.
- $R_0^p > 1$ if and only if $\rho(\Phi_{F-V}(T)) > 1$.

Thus, the disease-free equilibrium E_0^p is locally asymptotically stable if $R_0^p < 1$, and unstable if $R_0^p > 1$.

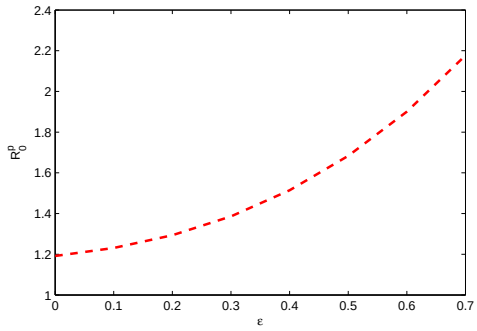

Figure 3.5: The graph of R_0^p versus with respect to ϵ.

By numerical computation, we get the curve of the basic reproduction number R_0^p (when $\Re = 1$) with respect to ϵ. In Fig.3.5, we can see that the basic reproduction number R_0^p increases with the increase of ϵ.

3.4.3 Simulations of the seasonal impact

Depending on the values of ϵ, and without changing the values of the other parameters, the basic reproduction number could remain above 1 or it could drop below 1. To see what could happen,

we plotted in Fig.3.6; choosing the value of the parameters when $\epsilon = 0, 0.1$ and 0.3.

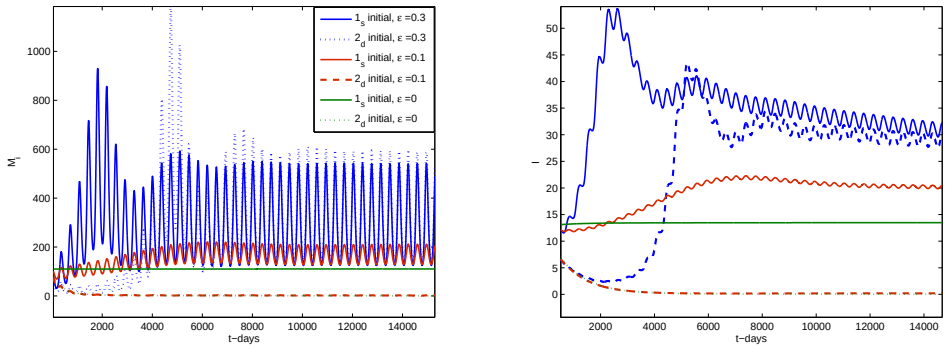

(a) Infected mosquitoes. (b) Infected humans.

Figure 3.6: Time series of model (3.2.1).

Fig.3.6 shows three different cases. The first one, while ignoring the impact of seasonality (i.e $\epsilon = 0$), we see the solutions are convergent to both the disease free equilibrium and the endemic equilibrium, depending on the initial sizes of the population. In the second case when $\epsilon = 0.1$, we note that the solutions oscillate with small amplitude to both the disease free equilibrium and the endemic equilibrium, depending on the initial sizes of the population. While in the third state when $\epsilon = 0.3$, the solutions oscillate to only the endemic equilibrium point at any initial size of the population. Thus, we can conclude that the dynamic behavior of the backward bifurcation state changes when the influence of the seasonal variation becomes stronger. Moreover, Fig.3.6 shows that when $\epsilon = 0$, the infected populations are almost constant to endemic point (as it is expected because the equilibrium is stable), while when ϵ increases, the peaks and valleys time series appear.

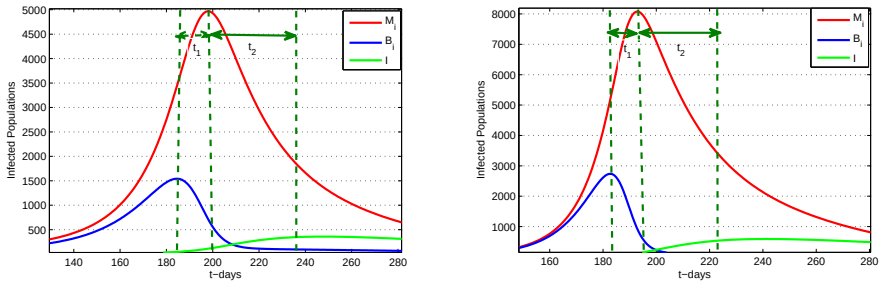

(a) $\epsilon = 0.25$. (b) $\epsilon = 0.5$.

Figure 3.7: Time series and peak time of model (3.2.1).

Furthermore, the amplitude of infected populations increases as ϵ increases. This is reflected in Fig.3.7 which shows one season with two different values of ϵ : 0.25 and 0.5. We note that when the seasonal variation has high force, it increases the infected cases. Also the highest peak number of infected populations when $\epsilon = 0.25$ comes later than when $\epsilon = 0.5$. This means that the time of applying the control could depend on the seasonal impact. Finally, from Fig.3.7(a), and (b) we can see that (t_1, t_2) (t_1 and t_2 are the difference in time between highest peaks of infected mosquitoes, and highest peaks of infected birds and humans, respectively) decreases from $(18, 35)$ when $\epsilon = 0.25$ to $(11, 27)$ when $\epsilon = 0.5$ days.

We deduce from numerical analysis that the strength of seasonality increases the number of infections. This agrees with the studies carried out that show that factors which influence mosquito dynamics such as mean values of temperature and rainfall are strong positive predictors of increased annual WNv incidence.

3.5 Conclusions and discussion

This chapter presented a comprehensive and continuous deterministic model for the transmission dynamics of WNv with and without seasonality. We started by analyzing the model without seasonality and verified the existence of backward bifurcation where the stable disease free equilibrium co-exists with a stable endemic equilibrium. The existence of the backward bifurcation indicated that the spread of the virus when R_0 is nearly below unity could depend on the initial sizes of the sub-population of the model. After that, we considered the model with seasonal variations - by assuming that the birth rate of mosquitoes follows a periodic pattern - to study the impact of seasonal variations of the mosquito population on the dynamics of WNv. In this latter model, we proved the existence of periodic solutions under specific condition using the classical Floquet method, which is based on the calculation of the monodromy matrix and an analysis of its eigenvalues. Moreover, we introduced and calculated the basic reproduction number for this seasonal forced model. Furthermore, we deduced from numerical analysis that the strength of seasonality increases the number of infections.

4 Optimal control of West Nile virus

4.1 Introduction

Control efforts are carried out to limit the spread of the disease, and in some cases, to prevent the emergence of drug resistance. Optimal control theory may be used to theoretically solve a minimization problem of the disease models. In the 1950 L.S. Pontryagin and his co-workers developed a formula of the maximum principle for optimal control of ordinary differential equations [68].

Consider the following general system of ordinary differential equations (ODE) with a parameter

$$\frac{dx}{dt} = g(t, x(t), u(t)), \quad x(t_0) = x_0, \tag{4.1.1}$$

where $x(t)$ is state variable, is the solution of the state differential equation (4.1.1), g is a continuously differentiable function and u is the control function. It is assumed that an objective functional with an integrand $f(t, x(t), u(t))$ and the state equation are both influenced by the control function $u(t)$. The objective function may be written as:

$$\min \int_{t_0}^{t_1} f(t, x(t), u(t))dt \tag{4.1.2}$$

with u is a Lebesgue measurable control functions on $[t_0, t_1]$.

For this simple optimal control problem, with f and g continuously differentiable in x and u, Pontryagins Maximum Principle [51] can be stated as:

Theorem 4.1.1. *If $u^*(t)$ and $x^*(t)$ are optimal for (4.1.2), then there exists a piecewise differentiable adjoint variable $\lambda(t)$ such that $H(t, x^*(t), u(t), \lambda(t)) \geq H(t, x^*(t), u^*(t), \lambda(t))$, where the Hamiltonian H is*

$$H(t, x(t), u(t), \lambda(t)) = f(t, x(t), u(t)) - \lambda(t) g(t, x(t), u(t)),$$

and adjoint equations

$$\frac{d\lambda(t)}{dt} = -\frac{\partial H(t, x^*(t), u^*(t), \lambda(t))}{\partial x}, \quad \lambda(t_1) = 0.$$

Solving the state and adjoint ODEs together with the optimal control representation requires an iterative scheme. This involves use of an algorithm such as Runge-Kutta of order four. In the Runge-Kutta method of order four, the interval $[t_0, t_1]$ is partitioned into N subdivisions of equal length, $N > 1$. First, we may solve the state equation (4.1.1), according to the following difference equation:

$$w_{j+1} = w_j + \frac{1}{6}(k_1 + 2k_2 + 2k_3 + k_4)$$

such that $w_0 = x(0)$, $k_1 = hg(t_i, w_i, u_i)$, $k_2 = hg(t_i + \frac{h}{2}, w_i + \frac{k_1}{2}, \frac{1}{2}(u_i + u_{i+1}))$, $k_3 = hg(t_i + \frac{h}{2}, w_i + \frac{k_2}{2}, \frac{1}{2}(u_i + u_{i+1}))$, $k_4 = hg(t_{i+1}, w_i + k_3, u_{i+1})$, for each $i = 1, 2, ..., N-1$, where $N >> 1$ and $h = \frac{t_{i+1} - t_i}{N}$ and t_i is the grid point [51].

One may use the same step technique to approximate $\lambda(t)$. However, since its value at the

final time is known instead of at the initial time, we set $w_N = 0$, with the difference equation:

$$w_{N-i-1} = w_{N-i} - \frac{1}{6}(k_1 + 2k_2 + 2k_3 + k_4)$$

such that $w_N = 0, k_1 = hG(t_{N-i}, w_{N-i}, u_{N-i}, x_{N-i}), k_2 = hG(t_{N-i} - \frac{h}{2}, w_{N-i} - \frac{k_1}{2}, \frac{1}{2}(u_{N-i} + u_{N-i-1}), \frac{1}{2}(x_{N-i} + x_{N-i-1})), k_3 = hG(t_{N-i} - \frac{h}{2}, w_{N-i} - \frac{k_2}{2}, \frac{1}{2}(u_{N-i} + u_{N-i-1}), \frac{1}{2}(x_{N-i} + x_{N-i-1})), k_4 = hG(t_{N-i-1}, w_{N-i} - k_3, u_{N-i-1}, x_{N-i-1})$, where $i = 1, 2, ..., N-1$, and $G = -\frac{\partial H}{\partial t}$.

Starting with an initial condition for the state variable and an initial guess for the control, forward sweep with the Runge-Kutta scheme may be used to obtain an approximate solution for the state equation. Using this estimate, the solution of the adjoint equation is approximated using backward sweep from the final time condition. The control is updated by using an average of its previous values and its values from the control characterization. Iterations continue until successive values of all variables from current and previous iterations are sufficiently close.

Optimal control theory can be applied to models of many infectious diseases. The authors in [7] used a time dependent model to study the effects of prevention and treatment on malaria. Similarly, the authors in [62] used a time dependent model to study the impact of a possible vaccination with treatment strategies in controlling the spread of malaria in a model that includes treatment and vaccination with waning immunity. Optimal control theory has been applied to models with vector-borne diseases [7, 20, 59, 71]. Time dependent control strategies have been applied for the studies of HIV/AIDS, Tuberculosis, Influenza and SARS [3, 15, 42, 95].

In this chapter we use the optimal control theory to study the strategies of control and minimizing the spread of WNv. The controls represent the level at which pesticide is applied to the

mosquito population and the prevention efforts to minimize human-mosquito contacts.

4.2 Existence of optimal control

The goal of this part is to show that it is possible to implement anti-WNv control techniques while minimizing the cost of implementation of such measures. So we formulate an optimal control problem for the transmission dynamics of WNv by extending the model (3.2.1) in two cases. One model without impact of seasonality and the other one is the modified mathematical model with the effect of seasonal variation (by assuming that the birth rate of mosquitoes satisfies the equation (3.2.2)).

In both cases, for the optimal control problem of the system (3.2.1), we consider the control variable in the set $\Gamma = \left\{(u_1, u_2, u_3) : [0, T] \longrightarrow R^3, s.t. 0 \leq u_j \leq U_j, j = 1, 2, 3\right\}$, where all control variables are bounded and Lebesgue measurable and $U_j, j = 1, 2, 3$ denote the upper bounds of the control variables.

In our controls $u_1(t)$ (representing the level of larvicide which means killing mosquito larva) and $u_2(t)$ (representing the level of adulticide which means killing adult mosquitoes) are used for mosquito control administered at mosquito breeding sites. Consequently, the reproduction rate of the mosquito population is reduced by the two factors $(1 - u_1(t))$ and $(1 - u_2(t))$. Furthermore, additional mortality rates of larval and adult mosquitoes (susceptible and infected) due to control represented by $d_0 u_1(t)$ and $d_0 u_2(t)$, where $d_0 > 0$ is a rate constant. In the human population, the associated force of infection is reduced by the factor $(1 - u_3(t))$ where $u_3(t)$ measures the level of successful prevention (personal protection) efforts.

We seek to minimize the human exposed and infected populations and minimize the total mosquito population. So we suppose that the costs of the control strategies are nonlinear and take quadratic form [7]. Thus, the objective (cost) functional is given by

$$J = \int_0^T (a_1 E(t) + a_2 I(t) + a_3 N_m(t) + c_1 u_1 L(t) + c_2 u_2 M(t) + c_3 u_3 S(t) + \frac{1}{2}\sum_{j=1}^{3} b_j u_j^2) dt, \quad (4.2.3)$$

subject to

$$\begin{cases}
\frac{dL_s}{dt} = r_m(M_s + (1-q)M_i)(1-u_2) - (d_L + m_L(1-u_1))L_s - d_0 u_1 L_s, \\
\frac{dL_i}{dt} = q r_m M_i (1-u_2) - (d_L + m_L(1-u_1))L_i - d_0 u_1 L_i, \\
\frac{dM_s}{dt} = m_L(1-u_1)L_s - \beta_m b_m \frac{B_{1i} + B_{2i}}{N} M_s - d_m M_s - d_0 u_2 M_s, \\
\frac{dM_i}{dt} = m_L(1-u_1)L_i + \beta_m b_m \frac{B_{1i} + B_{2i}}{N} M_s - d_m M_i - d_0 u_2 M_i,
\end{cases}$$

$$\begin{cases}
\frac{dB_{js}}{dt} = \gamma_{bj} - d_b B_{js} - \beta_b b_m \frac{B_{js}}{N} M_i, \\
\frac{dB_{ji}}{dt} = -(d_b + \nu_j + \mu_j) B_{ji} + \beta_b b_m \frac{B_{js}}{N} M_i, \qquad j = 1, 2 \\
\frac{dB_{jr}}{dt} = -d_b B_{jr} + \nu_j B_{ji},
\end{cases} \quad (4.2.4)$$

$$\begin{cases}
\frac{dS}{dt} = \gamma_h - \beta_h b_m \frac{S(1-u_3)}{N} M_i - d_h S, \\
\frac{dE}{dt} = \beta_h b_m \frac{S(1-u_3)}{N} M_i - \alpha E - d_h E, \\
\frac{dI}{dt} = \alpha E - (\gamma + \mu_l + r + d_h) I, \\
\frac{dH}{dt} = \gamma I - (\mu_h + \tau + d_h) H, \\
\frac{dR}{dt} = \tau H + r I - d_h R.
\end{cases}$$

Here, a_i, $i = 1, 2, 3$ are positive constants that represent, respectively, the weight constants of the exposed, infected human and the total mosquito populations. Similarly, b_i, $i = 1, 2, 3$ are also positive constants that represent, the weight constants for the quadratic cost of mosquito control (adult and larval) and personal protection (prevention of mosquito-human contacts), respectively. Also c_i, $i = 1, 2, 3$ are positive constants. The linear part of the cost of each type of control is proportional to the affected population, $c_1u_1L(t)+c_2u_2M(t)+c_3u_3S(t)$. For technical purposes, it is assumed that the cost of larvicide, adulticide and personal protection are given in quadratic form in the cost function (4.2.3). Using the control variables u_1, u_2 and u_3, our main goal here is to minimize the exposed and infected human populations, the total number of mosquitoes and the cost of implementing the control. So the terms $b_1u_1^2$, $b_2u_2^2$ and $b_3u_3^2$ describe the costs associated with mosquito control and prevention of mosquito-human contacts, respectively. Our purpose is to find an optimal control values (u_1^*, u_2^*, u_3^*) such that

$$J(u_1^*, u_2^*, u_3^*) = \min \{J(u_1, u_2, u_3) : (u_1, u_2, u_3) \in \Gamma\}.$$

The existence of optimal control can be proved by using the results in the paper of [31]. It is clear that system of equations given by (4.2.4) is bounded above by linear system. The boundedness of solution of system (4.2.4) for finite interval is used to prove the existence of an optimal control. Moreover, since the state system and the adjoint system (see the Appendix) are bounded and satisfy Lipschitz condition, the uniqueness of the optimal control can obtained by using the results in the paper of [51].

In order to find an optimal solution, first we should find the Hamiltonian of the optimal control problem (4.2.4) by defining the Hamiltonian $\hbar$ as follows:

Let $Q = (L_s, L_i, M_s, M_i, B_{1s}, B_{1i}, B_{1r}, B_{2s}, B_{2i}, B_{2r}, S, E, I, H, R)$, $u = (u_1, u_2, u_3)$ and $\lambda = (\lambda_i), i = 1, .., 15$ to obtain:

$$\hbar = a_1 E(t) + a_2 I(t) + a_3 N_m(t) + c_1 u_1 L(t) + c_2 u_2 M(t) + c_3 u_3 S(t) + \frac{1}{2}\sum_{j=1}^{3} b_j u_j + \sum_{j=1}^{15} \lambda_j f_j,$$

where f_j is the right side of the differential equation of the j-th state variable of (4.2.4). Based on that, we can demonstrate the next theory.

Theorem 4.2.1. *Consider the objective functional J. The unique optimal control $u^* = (u_1^*, u_2^*, u_3^*) \in \Gamma$ exists such that $J(u_1^*, u_2^*, u_3^*) = min_{(u_j, u_2, u_3)\in\Gamma} J$, subject to the control system (4.2.4).*

Proof. In this minimizing problem, the necessary convexity of the objective functional in u_1, u_2 and u_3 is satisfied. The set of controls Γ is also convex and closed by definition. The solutions of the state system and the adjoint system are bounded and satisfy Lipschitz condition, which together with the structure of the system gives the compactness needed for the existence and the uniqueness of the optimal control. In addition, the integrand of the objective functional is given by (4.2.3) on the control set Γ, which completes the existence of an optimal control [31]. □

The adjoint differential equations and final time conditions and the characterizations of optimal controls can be found using Pontryagin's Maximum Principle [68], and the details are in the Appendix.

Next, we discuss the numerical solutions of the optimality system for the model (4.2.4), the corresponding optimal control functions, the parameter choices, and the interpretations from various cases.

4.3 Numerical results of the control without the seasonality

In this part we start with an iterative method to obtain results of an optimal control problem for model (4.2.4) without the effect of the seasonal variation. We use Runge-Kutta fourth order procedure here to solve the optimality system consisting of 30 ordinary differential equations having 15 state equations as well as 15 adjoint equations and boundary conditions. With an initial guess we start for the control variables (u_1^*, u_2^*, u_3^*) and use Runge-Kutta fourth order forward in time for the state variables $L_s, L_i, M_s, M_i, B_{1s}, B_{1i},\ B_{1r}, B_{2s}, B_{2i}, B_{2r},\ S, E, I, H, R$. Then using the results from the state equations in the adjoint equations, we apply backward Runge-Kutta fourth order scheme due to transversality conditions. Then the control is updated and we iterate to find new state and adjoint variables [51].

The parameters values used in the simulations are tabulated in Table 2.1 and Table 3.1. In choosing upper bounds for the controls, since the control would not be 100% effective, so we chose the upper bound of u_1, u_2 to be 0.8 and u_3 to be 0.5 [8]. Since reducing the number of exposed and infected humans is important in our goal compared with reducing the total number of mosquitoes, then the weights in the objective functional are taken as $a_1 = 1, a_2 = 1, a_3 = 10^{-4}$ [8]. The cost associated with u_1 and u_2 mainly includes ways of eradicating the mosquito breeding (larvicide) and a little labor to spray it (adulticide), while u_3 essentially involves the cost of missing work during the infectious time, educating the public and health professionals. This means the cost of lowering the infectivity is higher than the cost of reducing the mosquito population, so we chose $b_3 = 10 > b_2 = b_1 = 1$. Since we assume that the total number of larval and adult population is constant, and the change in the human population is small then we

suppose that $c_j = 0, j = 1, 2, 3$.

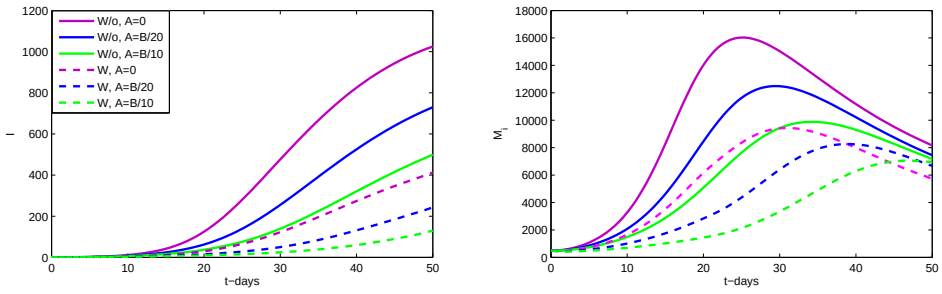

(a) Infected humans. (b) Infected Adult mosquitoes.

Figure 4.1: Time series of model (4.2.4) showing impact of A.

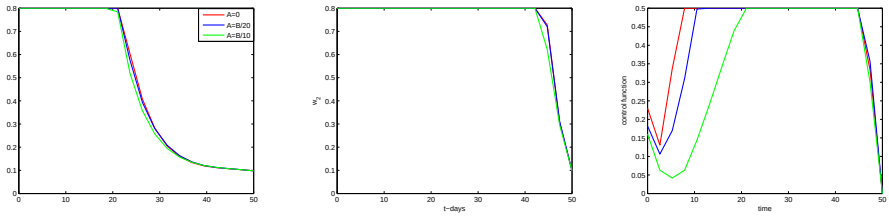

(a) u_1. (b) u_2. (c) u_3.

Figure 4.2: Control functions with different values of A.

The importance of the parameter A (representing the number of other living organisms that mosquitoes will bite) on the control is considered. Fig.4.1 illustrates the optimal trajectories of the infectious adult mosquitoes and infectious humans for three different values of A while keeping the other parameters unchanged. Fig.4.2 shows the three optimal control functions at those values of A. These optimal control functions are designed in such a way that they minimize

the cost functional J. We can see that when $A = 0, \frac{\tilde{B}}{20}$ and $\frac{\tilde{B}}{10}$, u_1 decreases a little and u_3 decreases more while u_2 does not change. Moreover, the objective functional value is reduced; $J = 8290, 7620$ and 6750 respectively. Thus, we can conclude that, if we do not include other mammals, any control impact and objective functional value will be over estimated.

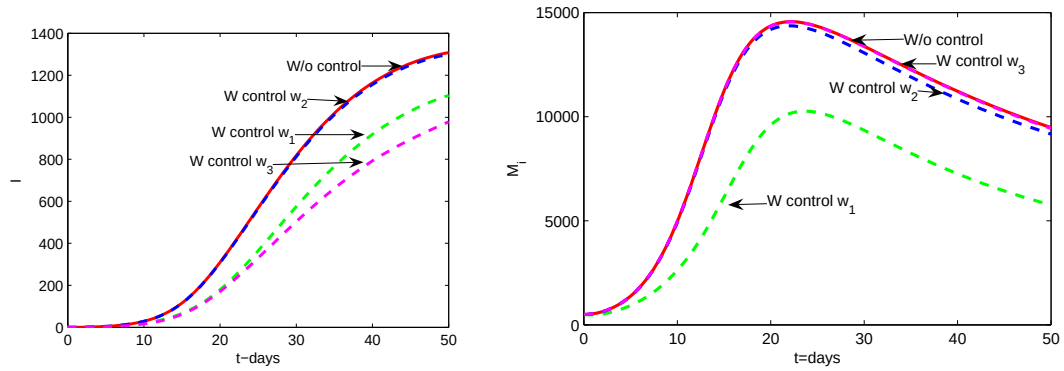

(a) Infected humans.

(b) Infected Adult mosquitoes.

Figure 4.3: Time series of model (4.2.4) under different optimal control strategies.

We investigate the use of one control at a time. Fig.4.3 illustrates the number of infected mosquitoes and humans under different optimal control strategies: (I) u_1, $(u_2 = u_3 = 0)$; (II) u_2, $(u_1 = u_3 = 0)$; (III) u_3, $(u_1 = u_2 = 0)$. The J value for implementing strategy (I) is much less than that for others strategies (II) or (III). In details, the J value of strategies (I), (II) and (III) are $5282, 5814$, and 6700 respectively. Moreover, the total number of infected mosquitoes using strategy (I) is the smallest while those with strategy (III) is the largest. While, the total number of infected humans using strategy (III) is the smallest; on the other hand, those with strategy (II) is the largest. Thus, we can conclude that, the most effective strategy to control

the WNv with only one control is by using larvicide during an ongoing epidemic in order to decrease the infected mosquitoes and humans with low cost. This conclusion further concurs the current control strategy used on Ontario: larviciding and not adulticiding is utilized to eradicate mosquitoes.

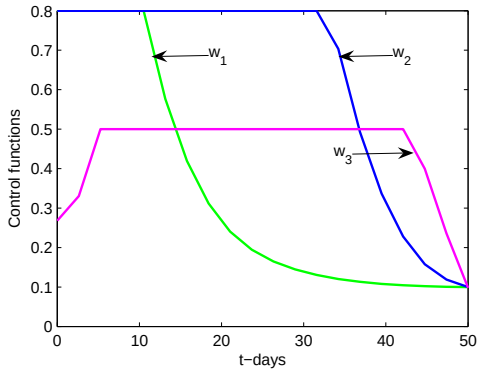

Figure 4.4: Control functions u_1, u_2 and u_3.

4.4 Optimal control with effect of the seasonal variations

Building on Section 4.2, and using numerical simulations, we carry out numerical experiment to study the impact of seasonal variations on control of WNv. We consider the same objective function (4.2.3), by assuming that $c_1 = c_2 = 1$ and $c_3 = 10$ and use the same values of the other weight factors (similar to the previous section).

From the available information on the schedule time of control in Ontario-Canada, it is worth mentioning that the control is usually applied for 50 to 60 days between May and August. Using these above fact, we performed different simulations using various initial populations. We will

explore the best time and strategy to apply the control.

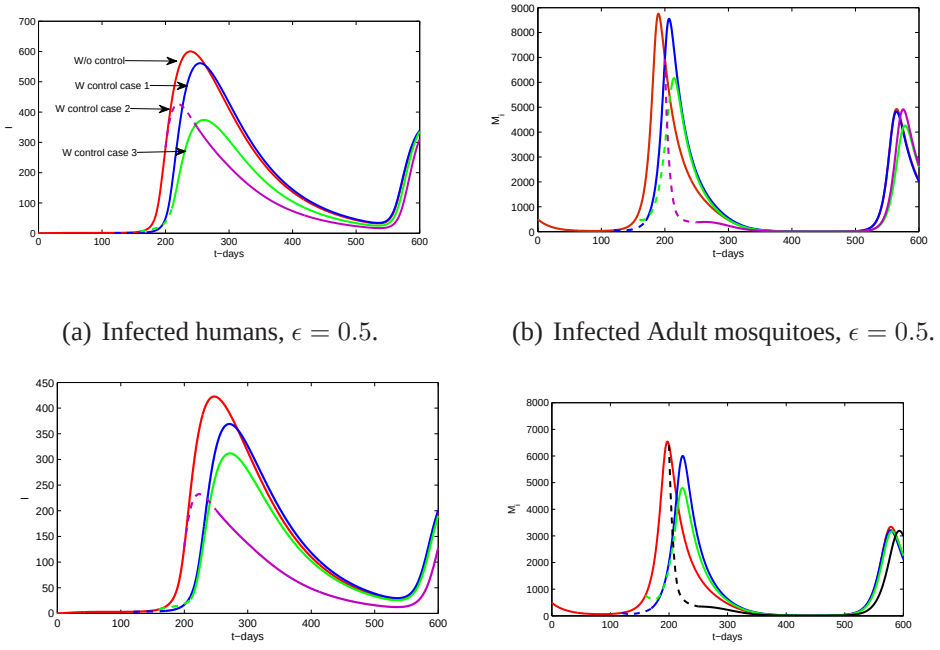

(a) Infected humans, $\epsilon = 0.5$. (b) Infected Adult mosquitoes, $\epsilon = 0.5$.

(c) Infected humans, $\epsilon = 0.25$. (d) Infected Adult mosquitoes, $\epsilon = 0.25$.

Figure 4.5: Time series of model (4.2.4) with seasonal impact.

In Fig.4.5, we investigated and compared numerical results of control for 50 days at different times of starting the control: case 1 (middle of May); case 2 (very early in July) and case 3 (middle of August). We perceived that, when $\epsilon = 0.5$ (see Fig.4.5(a) and (b)), if we start the control in July (case 2), the number of infected mosquitoes and humans and their highest peaks are lower than that of the other cases. It is worth-noting here that the J value of cases (1), (2) and (3) are 15282, 20814, and 24700 respectively. However, if $\epsilon = 0.25$ (see Fig.4.5(c) and (d)), case 3 (start the control on August) is the best time of starting the control. It is worth-noting here

that the J value when $\epsilon = 0.5$ will slightly increase than the cost of control when $\epsilon = 0.25$. Thus, when we focus the control in the course of 50 consecutive days, the optimal period to start depends on change in the temperatures. Whenever seasonal variations become stronger, our results recommend starting the control earlier.

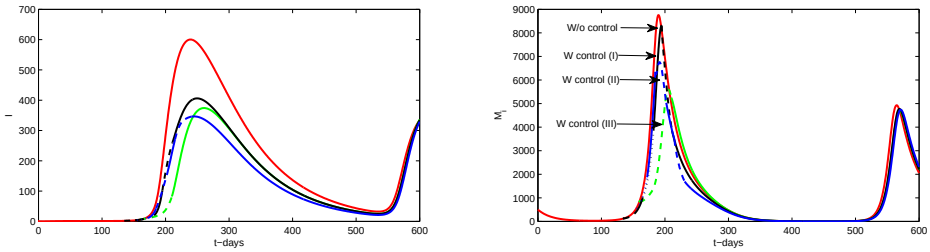

(a) Infected humans. (b) Infected Adult mosquitoes.

Figure 4.6: Time series of model (4.2.4) with seasonal impact (in case of $\epsilon = 0.5$).

In Fig.4.6, we used the same values of parameters and the same initial population as for Fig.4.5 (when $\epsilon = 0.5$) to compare the results of different optimal control strategies: (I) applying the control at three different times, each for 17 consecutive days (early in May, June and July); (II) applying the control at three different times, each for 17 consecutive days (end of May, June and July); (III) applying the control during 50 consecutive days in July. We can conclude that the best strategy of control depends on occurrence of infected cases of mosquitoes at a higher rate during May. If this takes place, then the best strategy is to apply the control at three different times (each time 17 days). Otherwise, it is best to apply the control one time for 50 days. Also the J values in cases (I) and (II) are almost the same but they are a little higher than the cost in case (III).

4.5 Conclusions and discussion

In this chapter we use the optimal control theory to study the strategies of control and minimizing the spread of WNv. The model formulated in Chapter 3 is extended to assess the impact of some anti-WNv control measures; by re-formulating the model as an optimal control problem in two cases with and without seasonality. The two models have been extended to assess the impact of some anti-WNv control measures, by re-formulating the models as an optimal control problem. This entails the use of three control functions: adulticide, larvicide and human protection. The results were analysed to determine the necessary conditions for the existence of an optimal control, using Pontrayagins maximum principle. From our numerical results, we found that Larvicide is the most effective strategy to control an ongoing epidemic in reducing disease cost when we apply only one control. The outcomes further stressed the importance of considering the other animals that could be infected in any region and its effect regarding the cost of control. Finally, the numerical results identified the time of applying the control to achieve the best control strategy. This work strongly justifies the importance of carefully taking into account the impact of the seasonal variation when applying the control.

5 West Nile virus risk assessment and forecasting using dynamical model

5.1 Introduction

There are different ways to estimate the risk of WNv in a area where virus is active. The two most commonly used risk assessment tools, or indices are the minimum infection rate (MIR) and the maximum likelihood estimation (MLE) [35].

The first index is MIR, is used as an indicator of the prevalence of WNv transmission intensity and therefore the risk for human disease. MIR is calculated using the equation below, which is the number of positive batches of mosquitoes of a given vector species divided by the total number of mosquitoes of the same species that were tested for the presence of the virus, expressed per 1,000 [35]. Therefore, if n is the number of positive pools and M is the total number of mosquitoes that tested, then the MIR is defined as:

$$MIR = \frac{n}{M} \times 1000.$$

The MIR is based on the assumption that infection rates are generally low and that only one mosquito is positive in a positive pool. The MIR can be expressed as a proportion or percent of

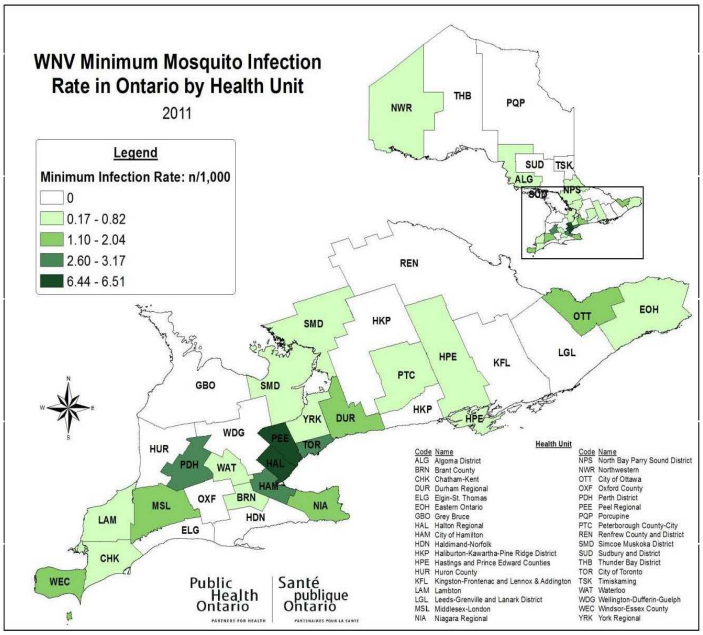

Figure 5.1: MIR of positive mosquito pools, 2011. Data from [85].

the sample that is WNv positive, but is commonly expressed as the number infected/1000 tested because infection rates are usually a small number. Fig.5.1, shows annual MIR in all health regions of Ontario in 2011 [85], and Fig.5.2, shows the incidence rate of WNv per 100,000 human population and number of confirmed and probable cases by health unit: Ontario, 2011 [85]. Fig.5.3, shows the weekly MIR and the number of infected cases of human at Peel region from 2002 to 2012 [86]. From Fig.5.1 and Fig.5.2, one can see that MIR is a effective tool to measure the risk of infection of WNv in Ontario.

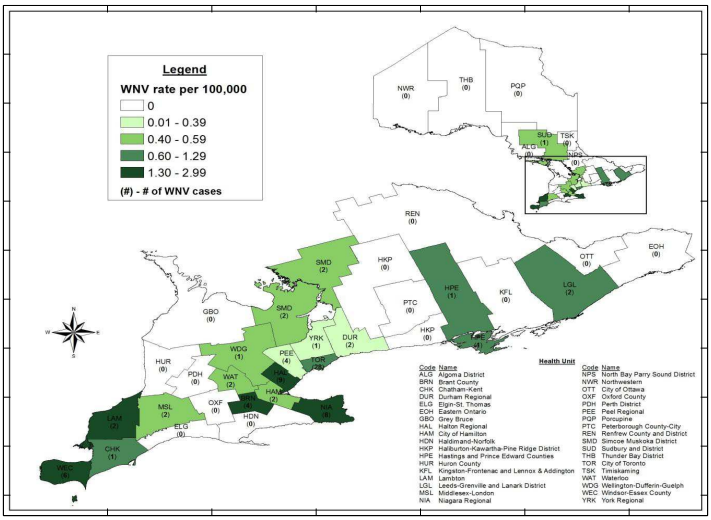

Figure 5.2: Incidence Rate of WNv per 100,000 human population and number of confirmed and probable cases by health unit: Ontario, 2011. Data from [85].

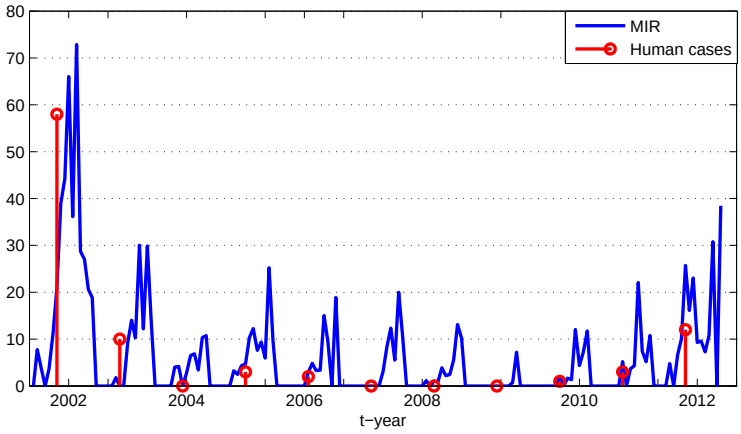

Figure 5.3: Reported human cases of WNv and MIR in Peel region; Ontario; Canada, from 2002 to 2012. Data from [86].

The second index to measure the WNv risk is MLE. The MLE is a statistical method used in the calculation of the proportion of infected mosquitoes, that maximizes the likelihood of k pools of size m to be virus positive [35], which is calculated using the following equation,

$$MLE = (1 - (k - \frac{n}{k})^{\frac{1}{m}}) \times 1000.$$

MLE does not require the assumption of one positive mosquito per positive pool, and provides a more accurate estimate when infection rates are high

The work of [21] evaluated both MIR and MLE to estimate WNv infection rates, and compared them for two mosquito species (*Culex* pipiens and *Culex* restuans) collected from three health units in Southern Ontario (Halton, Peel, and Toronto), from July to September 2002. They found good match between MIR and MLE using the pool size of 5. In general, MIR and MLE are similar when infection rates are low. Both MIR and MLE can provide a useful, quantitative

basis for comparison, allowing evaluation of changes in infection rate over time and space. These two indices also permit use of variable pool numbers and pool sizes while retaining comparability [5, 19].

Even though MIR and MLE provided useful information for the risk assessment for WNv, yet they still have some shortcomings. For instance, the calculation of MIR and MLE depends on the number of traps and number of species tested from established surveillance program. In addition to that both MIR and MLE are static numbers measuring the risk of the virus for the period of the week when the data were collected, so weather conditions (temperatures and perturbations) as important drivers for mosquito abundance and activities were ignored. Moreover, they also disregard the number of amplification host birds in the region. Therefore, it is essential and important to improve the indices of MIR and MLE to include the impact of the temperature and precipitation as well as the dynamical interaction of mosquitoes and birds by developing a new index.

In [89], a model for mosquitoes abundance incorporating the impact of the temperature and precipitation was developed to model and predict the average abundance of mosquitoes in Peel region. In this chapter, we will improve the MIR taking into account the impact of the weather (daily temperature and precipitation). We will utilise the dynamical models to measure the risk of WNv by considering the influence of birds. This is done by developing a new index, the dynamical minimum infection rate (DMIR) of WNv introduction into Ontario-Canada through different pathways. DMIR is the first WNv dynamical index to test and forecast the weekly risk of WNv by explicitly considering the temperature impact in the mosquito abundance, estimated

by statistical tools, and then comparing this new index with MIR, and with documented data available in Peel region-Ontario in order to justify our formula.

The current chapter is organized as follows. First, we demonstrate the statistical model for total mosquitoes abundance including the impact of the temperature and precipitation [89] in Section 5.2. Then in Section 5.3, based on one type of compartmental models for WNv, and combining with a weather impact model for total mosquitoes abundance, we will define the novel dynamical minimum infection rate (DMIR). The mosquitoes surveillance data and risk assessment data of MIR in the Peel region will then be used for model calibration and simulation in Section 5.4.

5.2 Statistical model for mosquito abundance of WNv

Mosquito abundance is crucial to the outbreak of mosquito-borne diseases [4,38,39,65,70,72,75, 87]. The intensity of WNv transmission is determined primarily by the abundance of competent mosquitoes and the prevalence of infection in mosquitoes. Therefore, understanding the dynamics of mosquito abundances is extremely helpful for efficient implementation of control measure and modeling of WNv.

Biologically, mosquitoes undergo complete metamorphosis going through four distinct stages of development, egg, pupa, larva, and adult, during a lifetime. After biting, adult females lay a raft of 40 to 400 tiny white eggs in standing water. Within a week, the eggs hatch into larvae that breathe air through tubes which they poke above the surface of the water. Larvae eat bits of floating organic matter and each other. Larvae molt four times as they grow; after the fourth

molt, they are called pupae. Pupae also live near the surface of the water, breathing through two horn-like tubes (called siphons) on their back. When the skin splits after a few days from a pupa, an adult emerges. The adult lives for only a few weeks and the full life-cycle of a mosquito takes about a month [57].

Mosquito populations such as *Culex pipiens* and *Culex restuans* (primary WNv vectors in southern Ontario [86]) are sensitive to long-term variations in climate and short-term variations in weather [74, 76, 89]. Combining the mosquito count and the related weather conditions, paper [63] concluded that the hot and dry conditions just before sampling were positively related to increased counts of *Culex pipiens* and *Culex restuans*. Also, high rainfall several weeks before sampling was positively related to *Culex pipiens* and *Culex restuans* counts under normal temperature conditions, because rainfall provided surface water for gravid females to lay eggs and larvae to develop [63]. These two types of extraordinary weather conditions can be used as indicators for taking action on mosquito control to prevent a disease outbreak by reducing the vector abundance.

The importance of the forecasting methods lies in its ability to warn of high-risk periods for WNv and this have been used with some success elsewhere in the world for vector borne diseases [55, 58, 83]. Recent efforts regarding forecasting arbovirus risk in North America include those of [26], who used a multiple linear regression model to build a biometeorological model for *Culex* populations on a monthly time scale, and [80] who used time series analysis techniques to forecast *Culex* pipiens - *restuans* populations on a weekly time scale. A weekly forecast model was also built by multiple linear regression techniques for *Culex tarsalis*, a vector for western

equine encephalitis virus, developed by [70]. These early studies showed that it is helpful for forecasting the mosquito abundance by understanding how weather conditions affect the count of vector mosquitoes.

In [89] used the average mosquito counts from 30 traps locations to represent the mosquito population at regional level and reached the conclusion that mosquito counts in Peel region, Ontario could be modeled by a gamma distribution. Then they used degree-days above $9^oC(dd)$, below which immature *Culex* mosquito development is effectively arrested, calculated as follows:

$$dd = \begin{cases} 0^oC & T_m \leq 9^oC, \\ T_m - 9^oC & T_m > 9^oC. \end{cases} \tag{5.2.1}$$

The arithmetic means of daily dd (ddm) from 1 to 60 day before each collection was explored as explanatory variables for mosquito abundance at the time of collection. The arithmetic means of daily precipitation (ppm) from 1 to 60 d before surveillance also was explored as explanatory variables for mosquito abundance at the time of collection. By using the surveillance data for mosquitoes and weather data in the Peel region, the authors in [89] discovered that the temperature from 1 to 34 d before mosquito capture was a significant predictor of mosquito abundance, with the highest test statistic being achieved when ddm11. Also, at ppm35, the test statistic reached its highest value, suggesting that the daily mean precipitation during the continuous 35 d before the mosquito capture had the most significant impact on the mosquito count. Using the most significant temperature (ddm11) and precipitation (ppm35) the model simulations match well with the data in the region. In Section 5.4, we will use the model in [89] (illustrated above) in order to update our model by the total number of mosquitoes (weekly) to predict the risk of

WNv using DMIR.

5.3 Risk assessment of WNv using the dynamical model

Compartmental models played an important role in gaining some insights into the transmission dynamics of WNv [1, 2, 10, 22, 56, 92]. In all of those models, due to various considerations of the factors related to the transmission of the virus, some models assumed that the total number of mosquito vectors remain constant [2, 22], others considered that the mosquito population satisfy the logistic growth [1]. While some models incorporated vertical transmission of the virus among vector mosquitoes [1, 2, 22], others did not [10, 54, 92]. Some models incorporated the aquatic life stage of the mosquitoes (eggs, larval and pupal stages) [2, 52] as well as seasonal effects in [2, 9, 23]. For the avian population, most of the models included a recovered class. Thus, one can see that all of the above models considered different aspects of transmission of WNv and that they determined the threshold conditions. The basic reproduction ratio were also calculated or estimated which serves as crucial control threshold for the reduction of the WNv. The dynamics from the above compartmental models make it possible to develop a quantity to measure the risk.

5.3.1 DMIR model

Our goal of this part is to develop an index to assess the risk of WNv. This is done by determining the dynamical minimum infection rate (DMIR) of WNv introduction into Ontario-Canada to test and forecast the weekly risk of WNv in the following weeks of the season and then identify possible mitigation strategies.

In the next model, M_s and M_i are the number of susceptible and infectious mosquitoes respectively. Due to its short life span, a mosquito never recovers from the infection and we do not consider the recovered class in the mosquitoes [34]. The total number of mosquitoes is $M = M_s + M_i$. The number of susceptible, infected and recovered birds are denoted by B_s, B_i and B_r respectively. Thus, $B = B_s + B_i + B_r$ is the total number of birds. The total human population denoted by H, is split into the populations of susceptible H_s, infectious H_i and recovered H_r humans.

According to the transmission cycle of the WNv and by extending the modeling for the WNv [1, 2, 10, 22, 52, 93], we propose to study the next compartment model:

$$\begin{cases} \frac{dM_s}{dt} = r_m(M_s + (1-q)M_i) - \beta_m b \frac{B_i}{B+H} M_s - d_m M_s, \\ \frac{dM_i}{dt} = q r_m M_i + \beta_m b \frac{B_i}{B+H} M_s - d_m M_i, \\ \frac{dB_s}{dt} = \Lambda_b - \beta_b b \frac{B_s}{B+H} M_i - d_b B_s, \\ \frac{dB_i}{dt} = -(d_b + \nu_b + \mu_b) B_i + \beta_b b \frac{B_s}{B+H} M_i, \\ \frac{dB_r}{dt} = \nu_b B_i - d_b B_r, \\ \frac{dH_s}{dt} = \Lambda_h - \beta_h b \frac{H_s}{B+H} M_i - d_h H_s, \\ \frac{dH_i}{dt} = -(d_h + \nu_h + \mu_h) H_i + \beta_h b \frac{H_s}{B+H} M_i, \\ \frac{dH_r}{dt} = \nu_h H_i - d_h H_r. \end{cases} \tag{5.3.2}$$

The definitions of the parameters used in the model (5.3.2) are summarized in Tables 2.1 and 3.1.

By considering the total number of mosquitoes is constant $\tilde{M}$ $(i.e, r_m = d_m)$ the model

(5.3.2) has a disease-free equilibrium $E_0 = (\tilde{M}, 0, \tilde{B}, 0, 0, \tilde{H}, 0, 0)$, where $\tilde{B} = \frac{\Lambda_b}{d_b}$, and $\tilde{H} = \frac{\Lambda_h}{d_h}$.

The basic reproduction number is obtained by using the second generating method [84]:

$$R_0 = \sqrt{q + \frac{4\beta_m \beta_b b_m^2 \tilde{B}\tilde{M}}{d_m(d_b + \nu_b + \mu_b)(\tilde{B} + \tilde{H})^2}}. \tag{5.3.3}$$

An endemic equilibrium is identified by the solution of the algebraic system obtained by setting the derivatives of model (5.3.2) equal to zero, then we can conclude the following results:

1. If $R_0 > 1$, there exists a unique positive stable endemic equilibrium

2. If $R_0 < 1$, there is no endemic equilibrium.

Which means if $R_0 < 1$, the disease dies out, whereas if $R_0 > 1$, the disease persists.

The formula of DMIR, derived from the method of calculating the MIR is as follows: Let $k(t)M(t)$ is the amount of mosquitoes collected which will be tested at any time t, for all $k(t)$ is the percentage of mosquitoes collected. Those mosquitoes will be placed in pools where each pool includes m mosquitoes. Then we can assume that the number of infected pools are $\frac{k(t)M_i(t)}{m}$. From the definition of MIR, we can conclude the formula of DMIR:

$$DMIR(t) = U\frac{M_i(t)}{M(t)}, \tag{5.3.4}$$

where the parameter U indicates the maximum value of DMIR which can be determined from the previous MIR data available at the region under study.

By considering this new variable, we can rewrite the model (5.3.2) to include the new index

as follows:

$$\begin{cases} \dfrac{dM_i}{dt} = qr_m M_i + \beta_m b \dfrac{B_i}{B+H} M_s - d_m M_i, \\ \dfrac{dB_s}{dt} = \Lambda_b - \beta_b b \dfrac{B_s}{B+H} M_i - d_b B_s, \\ \dfrac{dB_i}{dt} = -(d_b + \nu_b + \mu_b) B_i + \beta_b b \dfrac{B_s}{B+H} M_i, \\ \dfrac{dB_r}{dt} = \nu_b B_i - d_b B_r, \\ \dfrac{dH_s}{dt} = \Lambda_h - \beta_h b \dfrac{H_s}{B+H} M_i - d_h H_s, \\ \dfrac{dH_i}{dt} = -(d_h + \nu_h + \mu_h) H_i + \beta_h b \dfrac{H_s}{B+H} M_i, \\ \dfrac{dH_r}{dt} = \nu_h H_i - d_h H_r, \\ DMIR(t) = U \dfrac{M_i(t)}{M(t)}, \end{cases} \tag{5.3.5}$$

where the susceptible mosquitoes can be obtained from the next equation $M_s = M - M_i$, where M (the total number of mosquitoes) is updated weekly using the statistical model developed in [89] (and demonstrated in Section 5.2) in order to explain the dynamics of WNv infections with the impact of temperature in the mosquito abundance.

Note that U values are changed from week t_i to week t_{i+1} but are considered constant in the intervals $[t_i, t_{i+1})$. Thus, in the intervals $[t_i, t_{i+1})$ the change of DMIR can be identified by the next form

$$\frac{dDMIR(t)}{dt} = a(t)U - (a(t) + b(t))DMIR, \tag{5.3.6}$$

where $a(t) = \beta_m \frac{B_i}{B+H}$, is the infection rate per susceptible mosquito and $b(t) = (1-q)r_m$, is the rate of new susceptible mosquito.

From equation (5.3.6), we can conclude that the values of $DMIR(t)$ depends on the infection rate per susceptible mosquito $a(t)$ as well as the rate of new susceptible mosquito $b(t)$. However, the values of $a(t)$ and $b(t)$ are mutually dependant. This explains that in some regions of Ontario there is low risk of WNv where there are large number of birds.

5.3.2 The initial conditions in DMIR index

The model (5.3.5) is implemented with MATLAB program with a time step of 1 day. Our simulation starts from week 24 to week 39 in the summer. We considered that all the parameters value in the model (5.3.5) are constant (summarized in Tables 2.1 and 3.1). The initial value of mosquito population is set and updated weekly using the statistical model developed in [89]; hypothesizing that this number is 1% from the exact number of mosquitoes. The initial number of susceptible birds is set to the maximum bird population siz [44]. The initial human population can be specified from the information about the area under study. We will use the MIR data available at the region under study as a guide to consider the initial conditions for DMIR value by starting our simulation with the week where the MIR value is $\neq 0$ (i.e $DMIR(t_0) = MIR(t_0) > 0$). We can calculate the values of U by using the previous data of MIR at that region. Also we considered the initials of infected bird and human populations are zeros.

Once initialized with some infectious mosquitoes in the week where the $MIR(t_0) \neq 0$, we can calculate the value of U and then simulate our model for the entire period using 1-day time step for one week. This is repeated weekly while updating the total number of mosquitoes by using the statistical models developed in [89].

5.3.3 R_0 and DMIR

In [90], the authors listed R_0 calculated in the models [10, 22, 56, 92] and concluded that different models may induce different R_0 but all of these basic reproduction ratios are related to the ratio of the number of mosquitoes and hosts at the disease-free equilibrium, which implies that a reduction in mosquito density would help control the epidemic. The magnitude of R_0 is used to gauge the risk of an epidemic in emerging infectious disease. The author in [73] noted two fundamental properties commonly attributed to R_0, that an endemic infection can persist only if $R_0 > 1$ and provides a direct measure of the control effort required to eliminate the infection. He demonstrated that this statement can be false. The first property, as we have noted, can fail due to the presence of backward bifurcations. The second one can fail when control efforts are applied unevenly across different host types (such as a high-risk and a low-risk group) since R_0 is determined by averaging over all host types and does not directly determine the control effort required to eliminate infection. Thus, as we mentioned in almost every aspect that matters, R_0 is flawed.

In Fig.5.4 and Fig.5.5 we introduce the infected human and the DMIR (considering that total number of mosquitoes is constant) in three cases. From Fig.5.4, we can observe that the number of infected human are consistent with the DMIR values in three cases with different values of $R_0 = 0.8537, 1.1997, 1.515$. However in Fig.5.5, we can note the same thing but with different initial values of birds and humans but with same value of R_0 in all cases. Thus, we can conclude that the DMIR is a good method to test and forecast the weekly risk of WNv than R_0 and subsequently, we can provide a direct measure of the control effort required to eliminate the

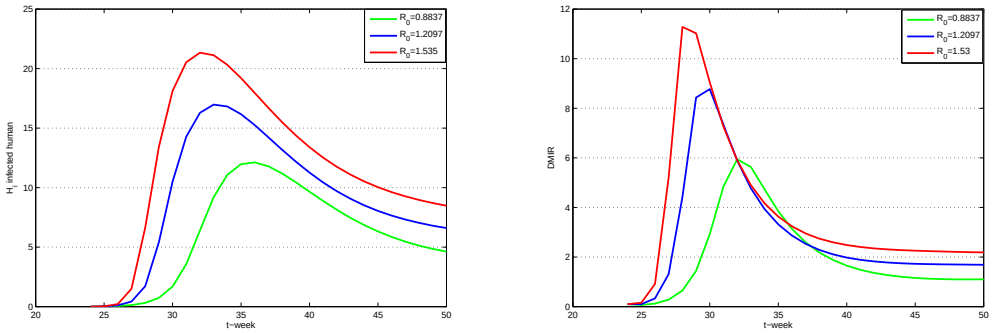

(a) H_i. (b) DMIR.

Figure 5.4: Comparison between the human infection H_i and DMIR in the model (5.3.2) in three cases when $R_0 = 0.8537, 1.1997$ and 1.515.

infection.

5.4 Forecasting WNv risk in Peel region, Ontario using real data

Peel region is a municipality in Southern Ontario on the north shore of Lake Ontario, between the City of Toronto and York region extending from latitude 43.35^oN to 43.52^oN and from longitude 79.37^oW to 80.00^oW. The region comprises the cities of Mississauga and Brampton and the Town of Caledon [86]. Mosquito data were obtained from a surveillance program of the Ontario Ministry of Health and Long-Term Care. The Peel region health unit used the Centers for Disease Control Miniature light trap with both CO_2 and light to attract host-seeking adult female mosquitoes [86].

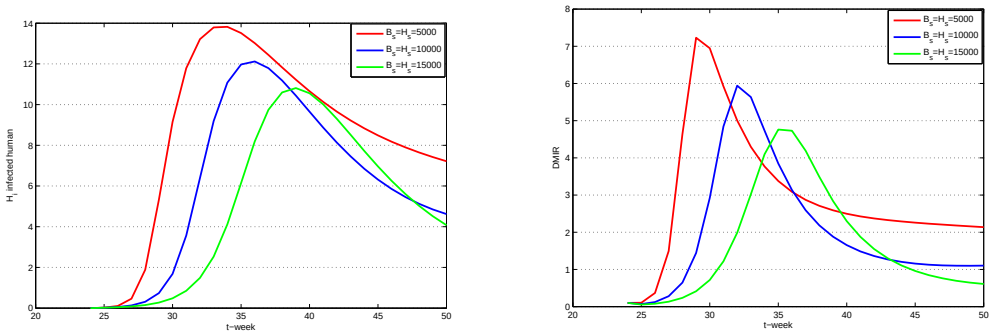

(a) H_i. (b) DMIR.

Figure 5.5: Comparison between the human infection H_i and DMIR in the model (5.3.2) in three cases when $B_s(t_0) = H_s(t_0) = 5000, 10000, 15000$. In all three cases $R_0 = 1.23$

5.4.1 Mosquito abundance

The Peel region has initiated a mosquito forecasting program started in 2011 and continued in 2012. Every week in mosquito season (from middle of June to earlier October), the mosquito traps were set up on Monday and Tuesday by the mosquito surveillance program in Peel region. The traps were collected the following morning and the mosquito data would be available on Wednesday. The previous weather data were collected through [86] and the weather data for the following two weeks were obtained through [86]. The mosquito predictive model developed by [89] has been used to provide the *Culex* mosquito abundance data for the next two weeks by using the mosquito surveillance and weather data collected. The forecasting results were posted and updated weekly on [86] and a weekly report was sent to Peel region public health department, Public Health of Ontario (PHO) and Environmental Issues Division of Public Health Agency of

Canada (PHAC).

5.4.2 WNv risk forecasting

The testing of mosquito pools gives an indication of which mosquito species harbor WNv and, if sufficient numbers are tested, infection rates can be calculated. However, the actual number of individual WNv positive mosquitoes in a pool is unknown. And then the estimation of the proportion of infected mosquitoes in a specific area can be calculated using MIR. From the data available at Peel region on MIR and the number of infected cases of human as shown in Fig.5.3, we can confirm that MIR is an good tool to identify the risk of infection of WNv in Peel region. Nevertheless, the method of identifying the MIR cannot predict what might happen in the following weeks. Consequently, we believe that our formula of DMIR is an appropriate method of predicting the risks of WNv in the following weeks through using the data available and some of the previously used dynamical models.

5.4.3 Numerical simulations

Because our simulation starts early in the summer, the initial values of infection birds and humans are set to zero. The initial number of susceptible birds is set to the maximum bird population size $B_s = 75000$. From [12], we specify the initial number of humans living $2005 - 2012$ in the Peel area. By starting with some infectious mosquitoes, our model simulates from the week t_0, such that $DMIR(t_0) = MIR(t_0) > 0$, to week t_1 using 1-day time step. The susceptible mosquito population is updated weekly using the form $M_s = M - M_i$ for all M is the total number of

Culex pipiens and *Culex restuans* mosquitoes. For the years 2005, 2006, 2008, 2010 and 2011, we try to verify our index so we update our model using the total number of mosquitoes previously collected M. As for the year 2012, we try to predict the risk of WNv using our index so we updated M using the statistical model developed in [89]. In all those years we considered the total number of mosquitoes to represent 1% from the exact number of mosquitoes.

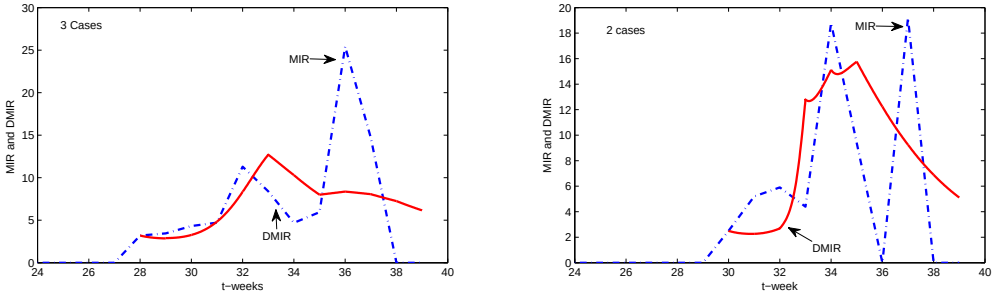

(a) 2005 (b) 2006

Figure 5.6: Compare MIR and DMIR in Peel region; Ontario; Canada 2005 and 2006.

The time series of our formula DMIR were compared with the MIR data available from 2005 to 2012 as shown in Fig.5.6, 5.7 and 5.8. It is worth noting that it was difficult to identify the DMIR values accurately in 2007 and 2009 (where the infection rate was very low in the first few weeks) since the first value of the $MIR > 0$ occurred in later weeks than the previous years.

For the validation period of 2005, 2006, 2008, 2010 and 2011 and the prediction in 2012, it was noticed that the DMIR values are directly proportional with the number of human cases. The magnitude of the peak values in DMIR was also close to the MIR peaks. Moreover, the rate of infection typically peaked in the middle of the season (in August) - a pattern that is consistent

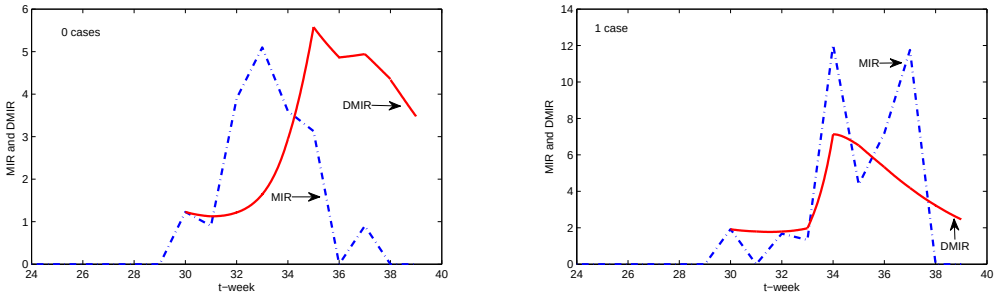

(a) 2008 (b) 2010

Figure 5.7: Compare MIR and DMIR in Peel region; Ontario; Canada 2008 and 2010.

across most of the years in our simulations. It is important to point out here that the DMIR index is more accurate in the years which are characterised by high level of infection (as in 2012, for instance) due to high fluctuations in temperatures in these years. Consequently, this has its direct impact on mosquitoes abundance.

5.5 Conclusions

The risk assessment tool uses information gathered through the surveillance mechanisms described to ascertain the level of risk for human transmission of WNv within an area. In this chapter we developed a new index to test and forecast the weekly risk of WNv named DMIR. The DMIR is the first index that employs the dynamical models while considering the temperature impact in the mosquito abundance for estimating the risk of WNv. And in order to verify our formula, we compared it with the data available at Peel region. The DMIR index would be useful than the other methods (MIR and MLE) for estimating the risk of WNv because DMIR

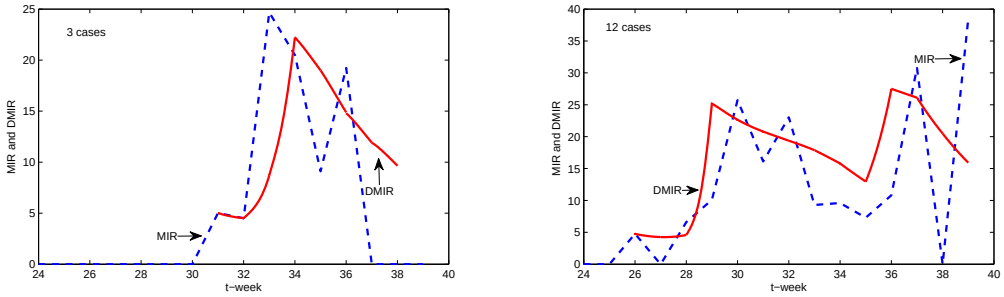

(a) 2011 (b) 2012

Figure 5.8: Compare MIR and DMIR in Peel region; Ontario; Canada 2011 and 2012.

considered the impact of quantity of the bird population as well as the linkage between mosquito abundance and preceding weather conditions (temperature and precipitation). This raises optimism for forecasting the risk of WNv with more accuracy.

During a WNv season, the DMIR predictive model would be useful to health units in identifying the relative risk of human infection within their jurisdiction. The DMIR tool could assist in guiding appropriate prevention and reduction activities such the need to increase public education (personal protection measures), expand larval control activities, enhance mosquito surveillance programs and assist in the decision making process to reduce the number of adult mosquitoes in areas of elevated risk to human health from WNv through the judicious use of pesticides. The application of pesticides to kill adult mosquitoes by ground or aerial application is called adulticiding. The timing of adulticiding is important as it should be undertaken prior or during the period of highest risk of human transmission. The DMIR could assist in projecting the high risk period in WNv season which would guide the timing of adulticiding spray events.

6 Conclusions and future work

Although discovering the transmission mechanism led to new insights into how to better control, WNv continue to pose a significant burden worldwide. The development of vector resistance to insecticides, changes in public health programs, seasonal climate changes, the increased mobility of humans, migration of birds and urban growth are all factors that contribute to the difficulty in controlling and eliminating WNv. Thus, in this thesis we tried to understand the behavior of the transmission of WNv in the mosquito-bird cycle and humans, as well as development of systems and procedures to reduce human risk by formulating dynamical models and using the optimal control to minimize the spread of WNv.

The first part of this work studied the impact of coexistence two avian populations in the transmission dynamics of WNv. We formulated a system of ordinary differential equations to model a single season of the transmission dynamics of WNv in the mosquito-bird cycle, by classifying avian populations as corvids and non-corvids. A detailed analysis of the model showed the existence of the backward bifurcation which indicates that the spread of the virus when R_0 is nearly below unity could be dependent on the initial sizes of the sub-population of the model. In this part we also generalized the results of backward bifurcation in previous work [41, 90], ana-

lyzed the effects of considering different amounts of corvid birds compared to noncorvid birds, and we concluded that the level of incidence (measured by the peak) and the reproduction number are completely different. For this reason, a field study is necessary to determine, in each region, the effectiveness of the avian and mosquito populations to transmit WNv in order to estimate the risk of the disease. In places where more effective avian populations are present, the infected level are high, having implications on the adopted mosquito reduction strategies. The results of this part suggest that even though dead corvids may not be seen in a given region, like in the early years of the endemic of the virus, there might be still a possibility of an outbreak due to the existence of the non-corvids as reservoirs. Furthermore, the outcomes also propose that it is essential to consider the diversity of the avian species, as well as the quantity of other mammals, when modeling WNv.

In the second part of this dissertation, we formulated a model to study the influence of seasonal variations of mosquito population on the transmission of WNv disease. We posed the question of how seasonal changes generate large outbreaks from an endemic equilibrium. Development, behavior and survival of mosquitoes are strongly influenced by climatic factors. In some places, the end of summer is the time where mosquito population notably increases. Thus, it is expected that such increase will increment the disease transmission. Hence, we presented a comprehensive and continuous deterministic model for the transmission dynamics of WNv in the mosquito-bird cycle and human with and without seasonality. We started by analyzing the model without seasonality and verified the existence of backward bifurcation. With reference to equation (3.3.23), we noticed that the existence of two important conditions that are required for

the occurrence of backward bifurcation: one is similar to one condition in [8] (which is considered a generalization of the same form in [1, 90]), and the other one which is the ratio between total number of birds and the other mammals that can be infected by mosquitoes is greater than unity. After that, we considered the model with seasonal variations (by assuming that the birth rate of mosquitoes follows a periodic pattern) to study the impact of seasonal variations of the mosquito population on the dynamics of WNv. In this latter model, we proved the existence of periodic solutions under specific conditions using the classical Floquet method, which is based on the calculation of the monodromy matrix and an analysis of its eigenvalues. Moreover, we introduced and calculated the basic reproduction number for this seasonal forced model. Numerical simulations of the model indicated that a sudden recrudescence from an endemic situation could have its origin in the interplay between intrinsic and extrinsic oscillations. Therefore, it is not just a simple consequence of the vector population growth that could be associated with climatic changes.

In the third part, we adopt the optimal control theory to study the strategies of control and minimiz the spread of WNv. The model formulated in Chapter 3 is extended to assess the impact of some anti-WNv control measures; by re-formulating the model as an optimal control problem in two cases with and without seasonality. This necessitates the use of three control functions: adulticide, larvicide and human protection. The results were analysed to determine the necessary conditions for the existence of an optimal control, using Pontrayagins maximum principle. The resulting non-autonomous system was examined to determine the necessary conditions for existence of an optimal control, using Pontrayagins maximum principle. Numerical simulations of the

model suggested that the Larvicide is the most effective strategy to control an ongoing epidemic in reducing disease cost when we apply only one control. But we noted that more knowledge about the actual effectiveness and costs of these intervention measures in specific applications would give more realistic parameters and results. The outcomes further stressed the importance of considering the other animals that could be infected in any region and its effect regarding the cost of control. Finally, the numerical results identified the time of applying the control to achieve the best control strategy. This work strongly justified the importance of carefully taking into account the impact of the seasonal variation when applying the control.

In the last part, we presented new methods to measure and forecast the risk of WNv. This is done by determining the dynamical minimum infection rate (DMIR) of WNv introduction into Ontario-Canada through different pathways. DMIR could be regarded as the first WNv dynamical model to test and forecast the weekly risk of WNv by being updated weekly of the total number of mosquitoes using the statistical models [89]. Finally, we compared our formula with the data available at Peel region to verify our formula.

As discused earlier in Chapters two and three, it is noticed that backward bifurcations have recently received much attention due to the adaptation, continual evolution of infectious agents and the reemergence of disease (The epidemiological significance of the backward bifurcation is that the usual requirement of $R_0 < 1$ is, although necessary, no longer sufficient for disease elimination). However, backward bifurcation occurs for certain ranges of the parameters. Thus, in future work we plan to find answers for the following questions as extended work for this dissertation:

- What is the biological interpretation (mechanism) of the occurrence of these backward bifurcations?.
- How will seasonal change affect the disease development as well as the equilibrium points in case of backward bifurcation and how this improves our understanding of the economics of WNv disease control?
- How to introduce WNv model presence of the oscillations without recourse to external seasonal forcing and then study the impact of the seasonal variations of the vector populations on the dynamics of the transmission of the disease in that model.
- How do we test the DMIR model with the occur of backward bifurcations when we estimate the risk assessment?

Bibliography

[1] Abdelrazec A, Lenhart S and Zhu H, (2014). Transmission Dynamics of West Nile Virus in Mosquito and Corvids and Non-Corvids. *Journal of Mathematical Biology,* **68**(6): 1553–1582.

[2] Abdelrazec A, Lenhart S and Zhu H, (2014). Dynamics and Optimal Control of a West Nile Virus Model with Seasonality. *to appear in Journal of Theoretical Biology*.

[3] Agusto F and Gumel A, (2010). Theoretical Assessment of Avian Influenza Vaccine. *Discrete and Continuous Dynamical Systems Series B,* **13**(1): 1–25.

[4] Barker C, Reisen W, Eldridge B, Park B and Johnson W, (2009). Culex Tarsalis Abundance as a Predictor of Western Equine Encephalomyelitis Virus Transmission. *Publications - Mosquito and Vector Control Association of California*, **77**: 65–68.

[5] Bernard A, Maffei G and Jones A, (2001). West Nile Virus Infection in Birds and Mosquitoes, New York State, 2000. *Emerging infectious disease,* **7**: 679–685.

[6] Bin H, Grossman Z, Pokamunski S, Malkinson M, Weiss L, Duvdevani P, Banet C, Weisman Y, Annis E, Gandaku D, Yahalom V, Hindyieh M, Shulman L and Mendelson E, (2001).

West Nile Fever in Israel 1999–2000: From Geese to Humans. *Annals of the New York Academy of Sciences*, **951**: 127–142

[7] Blayneh K, Cao Y and Kwon H, (2009). Optimal Control of Vector-Borne Diseases: Treatment and Prevention. *Discrete and Continuous Dynamical Systems Series B*, **11**(3): 587–611.

[8] Blayneh K, Gumel A, Lenhart S and Clayton T, (2010). Backward Bifurcation and Optimal Control in Transmission Dynamics of West Nile Virus. *Bulletin of Mathematical Biology*, **72**(4): 1006–1028.

[9] Bolling B, kennedy J and Zimmerman E, (2005). Seasonal Dynamics of Four Potential West Nile Vector Species in North-Central Texas. *Journal of Vector Ecology*, **30**: 186–194.

[10] Bowman C, Gumel A, van den Driessche P, Wu J and Zhu H, (2005). A mathematical Model for Assessing Control Strategies Against West Nile Virus. *Bulletin of Mathematical Biology*, **67**(5): 1107–1133.

[11] Buck P, Liu R, Shuai J, Wu J and Zhu H, (2009). Modeling and Simulation Studies of West Nile Virus in Southern Ontario Canada. In the book *"Modeling and Dynamics of Infectious Diseases"* edited by Ma Z, Wu J and Zhou Y. World Scientific Publishing.

[12] Canada's National Climate Archive, *http://climate.weather.gc.ca/*

[13] Carr J, (1981). Applications of Centre Manifold Theory. Springer-Verlag, Berlin.

[14] Castillo C and Song B, (2004). Dynamical Models of Tuberculosis and Their Applications. *Mathematical Biosciences and Engineering*. **1**(2): 361–404.

[15] Castillo C, (2006). Optimal Control of an Epidemic Through Educational Campaigns. *Electronic Journal of Differential Equations*, **2006**(125): 1–11.

[16] Center for Disease Control and Prevention (CDC), (2002). Weekly update: West Nile Virus Activity-United States. *Morbidity and Mortality Weekly Report (MMWR)*, **50**: 1061–1063.

[17] Centers for Disease Control (CDC), (2011). Statistics, Surveillance and Control of West Nile Virus.

[18] Center for Disease Control and Prevention (CDC), (2013). Weekly update: West Nile Virus Activity-United States. *Morbidity and Mortality Weekly Report (MMWR)*, **50**: 106–113.

[19] Chiang L and Reeves C, (1995). Statistical Estimation of Virus Infection Rates in Mosquito Vector Populations. *American Journal of Hygiene*, **75**: 377–391.

[20] Chitnis N, (2005). Using Mathematical Models in Controlling the Spread of Malaria. *PhD thesis University of Arizona, Program in Applied Mathematics*.

[21] Condotta S, Hunter F and Bidochka M, (2004). West Nile Virus Infection Rates in Pooled and Individual Mosquito Samples. *Vector-Borne and Zoonotic Diseases*, **4**(3): 198–203.

[22] Cruz-Pacheco G, Esteva L, Montano-Hirose, J and Vargas D, (2005). Modelling the Dynamics of West Nile Virus. *Bulletin of Mathematical Biology*, **67**: 1157–1172.

[23] Cruz-Pacheco G, Esteva L and Vargas C, (2009). Seasonality and Outbreaks in West Nile Virus Infection. *Bulletin of Mathematical Biology*, **71**(6): 1378–1393.

[24] Cruz-Pachecoa G, Estevab L and Vargas C, (2012). Multi-Species Interactions in West Nile Virus Infection. *Journal of Biological Dynamics*, **6**(2): 281–298.

[25] Dowell F, (2002). Seasonal Variation in Host Susceptibility and Cycles of Certain Infectious Disease. *Emerging Infectious Diseases*, **7**(3): 369–373.

[26] DeGaetano T, (2005). Meteorological Effects on Adult Mosquito *Culex* Population in Metropolitan New Jersey. *International Journal of Biometeorology*. **49**: 345–353.

[27] Diallo O and Kone Y, (2007). Melnikov Analysis of Chaos in a General Epidemiological Model. *Nonlinear Analysis: Real World Applications*, **8**(1): 20–26.

[28] Dohm J, Sardelis M, and Turell M, (2002). Experimental Vertical Transmission of West Nile Virus by Culex Pipiens (Diptera: Culicidae). *Journal of Medicine and Entomology*, **39**: 640–644.

[29] Durand B, Balanca G, Baldet T and Chevalier V, (2010). A metapopulation Model to Simulate West Nile Virus Circulation in Western Africa, Southern Europe and the Mediterranean Basin. *Veterinary Research*, **41**: 32.

[30] Fan G, Junli P, van den Driessche P, Wu J and Zhu H, (2010). The Impact of Maturation Delay of Mosquitoes on the Transmission of West Nile Virus. *Mathematical Biosciences*, **228**(2): 119–126.

[31] Fleming H and Rishel W, (1975). Deterministic and Stochastic Optimal Control. Springer, New York.

[32] Greenhalgh D and Moneim I, (2003). SIRS Epidemic Model and Simulations Using Different Types of Seasonal Contact Rate. *Systems Analysis Modelling Simulation*, **43**(5): 573–600.

[33] Guckenheimer J and Holmes P, (1983). Nonlinear Oscillations, Dynamical Systems and Bifurcations of Vector Fields, Springer-Verlag, Berlin.

[34] Gubler J, (1989). The Arboviruses: Epidemiology and Ecology. **II**. CRC Press, Florida, 213–261.

[35] Gu W, Lampman R and Novak R, (2003). Problems in Estimating Mosquito Infection Rates Using Minimum Infection Rate. *Journal of Medical Entomology*, **40**(5): 595–596.

[36] Hamer L, Kitron D, Goldberg L, Brawn D, Loss R, Ruiz O, Hayes B and Walker D, (2009). Host Selection by *Culex Pipiens* Mosquitoes and West Nile Virus Amplification. *The American Journal of Tropical Medicine and Hygiene*, **80**(2), 268–278.

[37] Hilker F and Westerhoff F, (2007). Preventing Extinction and Outbreaks in Chaotic Populations. *American Naturalist*, **170**(2): 232–241.

[38] Hu W, Nicholls N, Lindsay M, Dale P, McMichael J, Mackenzie S and Tong S, (2004). Development of a Predictive Model for Ross River Virus Disease in Brisbane, Australia. *The American Journal of Tropical Medicine and Hygiene*, **7**(12): 129–137.

[39] Hu W, Tong S, Mengersen K and Oldenbury B, (2006). Rainfall, Mosquito Density and the Transmission of Ross River Virus; A time-series forecasting model. *Ecological modeling*, **196**: 505–514.

[40] Hu X, Liu Y and Wu J, (2009). Culling Structured Hosts to Eradicate Vector-Borne Diseases. *Mathematical Biosciences and Engineering*, **6**(2): 301–310.

[41] Jiang J, Qiu Z, Wu J and Zhu H, (2009). Threshold Conditions for West Nile Virus Outbreaks. *Bulletin of Mathematical Biology*, **71**(3): 627–647.

[42] Karrakchou M and Gourari S, (2006). Optimal Control and Infectiology: Application to an HIV/ AIDS Model. *Applied Mathematics and Computation*, **177**(2): 807–818.

[43] Keeling M, Rohani P and Grenfell P, (2001). Seasonally Forced Disease Dynamics Explored as Switching Between Attractors. *Physica D*, **148**: 317–335.

[44] Kennedy J, Pam D and Erskine A, (1999). National Office 1999 Canadian Wildlife Service Environment Canada. Technical Report Series No 342.

[45] Kenkre M, Parmenter R, Peixoto D and Sadasiv L, (2006). A Theoretic Framework for the Analysis of the West Nile Virus Epidemic. *Journal of Computational Mathematics*, **42**: 313–324.

[46] Komar N and Clark G, (2006). West Nile Virus Activity in Latin America and the Caribbean. *Revista Panamericana de Salud Pblica*, **19**(2): 112–117.

[47] Komar N, Langevin S, Hinten S, Nemeth N and Edwards E, (2003). Experimental Infection of North American Birds with the New York 1999 Strain of West Nile Virus. *Emerging Infectious Diseases*, **9**(3): 311–322.

[48] Kurt D, Reed M, Jennifer K, James S, Henkel S and Sanjay K, (2003). Birds, Migration and Emerging Zoonoses: West Nile Virus, Lyme Disease, Influenza A and Enteropathogens. *Journal of Clinical Medicine Research*, **1**(1): 5–12.

[49] Lanciotti S, Roehrig T, Deubel V, Smith J, Parker M, Steele K, Crise B, Volpe E, Crabtree B, Scherret H, Hall A, MacKenzie S, Cropp B, Panigrahy B, Ostlund E, Schmitt B, Malkinson M, Banet C, Weissman J, Komar N, Savage M, Stone W, McNamara T and Gubler J, (1999). Origin of the West Nile Virus Responsible for an Outbreak of Encephalitis in the Northeastern United States. *Science*, **286**(5448): 2333–2337.

[50] Laperriere V, Brugger K and Rubel F, (2011). Simulation of the Seasonal Cycles of Bird, Equine and Human West Nile Virus Cases. *Institute for Veterinary Public Health, University of Veterinary Medicine Vienna, Veterinrplatz*.

[51] Lenhart S and Workman J, (2007). Optimal Control Applied to Biological Models. *Mathematical and Computational Biology Series*.

[52] Lewis M, Renclawowicz J and van den Driessche P, (2006a). Traveling Waves and Spread Rates for a West Nile Virus Model. *Bulletin of Mathematical Biology*, **66**: 3–23.

[53] Lewis M, Renclawowicz J, van den Driesssche P and Wonham M, (2006b). A Comparison of Continuous and Discrete-Time West Nile Virus Models. *Bulletin of Mathematical Biology*, **68**: 491–509.

[54] Liu R, Shuai J, Wu J and Zhu H, (2006). Modelling Spatial Spread of West Nile Virus and Impact of Directional Dispersal of Birds. *Mathematical Biosciences and Engineering*, **3**: 145-160.

[55] Li J, Blakeley D and Smith R, (2011). The Failure of R_0. *Computational and Mathematical Methods in Medicine*, **2011**: 511–527.

[56] Lord C and Day J, (2005). Simulation Studies of St. Louis Encephalitis Virus in South Florida. *Vector Borne Zoonotic Diseases*, **1**(4): 299–315.

[57] Madder D, Surgeoner G and Helson B, (1983). Number of Generations, Egg Production, and Developmental Time of *Culex Pipiens* and *Culex Restuans* (*Diptera: Culicidae*) in Southern Ontario. *Journal of Medical Entomology*, **22**: 275–287.

[58] Makridakes S, Wheelwright S and Hyndman R, (1998). Forecasting Methods and Applications. *John Wiley, New York*.

[59] Makinde D and Okosun O, (2011). Impact of Chemo-Therapy on Optimal Control of Malaria Disease with Infected Immigrants. *Biosystems*, **104**(1): 32–41.

[60] Maidana N and Yang H, (2011). Dynamic of West Nile Virus Transmission Considering Several Coexisting Avian Populations. *Mathematical and Computer Modelling*, **53**(5–6): 1247–1260.

[61] Murgue B, Murri S, Triki H, Deubel V and Zeller G, (2001). West Nile in the Mediterranean Basin: 1950–2000. *Annals of the New York Academy of Sciences*, **951**: 117–126.

[62] Okosun K, (2010). Mathematical Epidemiology of Malaria Disease Transmission and its Optimal Control Analyses. *PhD thesis, University of the Western Cape, South Africa*.

[63] Paz S and Albersheim I, (2008). Influence of Warming Tendency on *Culex Pipiens* Population Abundance and on the Probability of West Nile Fever Outbreaks. EcoHealth, **5**: 40–48.

[64] Patrick Z, (2005). West Nile Virus National Report on Dead Bird Surveillance. Canadian Cooperative Wildlife Health Centre.

[65] Pecoraro H, Day H, Reineke R, Stevens N, Withey J, Marzluff J and Meschke J, (2007). Climate and Landscape Correlates for Potential West Nile Virus Mosquito Vectors in the Seattle Region. *Journal of Vector Ecology*, **32**(1): 22–28.

[66] Peterson R and Marfin A, (2002). West Nile Virus: A Primer for the Clinician. *Annals of Internal Medicine*, **137**: 173–179.

[67] Public Health Agency of Canada, West Nile Virus MONITOR, 2013. http://www.phac-aspc.gc.ca/index-eng.php.

[68] Pontragin L, Gamkrelize R, Boltyanskii V and Mishchenko E, (1962). The Mathematical Theory of Optimal Processes. *Wiley*.

[69] Puente D, Delgado P, Perez D, Tapia C, Sanchez V and Murillo D, (2004). The Impact of Mosquito-Bird Interaction on the Spread of West Nile Virus to Human Populations. *Mathematical and Theoretical Biology Institute*, **58**: 31–42

[70] Raddatz R, (1986). A Biometeorological Model of an Encephalitis Vector. *Boundary layer meteorology*, **34**: 185–199.

[71] Rafikov M, Bevilacqua L and Wyse P, (2008). Optimal Control Strategy of Malaria Vector Using genetically Modified Mosquitoes. *Journal of Theoretical Biology*, **258**: 418–425.

[72] Reisen W, Gayan D, Tyree M, Barker C, Eldridge B and Dettinger M, (2008). Impact of Climate Variation on Mosquito Abundance in California. *Journal of Vector Ecology*, **32**(1): 89–98.

[73] Roberts M, (2007). The Pluses and Minuses of R_0. *Journal of the Royal Society Interface*, **4**(16): 949–961.

[74] Ruiz M, Chaves L, Hamer G, Sun T, Brown W, Walker E, Haramis L, Goldberg T and Kitron U, (2010). Local Impact of Temperature and Precipitation on West Nile Virus Infection on *Culex* Species Mosquitoes in Northeast Illinois, USA. *Parasites & Vectors*, **2**: 3–19.

[75] Shone S, Curriero F, Lesser C and Glass G, (2006). Characterizing Population Dynamics of Aedes Sollicitans (Diptera: Culicidae) Using Meteorological Data. *Journal of Medical Entomology*, **43**(2): 393–402.

[76] Shelton R, (1973). The Effects of Temperature on Development of Eight Mosquito Species. *Mosque News*, **33**: 1–12.

[77] Smithburn K, Hughes T and Burke A, (1940). A Neurotropic Virus Isolated from the Blood of a Native of Uganda. *The American Journal of Tropical Medicine and Hygiene*, **20**: 471–492.

[78] Swayne D, Beck R and Zaki S, (2002). Pathogenicity of West Nile Virus for Turkeys. *Avian Diseases*, **44**: 932–937.

[79] Thomas M and Urena B, (2001). A Model Describing the Evolution of West Nile-Like Encephalitis in New York City. *Mathematical Computational Modelling*, **34**(7): 771–781.

[80] Trawinski R and MacKay D (2008). Meteorologically Conditioned Time-Series Predictions of West Nile Virus Vector Mosquitoes. *Vector-Borne Zoonotic Diseases*, **8**: 505–521.

[81] Triki H, Murri S, Le Guenno B, Bahri O, Hili K, Sidhom M and Dellagi K, (2001). West Nile Viral Meningoencephalitis in Tunisia. *Med Trop*, **61**(6): 487–490.

[82] Tsai F, Popovici F, Cernescu C, Campbell L and Nedelcu I, (1998). West Nile Encephalitis Epidemic in South-Eastern Romania. *Lancet*, **352**(9130): 767–771.

[83] Turell D, Dohm D, Sardelis R and Guinn L, (2005). An Update on the Potential of North American Mosquitoes to Transmit West Nile Virus. *Journal of Medical Entomology*, **42**: 57–62.

[84] van den Driessche P and Watmough J, (2002). Reproduction Numbers and Sub-Threshold Endemic Equilibria for Compartmental Models of Disease Transmission. *Mathematical Biosciences,* **180**: 29–48.

[85] Vector-Borne Diseases 2011 Summary Report,Public Helth Ontario, Canada.

[86] Vector-Borne Diseases 2013 Summary Reports. Peel Public Health.

[87] Walsh A, Glass G, Lesser C and Curriero F, (2008). Prediction Seasonal Abundance of Mosquitoes Based on off-Season Meteorological Conditions. *Environmental and Ecological Statistics*, **15**: 279–291.

[88] Wang W and Zhao X, (2008). Threshold Dynamics for Compartmental Epidemic Models in Periodic Environments. *Journal of Dynamics and Differential Equations*. **20**: 699–717.

[89] Wang J, Ogden N and Zhu H, (2011). The Impact of Weather Conditions on *Culex Pipiens* and *Culex Restuans* (Diptera: Culicidae) Abundance: A Case Study in Peel Region. *Journal of Medical Entomology*, **48**(2): 468–475.

[90] Wan H and ZHU H, (2010). The Backward Bifurcation in Compartmental Models for West Nile Virus. *Mathematical Biosciences*, **227**(1): 20-28.

[91] Weber A, Weber M and Milligan P, (2001). Modeling Epidemics Caused by Respiratory Syncytial Virus (RSV). *Mathematical Biosciences*, **172**: 95–113.

[92] Wonham M, de-Camino-Beck T and Lewis M, (2004). An Epidemiological Model for West Nile Virus: Invasion Analysis and Control Applications. *Proceedings of the Royal Society B: Biological Sciences*, **271**: 501–507.

[93] Wonham M, Lewis M, Rencawowicz J and van den Driessche P, (2006). Transmission Assumptions Generate Conflicting Predictions in HostVector Disease Models: a Case Study in West Nile Virus. *Ecology Letters*, **9**: 706-725.

[94] Weir E, (2000). West Nile Fever Heads North. *Canadian Medical Association Journal*, **163**(7): 878.

[95] Yan X, Zou Y and Li J, (2007). Optimal Quarantine and Isolation Strategies in Epidemics Control. *World Journal of Modelling and Simulation*, **3**(3): 202–211.

A Appendices

In the following theorem, we present the adjoint system and control characterization.

Theorem A.0.1. *For an optimal control variable* (u_1^*, u_2^*, u_3^*) *and optimal corresponding state solutions* Q^**, then there exist adjoint variables* λ_j*,* $j = 1, ..., 15$*, satisfying,*

$$\begin{aligned}
\acute{\lambda_1} &= -a_3 - c_1 w_1 + \lambda_1(d_L + d_0 u_1) + (\lambda_1 - \lambda_3) m_L (1 - u_1), \\
\acute{\lambda_2} &= -a_3 - c_1 u_1 + \lambda_2(d_L + d_0 u_1) + (\lambda_2 - \lambda_4) m_L (1 - u_1), \\
\acute{\lambda_3} &= -a_3 - c_2 u_2 - \lambda_1(r_m(1 - u_2) - \lambda_3(d_m + d_0 u_2) + (\lambda_3 - \lambda_4)\tfrac{\beta_m b_m (B_{1i} + B_{2i})}{N}, \\
\acute{\lambda_4} &= -a_3 - c_2 u_2 - r_m(1 - u_2)\lambda_1 + \lambda_4(d_m + d_0 u_2) + (\lambda_1 - \lambda_2) q r_m (1 - u_2) \\
&+ (\lambda_5 - \lambda_6)\tfrac{\beta_b b_m B_{1s}}{N} + (\lambda_8 - \lambda_9)\tfrac{\beta_b b_m B_{2s}}{N} + (\lambda_{11} - \lambda_{12})\tfrac{\beta_h b_m S}{N}(1 - u_2), \\
\acute{\lambda_5} &= \lambda_5 d_b + (\lambda_4 - \lambda_3)\left(\tfrac{\beta_m b_m (B_{1i} + B_{2i})}{N^2} M_s\right) + (\lambda_5 - \lambda_6)\left(\tfrac{\beta_b b_m (N - B_{1s})}{N^2} M_i\right) \\
&+ (\lambda_9 - \lambda_8)\left(\tfrac{\beta_b b_m B_{2s}}{N^2} M_i\right) + (\lambda_{12} - \lambda_{11})\left(\tfrac{\beta_h b_m S}{N^2} M_i (1 - u_3)\right), \\
\acute{\lambda_6} &= \lambda_6 \delta_1 - \lambda_7 \nu_1 + (\lambda_3 - \lambda_4)\left(\tfrac{\beta_m b_m (N - (B_{1i} + B_{2i}))}{N^2} M_s\right) + (\lambda_6 - \lambda_5)\left(\tfrac{\beta_b b_m B_{1s}}{N^2} M_i\right)
\end{aligned}$$

$$+ \quad (\lambda_9 - \lambda_8)\left(\tfrac{\beta_b b_m B_{2s}}{N^2} M_i\right) + (\lambda_{12} - \lambda_{11})\left(\tfrac{\beta_h b_m S}{N^2} M_i(1-u_3)\right),$$

$$\acute{\lambda_7} = \lambda_7 d_b + (\lambda_4 - \lambda_3)\left(\tfrac{\beta_m b_m (B_{1i}+B_{2i})}{N^2} M_s\right) + (\lambda_6 - \lambda_5)\left(\tfrac{\beta_b b_m B_{1s}}{N^2} M_i\right)$$

$$+ \quad (\lambda_9 - \lambda_8)\left(\tfrac{\beta_b b_m B_{2s}}{N^2} M_i\right) + (\lambda_{12} - \lambda_{11})\left(\tfrac{\beta_h b_m S}{N^2} M_i(1-u_3)\right),$$

$$\acute{\lambda_8} = \lambda_6 d_b + (\lambda_4 - \lambda_3)\left(\tfrac{\beta_m b_m (B_{1i}+B_{2i})}{N^2} M_s\right) + (\lambda_6 - \lambda_5)\left(\tfrac{\beta_b b_m B_{1s}}{N^2} M_i\right)$$

$$+ \quad (\lambda_8 - \lambda_9)\left(\tfrac{\beta_b b_m (N-B_{2s})}{N^2} M_i\right) + (\lambda_{12} - \lambda_{11})\left(\tfrac{\beta_h b_m S}{N^2} M_i(1-u_3)\right),$$

$$\acute{\lambda_9} = \lambda_9 \delta_2 - \lambda_{10}\nu_2 + (\lambda_3 - \lambda_4)\left(\tfrac{\beta_m b_m (N-(B_{1i}+B_{2i}))}{N^2} M_s\right) + (\lambda_6 - \lambda_5)\left(\tfrac{\beta_b b_m B_{1s}}{N^2} M_i\right)$$

$$+ \quad (\lambda_9 - \lambda_8)\left(\tfrac{\beta_b b_m B_{2s}}{N^2} M_i\right) + (\lambda_{12} - \lambda_{11})\left(\tfrac{\beta_h b_m S}{N^2} M_i(1-u_3)\right),$$

$$\acute{\lambda_{10}} = -c_3 u_3 + \lambda_{10} d_b + (\lambda_2 - \lambda_1)\left(\tfrac{\beta_m b_m (B_{1i}+B_{2i})}{N^2} M_s\right) + (\lambda_6 - \lambda_5)\left(\tfrac{\beta_b b_m B_{1s}}{N^2} M_i\right)$$

$$+ \quad (\lambda_9 - \lambda_8)\left(\tfrac{\beta_b b_m B_{2s}}{N^2} M_i\right) + (\lambda_{12} - \lambda_{11})\left(\tfrac{\beta_h b_m S}{N^2} M_i(1-u_3)\right),$$

$$\acute{\lambda_{11}} = \lambda_{11} d_h + (\lambda_4 - \lambda_3)\left(\tfrac{\beta_m b_m (B_{1i}+B_{2i})}{N^2} M_s\right) + (\lambda_6 - \lambda_5)\left(\tfrac{\beta_b b_m B_{1s}}{N^2} M_i\right)$$

$$+ \quad (\lambda_9 - \lambda_8)\left(\tfrac{\beta_b b_m B_{2s}}{N^2} M_i\right) + (\lambda_{11} - \lambda_{12})\left(\tfrac{\beta_h b_m (N-S)}{N^2} M_i(1-u_3)\right),$$

$$\acute{\lambda_{12}} = -a_1 + \lambda_{12} d_h + (\lambda_4 - \lambda_3)\left(\tfrac{\beta_m b_m (B_{1i}+B_{2i})}{N^2} M_s\right) + (\lambda_6 - \lambda_5)\left(\tfrac{\beta_b b_m B_{1s}}{N^2} M_i\right)$$

$$+ \quad (\lambda_9 - \lambda_8)\left(\tfrac{\beta_b b_m B_{2s}}{N^2} M_i\right) + (\lambda_{12} - \lambda_{11})\left(\tfrac{\beta_h b_m S}{N^2} M_i(1-w_3)\right)$$

$$+ \quad (\lambda_{12} - \lambda_{13})\alpha,$$

$$
\begin{aligned}
\acute{\lambda_{13}} &= -a_2 + (\gamma + \mu_l + r + d_h)\lambda_{13}(\lambda_4 - \lambda_3)\left(\tfrac{\beta_m b_m (B_{1i}+B_{2i})}{N^2} M_s\right) \\
&+ (\lambda_9 - \lambda_8)\left(\tfrac{\beta_b b_m B_{2s}}{N^2} M_i\right) + (\lambda_{10} - \lambda_9)\left(\tfrac{\beta_h b_m S}{N^2} M_i(1-u_3)\right) - \gamma, \lambda_{14} - r\lambda_{15} \\
&+ (\lambda_6 - \lambda_5)\left(\tfrac{\beta_b b_m B_{1s}}{N^2} M_i\right), \\
\acute{\lambda_{14}} &= (\mu_h + \tau + d_h)\lambda_{14} - \tau\lambda_{15} + (\lambda_4 - \lambda_3)\left(\tfrac{\beta_m b_m (B_{1i}+B_{2i})}{N^2} M_s\right) \\
&+ (\lambda_9 - \lambda_8)\left(\tfrac{\beta_b b_m B_{2s}}{N^2} M_i\right) + (\lambda_{12} - \lambda_{11})\left(\tfrac{\beta_h b_m S}{N^2} M_i(1-u_3)\right), \\
&+ (\lambda_6 - \lambda_5)\left(\tfrac{\beta_b b_m B_{1s}}{N^2} M_i\right), \\
\acute{\lambda_{15}} &= d_h\lambda_{15} + (\lambda_4 - \lambda_3)\left(\tfrac{\beta_m b_m (B_{1i}+B_{2i})}{N^2} M_s\right) + (\lambda_6 - \lambda_5)\left(\tfrac{\beta_b b_m B_{1s}}{N^2} M_i\right) \\
&+ (\lambda_9 - \lambda_8)\left(\tfrac{\beta_b b_m B_{2s}}{N^2} M_i\right) + (\lambda_{12} - \lambda_{11})\left(\tfrac{\beta_h b_m S}{N^2} M_i(1-u_3)\right),
\end{aligned}
$$

with transversality conditions (or final time conditions)

$$\lambda_i(T) = 0, \quad i = 1, ..., 15. \tag{A.0.1}$$

Furthermore, optimal control functions are given as follows:

$$u_1^* = \max\left(0, \min\left(U_1, \frac{1}{b_1}((\lambda_3 - \lambda_1)m_L L_s + (\lambda_4 - \lambda_2)m_L L_i + d_0 L_s\lambda_1 + d_0 L_i\lambda_2 - c_1 L)\right)\right),$$

$$u_2^* = \max\left(0, \min\left(U_2, \frac{1}{b_2}(r_m M\lambda_1 + (\lambda_2 - \lambda_1)q r_m M_i + \lambda_3 d_0 M_s + \lambda_4 d_0 M_i - c_2 M)\right)\right),$$

$$u_3^* = \max\left(0, \min\left(U_3, \frac{1}{b_3}((\lambda_{12} - \lambda_{11})\frac{\beta_h b_m S}{N} M_i - c_3 S)\right)\right).$$

Proof. The adjoint system results from Pontryagin's Principle [68],

$$\acute{\lambda_1} = -\frac{\partial \hbar}{\partial L_s}, \quad \acute{\lambda_2} = -\frac{\partial \hbar}{\partial L_i}, \quad \ldots\ldots\ldots\ldots \quad \acute{\lambda_{15}} = -\frac{\partial \hbar}{\partial R}.$$

The optimality conditions (characterization of the optimal control) given by

$$\frac{\partial \hbar}{\partial u_1} = 0, \qquad \frac{\partial \hbar}{\partial u_2} = 0, \qquad \frac{\partial \hbar}{\partial u_3} = 0,$$

on the interior of the control set. Using the bounds on the controls, we obtain the desired characterization. □